Fractalkine Receptor Regulates Cellular Response to X-ray Radiation in Ovarian Cancer Cells

By

Jia Xie
B.S.,Wuhan University, 2010

Dissertation

Submitted as partial fulfillment of the requirements
For the degree of Doctor of Philosophy in Biopharmaceutical Sciences
In the Graduate College of the University of Illinois at Chicago, 2015

Chicago, Illinois

Defense Committee:

Maria Barbolina, Chair and Advisor
John Nitiss
Hyun-Young Jeong
Joanna Burdette, Medicinal Chemistry and Pharmacognosy
Alan Diamond, Pathology

This dissertation is dedicated to my parents.

ACKNOWLEDGEMENTS

I would like to thank my advisor Dr. Maria Barbolina for giving me invaluable guidance in scientific research. Her dedication towards ovarian cancer research has motivated me to pursue a career in cancer research. She gave me a lot of insightful suggestions on designing experiments and preparing posters and presentations.

I also want to thank my thesis committee members, Dr. John Nitiss, Dr. Joanna Burdette, Dr. Hyun-Young Jeong, Dr. Alan Diamond and Dr. Xiaolong He for their generous time and constructive criticism. I truly benefited from all their advice, which greatly improved my research work.

Furthermore, I would like to thank Brett Smith from the Department of Radiation Oncology at University of Illinois at Chicago for his technical support in doing radiation.

I would also like to express my gratitude to my labmates – Hilal Gurler, Goda Muralidhar and Joelle Sacks. Working with them for the past few years is an enjoyable experience.

Lastly, I would like to thank my family members. Without their love and support, I could not finish my Ph.D. study.

TABLE OF CONTENTS

TABLE OF CONTENTS (continued)

LIST OF TABLES

LIST OF FIGURES

LIST OF ABBREVIATIONS

7TM	Seven Helical Transmembrane
A	Adenine
ABCC	ATP-Binding Cassette/Multidrug Resistance-Associated Protein
ACC	Animal Care Committee
Akt	Protein Kinase B
Alt-NHEJ	Alternative-NHEJ
ANOVA	Analysis of Variance
APE1	Apurinic Endonuclease I
ApoA1	Apolipoprotein A1
ARID1A	AT-rich interactive domain-containing protein 1A
ASK1	Apoptosis Signal-regulatory Kinase 1
ATF2	Activating Transcription Factor 2
ATM	Ataxia Telangiectasia Mutated
ATR	Ataxia Telangiectasia and Rad3 Related
AZD8797	Substituted 7-amino-5-thio-thiazolo [4,5-d] pyrimidines.
BER	Base Excision Repair
BLM	Bloom Syndrome Protein
BRAF	V-Raf Murine Sarcoma Viral Oncogene Homolog B
BRCA1/2	Breast Cancer 1/2
BSA	Bovine Serum Albumin
C	Cytosine

LIST OF ABBREVIATIONS (CONTINUED)

CA-125	Cancer Antigen 125
CAMKII	Calmodulin-dependent Protein Kinase II
CASMC	Coronary Artery Smooth Muscle Cells
CCC	Clear Cell Carcinoma
CCNE1	G_1/S-Specific Cyclin E1
Cdc25	Cell Division Cycle 25
CDK	Cyclin-dependent Kinase
CDK12	Cyclin-Dependent Kinase 12
Chk1	Checkpoint Kinase 1
Chk2	Checkpoint Kinase 2
C-NHEJ	Classical NHEJ
CNS	Central Nervous System
CO_2	Carbon Dioxide
CR	Complete Response
c-Rel	Proto-oncoprotein c-Rel
CRISPR-Cas9	Clustered Regularly Interspaced Short Palindromic Repeat Associated Protein 9
CSB/A	Cockayne Syndrome Proteins B/A
CtIP	CtBP-interacting Proteins
CX1	CX_3CR1 shRNA Transfected SKOV3 Clone6
CX2	Id8 Cells Transfected with CX_3CR1 shRNA Clone 2
CX_3CL1	Fractalkine

LIST OF ABBREVIATIONS (CONTINUED)

CX_3CR1	Fractalkine Receptor
CX6	CX_3CR1 shRNA Transfected SKOV3 Clone1
CX6	Id8 Cells Transfected with CX_3CR1 shRNA Clone 6
D	Radiation Dose
DAPI	4’,6-diamidino-2-phenylindole
DCFDA	2’,7’-dichlorofluorescin Diacetate
DDR	DNA Damage Repair
DEF	Dose Enhancement Factor
DGCR8	DiGeorge Syndrome Chromosomal Region 8
DMF	Dose Modifying Factor
DMSO	Dimethyl Sulfoxide
DNA	Deoxyribonucleic Acid
DNA-PKcs	DNA-Dependent Protein Kinase, Catalytic Subunit
DSB	DNA Double Strand Break
DsRed	Red Fluorescent Protein
EC	Endometrioid Carcinoma
ECL	Enhanced Chemoluminescence
ECLs	Extracellular Loops
ECM	Extracellular Matrix
EGFR	Epidermal Growth Factor Receptor
EOC	Epithelial Ovarian Carcinoma

LIST OF ABBREVIATIONS (CONTINUED)

ERBB2	Receptor Tyrosine-Protein Kinase
ERCC1	Exchange Repair Cross Complementing 1
ERK	Extracellular Signal-regulated Kinases
FABP4	Fatty Acid-binding Protein 4
FBS	Fetal Bovine Serum
FDA	Food and Drug Administration
FIGO	The International Federation of Gynecology and Obstetrics
G	Guanine
GABRA6	Gamma-Amino Butyric Acid Receptor Subunit Alpha-6
GAPDH	Glyceraldehyde 3-phophate Dehydrogenase
GDP	Guanine Diphosphate
GEF	Guanine Nucleotide Exchange Factor
GFP	Green Fluorescent Protein
GGR	Global Genomic NER
GI	Gastrointestinal
GPCR	G-Protein Coupled Receptor
GPx	Glutathione Peroxidase
gRNA	Guided RNA
GSH	Glutathione
GSK3β	Glycogen Synthase Kinase 3 β
GST	Glutathione S-transferase

LIST OF ABBREVIATIONS (CONTINUED)

GTP	Guanine Triphosphate
GTPase	Guanine Triphosphate Hydrolase
Gy	Gray
H	Hydrogen
H2A.X	H2A Histone Family, Member X
H_2O_2	Hydrogen Peroxide
HE4	Human Epididymics Protein 4
HGSC(HGSOC)	High Grade Serous Ovarian Carcinoma
HIPEC	Hyperthermic Intraperitoneal Chemotherapy
HIV	Human Immunodeficiency Virus
HJ	Holiday Junction
HO-1	Hemeoxygenase-1
HOSEpiC	Normal Ovarian Surface Epithelial Cells
HR	Homologous Recombination
HRP	Horseradish Peroxidase
HSP	Heat Shock Protein
HT	Helical Tomotherapy
ICRU	The International Commission on Radiological Units and Measurements
IgG	Immunoglobulin G
IL6,8	Interleukin 6,8
IMAT	Volumetric Intensity-modulated Arc Therapy

LIST OF ABBREVIATIONS (CONTINUED)

IMRT	Intensity-modulated Radiotherapy
IR	Ionizing Radiation
IκB	Inhibitor of kappa B
JNK	c-Jun N-terminal Kinase
KLK	Kallikreins
KRAS	V-Ki-ras2 Kirsten Rat Sarcoma Viral Oncogene Homolog
L	Length
LA	Linear Accelerator
LET	Linear Energy Transfer
LGSC	Low Grade Serous Ovarian Carcinoma
LIG3/4	Ligase III/IV
MAPK	Mitogen-Activated Protein Kinase
MAPKK	MAP Kinase Kinase
MAPKKK	MAP Kinase Kinase Kinase
MC	Mucinous Carcinoma
MDC1	Mediator of DNA Damage Checkpoint Protein 1
MECOM	MDS1 and EVI1 Complex Locus Protein EVI1
MEM	Minimal Essential Media
miRNA	microRNA
MLK3	Mixed-lineage Kinase 3
MMEJ	Microhomology-Mediated End Joining

LIST OF ABBREVIATIONS (CONTINUED)

MRE11A	Meiotic Recombination II Homolog A
MRN	MRE11-RAD50-NBS1
mRNA	Messenger RNA
MS	Multiple Sclerosis
NaCl	Sodium Chloride
NADPH	Nicotinamide Adenine Dinucleotide Phosphate
NBS1	Nibrin
NCI	National Cancer Institute
NER	Nucleotide Excision Repair
NF-κB	Nuclear Factor Kappa-light-chain-enhancer of Activated B Cells
NHEJ	Non-homologous End Joining
NIK	NF-κB-inducing Kinase
NK	Natural Killer
Nox4	NADPH Oxidase 4
NP40	Nonyl Phenoxypolyethoxylethanol
NQO1	NADP(H) Quinone Oxidoreductase
Nrf-2	Nuclear Factor-like 2
NSCLC	Non-small Cell Lung Cancer
NT	Non-transfected
OACIB	Office of Animal Care and Institutional Biosafety
OAR	Organs at Risk

LIST OF ABBREVIATIONS (CONTINUED)

OE	Overexpressor
OH	Hydroxyl
OPN	Osteopontin
OSE	Ovarian Surface Epithelium
P	Phosphorus
PACT	Protein ACTivator of the Interferon-Induced Protein Kinase
pADPr	Poly (ADP) Ribose
PAGE	Polyacrylamide Gel Electrophoresis
PAM	Protospacer Adjacent Motif
PARP	Poly ADP Ribose Polymerase
PBS	Phophate-buffered Saline
PCNA	Proliferating Cell Nuclear Antigen
PDAC	Pancreatic Ductal Adenocarcinoma
PFA	Para-formaldehyde
PFS	Progression Free Survival
PI	Propidium Iodide
PI3K	Phosphoinositide 3-kinase
PIKKs	Phosphoinositide 3-kinase-related Protein Kinase
pL	Amino Acid Leucine
PLD	Potentially Lethal Damage
Polβ	Polymerase β

LIST OF ABBREVIATIONS (CONTINUED)

PP2A	Protein Phosphatase 2A
pQ	Amino Acid Glutamine
pR	Amino Acid Arginine
pS	Amino Acid Serine
PT	Bordetella Pertussis Toxin
PTEN	Phosphatase and Tensin Homolog
PVDF	Polyvinylidene Fluoride
pVec	pVector Transfected
R	Rontgen
Rad51C	Rad51 Homolog C
RB1	Retinoblastoma Protein 1
REF	Radiation Enhancement Factor
RelA	Transcription Factor p65
RelB	Transcription Factor RelB
RF-C	Replication Factor C
RIPA	Radioimmunoprecipitation Assay Buffer
RISC	RNA-Inducing Silencing Complex
RNA	Ribonucleic Acid
RNAi	RNA Interference
RNase	Ribonuclease
ROS	Reactive Oxygen Species

LIST OF ABBREVIATIONS (CONTINUED)

RPA	Replication Protein A
RPMI	Roswell Park Memorial Institute Medium
RSF-1	Remodeling and Spacing Factor 1
RT	Room Temperature
SC	Serous Carcinoma
SCR	Id8 Cells Transfected with Scrambled shRNA
SD	Standard Deviation
SDS	Sodium Dodecyl Sulfate
SEM	Standard Error of the Mean
SER	Sensitizing Enhancement Ratio
Ser	Serine
SF	Surviving Fraction
shRNA	Short Hairpin RNA
siCTRL/CTRL	Control siRNA Transfected
siCX/CX	CX_3CR1 siRNA Transfected
siRNA	Small Interfering RNA
SLD	Sublethal Damage
SOD	Superoxide Dismutases
ssDNA	Single Strand DNA
STAT1	Signal Transducers and Activators of Transcription 1
STIC	Serous Tubal Intraepithelial Component

LIST OF ABBREVIATIONS (CONTINUED)

T	Thymidine
T	Thr (Threonine)
TAO	Thousand-and-one Amino Acids 1 and 2
TBST	Tris-buffered Saline with Tween
TCC	Transitional Cell Carcinoma
TCGA	The Cancer Genome Atlas
TCR	Transcription-coupled Repair
TFIIH	Transcription Factor II Human
TP53	Tumor Protein P53
TRBP	RISC-Loading Complex Subunit TARBP2
Tris	Tris (Hydroxymethyl) Aminomethane
Trx	Thioredoxin
TTR	Transthyretin
UNG	Uracil-DNA Glycosylase
UTR	Untranslated Region
UV	Ultraviolet
VCAM-1	Vascular Cell Adhesion Molecule 1
VEGF	Vascular Endothelial Growth Factor
W	Width
WAR	Whole Abdomen Radiation
WRN	Werner Syndrome ATP-dependent Helicase

LIST OF ABBREVIATIONS (CONTINUED)

XCR1	Lymphotactin Receptor
XLF	XRCC4-like Factor
XPA/B/C/G	Xeroderma Pigmentosum, Complementation Group A/B/C/G
XRCC1/4	X-Ray Repair Cross-complementing Group 1/4

SUMMARY

Epithelial ovarian carcinoma (EOC) is a leading cause of death from gynecologic malignancies. X-ray radiotherapy is one of the treatments against the disease. Multiple complications, such as dose-associated toxicity, preclude widespread use of this method. However, clinical studies indicate that this method could be useful against late and recurrent metastatic EOC. Therefore, modifications of the therapy could offer benefits to overcome current problems and treat the disease. Fractalkine receptor (CX_3CR1) belongs to a chemokine family of G protein-coupled receptors and our previous publications reported that transient downregulation of CX_3CR1 in ovarian cancer cells will impair their proliferation as well as their migration and adhesion to peritoneal mesothelial cells. Hence, combining CX_3CR1 downregulation and radiation could be one of the strategies for reducing the dose of radiation used in therapy while keeping its efficiency at a therapeutically effective level.

Our data indicate that transient downregulation of CX_3CR1 in most p53 mutant/null epithelial ovarian cancer cell lines can lead to radiosensitization, as determined by clonogenic assay. However, loss of CX_3CR1 does not affect radiosensitivity in cells that express wild-type p53. The mechanisms behind the CX_3CR1-dependent radiosensitization include the regulation of DNA double strand break repair. Specifically, CX_3CR1 knockdown can impair the activity of DNA damage repair related proteins and thereby lead to accumulated DNA damage. Another mechanism by which CX_3CR1 knockdown alters radiosensitivity is the regulation of cellular redox capacity, where loss of CX_3CR1 leads to elevated ROS levels.

SUMMARY (CONTINUED)

Taken together, our data indicate that disruption of the CX_3CR1 signaling could sensitize ovarian carcinoma to radiation therapy.

CHAPTER 1.

INTRODUCTION

1.1 Epithelial Ovarian Carcinoma

Epithelial ovarian carcinoma (EOC) is the most frequent cause of death among the gynecological malignancies (1, 2). The symptoms include pleural effusion, small bowel obstruction, venous thromboembolism, abdominal pain, gastrointestinal symptoms, etc. EOC contains four different stages according to FIGO staging system: stage I, II, III and IV. At stage I, malignant cells are usually confined in either or both of the ovaries; at stage II, besides the involvement of ovary, cancer has spread to the organs in the pelvis, including the fallopian tubes and uterus; at stage III, together with the involvement of the ovary, cancer has spread to the organs in the abdominal cavity, as well as lymph nodes; at stage IV, cancer has metastasized to distant sites, with the involvement of ovaries (3). According to the histopathology, immunohistochemistry, and molecular genetic analysis of the tumor, EOC is composed of several histotypes, including serous, endometrioid, mucinous, clear cell and transitional cells carcinoma. Serous carcinoma (SC) is the most common of the ovarian epithelial malignancies, accounting for approximately 80% of the cases. Other types are less common, where 10% are endometrioid carcinomas (EC), 3% are mucinous carcinomas (MC), 6% are clear cell carcinomas (CCC) and 1% are transitional cell carcinomas (TCC) (4). Some studies have shown that EC might arise from endometriosis, and the survival is slightly better compared to SC (90, 91). MC histologically resemble intestinal or endocervical epithelium, which lead to the difficulty in distinguishing them from metastatic mucinous tumors from the colon/rectum, appendix, cervix or pancreas (92, 93). CCC sometimes

originate from atypical endometriosis, with the pathogenesis partially due to the aberrant chromatin remodeling caused by ARID1A mutation. The prognosis of this disease is usually poor (1). SC can be further segregated into two types: high grade serous carcinomas (HGSCs) (Figure 1.1) and low grade serous carcinomas (LGSCs). More than 90% of the serous carcinomas are high grade serous carcinomas. This classification is based on morphological appearance, molecular changes, clinical behavior and distinct precursor lesions (4). Since high grade serous carcinomas are the most prevalent and deadly subtype, my thesis is mainly focus on this model.

"Malpica *et al*. have developed a two-tier grading scheme specifically for serous carcinoma that evaluates mitotic index and nuclear atypia. Tumors with uniform nuclei and <12 mitoses per 10 high-power fields are classified as low-grade serous carcinoma (LGSC), and those with marked cytological atypia (≥3 times variation in nuclear size) or 12 or more mitoses are classified as high-grade serous carcinoma (HGSC)" (Delair and Soslow, 2012, p.330).

High grade serous carcinoma is also different from low grade serous carcinoma in molecular changes. According to TCGA (The Cancer Genome Atlas) and a study recently published by Vang R., *et al*., 100% HGSC cases harbor a TP53 mutation (94), while only 8% of LGSC have TP53 mutations. In addition, HGSC is associated with BRCA (breast cancer genes) abnormalities, with 10-15% BRCA1/2 (breast cancer gene 1/2) germline mutation, 5-10% BRCA1/2 somatic mutation and 5-30% BRCA promoter methylation. BRCA1/2 plays a crucial role in DNA double strand break repair, and their mutations will increase cancer susceptibility (95). Moreover, most HGSCs share the phenotypic characteristics with tumors that harbor BRCA germline mutations. They also have molecular defects in DNA damage repair pathways that cause a common biological behavior with the ones caused by BRCA mutations. For example, 2%

of ovarian carcinomas have an ATM (Ataxia Telangiectasia Mutated) /ATR (Ataxia Telangiectasia and Rad3 Related) mutation, and 3% of them contain Rad51c (Rad51 Homolog C) mutation (96). HGSCs are also absent of mutations of KRAS, BRAF, or ERBB2, in contrast, 67% of LGSC have one mutation from KRAS, BRAF and ERBB2, and they are mutually exclusive (97). HGSCs also have aberrant DNA copy number changes, while low DNA copy number changes are found in LGSCs (4, 5).

The origin of serous ovarian carcinoma remains debatable, while some suggested that ovarian surface epithelium is the origin, others indicated that fallopian tube is the origin of the disease. It is now known that ovarian surface epithelium (OSE), which is a mesodermally derived mesothelium, are damaged during ovulation. Repeated ovulation with trauma is one of the theories for the pathogenesis of EOC, due to the formation of ovarian cysts after the internalization of OSE (98, 99). The aberrant hormone production would trigger these cysts to become metaplastic, undergo dysplasia, and eventually become ovarian carcinoma. However, serous ovarian carcinoma histologically and molecularly resembles malignant cells found in fallopian tube cancers: they contained tense areas of serous tubal intraepithelial component (STIC) which are found to be located in the distal fimbriated end of the fallopian tube (Figure 1.1); 10-15% of fallopian tubes from patients with BRCA mutation contain STIC; the majority of both STIC and HGSC have TP53 mutation; cyclin E1, Rsf-1 and fatty acid synthase are overexpressed in both STIC and HGSC (6, 7).

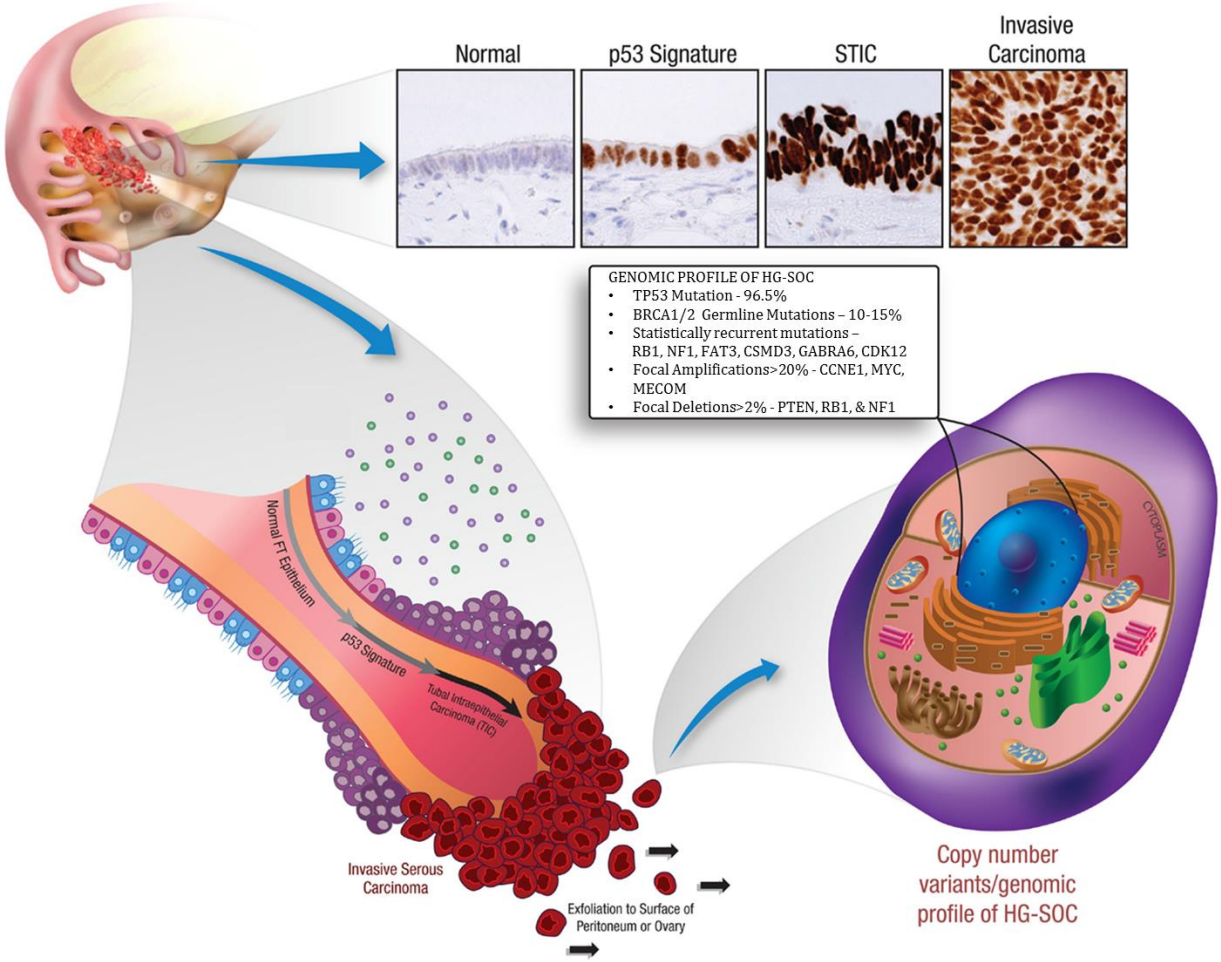

Figure 1.1. Early Tumor Progression within the Fallopian Tube and the Resultant Genetic Profile of HG-SOC. This illustration depicts the recently identified precursor lesions of HG-SOC that are present in the fallopian tube. Mutations in the TP53 tumor suppressor gene are a very early event in the pathogenesis of HG-SOC, occurring exclusively in benign-appearing secretory cells. These preneoplastic lesions are referred to as 'p53 signatures'. Acquisition of a neoplastic phenotype and proliferative capacity results in the development of serous tubal intraepithelial carcinoma (STIC). Breaching of the basement membrane and localized dissemination to the ovary and/or peritoneal cavity heralds the development of invasive HG-SOC and the associated clinical scenario. HG-SOCs that involve the ovary or peritoneum are characterized by mutations in TP53 (and BRCA1 in familial cases) and display a complex genomic terrain with widespread copy number alterations throughout the genome. Modified from Jones PM and Drapkin R, 2013. (Figure as originally published in Jones PM and Drapkin R (2013) Modeling high-grade serous carcinoma: how converging insights into pathogenesis and genetics are driving better experimental platforms. *Front. Oncol.* **3**:217. doi: 10.3389/fonc.2013.00217)

"Clinical presentation of HGSCs and LGSCs are also different. Although the overall long-term survival for both groups of patients is similar, the difference being that those with HGSC succumb to their disease sooner than those with LGSC. And patients with LGSC have a median survival of 4.2 years after diagnosis, as compared with 1.7 years for those with HGSC" (Delair and Soslow, 2012, p.335).

1.2 Ovarian Cancer Biomarkers

EOC is a heterogeneous disease and can progress to the late stage rapidly. Due to the lack of symptoms from patients and detection tools, early diagnosis of ovarian cancer is difficult. Currently, CA-125 (Cancer Antigen-125) and transvaginal ultrasonography are recommended for ovarian cancer screening, even though only 30-45% of women with early stage disease can be detected using this approach (2).

Several risk factors can lead to the development of ovarian cancer, and the most important one is the family history. Women with a family history of ovarian or breast cancer have higher risk of disease, because they might have inherited BRCA1/2 mutations (100). The approaches that may help lower the risk of developing ovarian cancer include oral contraceptive use, children breastfeeding, hysterectomies and tubal ligations (8, 9).

Due to the low sensitivity and specificity in ovarian cancer screening, a lot of studies have investigated novel serum biomarkers of the disease. HE4, mesothelin, VCAM-1, IL6, IL8, B7-H4, serum amyloid A, osteopontin (OPN), kallikreins (KLK), OVX1 and VEGF are elevated in ovarian cancer patients, while transthyretin (TTR), ApoA1 and transferrin are decreased (10). Besides these protein biomarkers, miRNAs are under extensive evaluation (11). miRNAs are small non-coding RNAs which contain approximately 22 nucleotides that can post-transcriptionally regulate gene expression (12). Ovarian cancer and its development are

correlated with differentially expressed miRNAs. According to miRNA-expression profiling, miR-21, miR-29a, miR-92, miR-93 and miR-126 are overexpressed while miR-127, miR-155 and miR-99 are underexpressed (13). Moreover, exosomes which are one sub-type of secreted microvesicles are also correlated with ovarian cancer development. Taylor *et al.* reported that the level of the circulating tumor-derived exosomes increases with the progression of ovarian cancer. These exosomes contain miRNAs that can affect recipient cell's function and therefore affect disease progression (14).

Since multiple biomarker analysis can increase sensitivity and specificity in detecting ovarian cancer, the analysis of biomarkers, in combination with advanced diagnostic imaging technologies, will enable early diagnosis of ovarian cancer and therefore, improve the treatment of the disease.

1.3 Current Treatment

Most EOC patients are diagnosed when the disease has progressed to an advanced stage. These patients are often treated with staging laparotomy, total abdominal hysterectomy, bilateral salpingo-oophorectomy, omentectomy, cytoreductive tumor debulking, followed by assessment of the pelvic and para-aortic lymph node (15). Six cycles of a platinum-/taxane-based chemotherapy is the standard adjuvant therapy, with 3-week treatment-free intervals. Most patients initially respond to the treatment, with 75% clinical complete response (CR) rates (16). Unfortunately, 75% of these CR patients experience disease recurrence and the median time to relapse is 12-18 months (16). Clinical studies have shown that compared to chemotherapy, radiation therapy may show advantage in long-term overall survival (17, 18, 19, 20, 21). For

instance, researchers from Australia treated 64 women with advanced ovarian cancer who underwent cytoreductive surgery and standard chemotherapy with either radiation therapy or chemotherapy. The 5-year survival rates were 59% for the radiation treated group and 33% for the chemotherapy treated group (22). However, radiation therapy is not used as a first-line therapy, because even though high dose of radiation could achieve better treatment effect, severe toxicity would also be caused. Thrombocytopenia, neutropenia, nausea, vomiting, diarrhea and small bowel obstruction are commonly observed and they are not very easy to treat (23, 24). Therefore, radiation therapy is usually effective in "palliating" the symptoms caused by chemotherapy, such as pain, because chemotherapy may destroy spinal cord (25, 26). Approximately 50% to 75% of patients experience significant local abdominopelvic symptoms relief from a short course of external beam radiation (27). Second-line therapy is composed of maintenance therapy and consolidation therapy. They are used after first-line therapy to prevent disease recurrence, because only a minority of the patients won't suffer from disease recurrence with chemotherapy. Maintenance therapy includes prolonged administration of single-agent therapy, continuation of induction chemotherapy, intraperitoneal chemotherapy, hormonal therapy and immunotherapy with interferon or monoclonal antibodies. However, several clinical studies indicated that prolonged or continuate administration of chemotherapy showed no benefits in clinical outcomes. To be more specific, 12 cycles of platinum-based chemotherapy showed no better response compared to 6 cycles of platinum-based therapy. Administration of other drugs, such as topotecan and doxorubicin, which are topoisomerase inhibitors, also showed no benefit in the treatment of advanced stage EOC. Consolidation therapy includes high-dose chemotherapy with stem cell support, whole-abdominal radiotherapy, and intraperitoneal administration of ^{32}P or antibodies labeled with radioisotopes (Brachytherapy). Among all of

them, whole abdominal radiotherapy is the most commonly used consolidation therapy. It could achieve greater clinical outcome especially when the diameter of the residual tumor is less than 5mm (19). The planned whole-abdominal radiation dose varied between 20 and 30 Gy, given in 22 fractions, 5 fractions per week with the maximal kidney dose of 20 Gy. The majority of studies performed a routine boost of 45 or 50 Gy to the pelvis regardless of the site of the residual tumor, also given in 22 fractions with 5 fractions per week. Several studies also employed a boost to the para-aortic nodes (16). Although radiation therapy is commonly used as a consolidation therapy, its toxic side effects cannot be ignored. Therefore, it is very important to find a new way to reduce the dose of radiation to avoid toxicity while maintaining its therapeutic efficacy. The following sections will be a detailed introduction to radiation therapy, chemotherapy and radiosensitizers.

1.3.1 Ionizing Radiation

After the first discovery of "x-rays" in 1895 by the German physicist Wilhelm Conrad Rontgen (28), x-rays were widely used in medical therapeutics. X-ray is one type of ionizing radiation which is classified as electromagnetic radiation (29). There are two types of electromagnetic radiation, x- and r-rays, and they are different in the ways they produced (29). X-rays are produced extranuclearly, which is from an electrical device such as linear accelerator that accelerates electrons to high energy and stops them abruptly in a target (29). γ-rays are produced intranuclearly, which means they are emitted by radioactive isotopes (29). They are the excessive energy that are released during the process of the transformation of an unstable nucleus becomes stable (29). Other types of radiation which can be classified as particulate radiations are electrons, protons, α-particles, neutrons and heavy charged particles (29). While all of these charged

particles are directly ionizing with high linear energy transfer (LET), x-rays are indirectly ionizing, which do not produce biological and chemical damage themselves, but when they are absorbed in tissues and organs, they interact with water molecules to produce free radicals that are able to damage deoxyribonucleic acid (DNA) (29). DNA lesions produced by x-rays could be effectively modified by chemical sensitizers and protectors (29).

"Quantity of radiation is expressed in rontgen, rad, or gray. The rontgen (R) is the unit of exposure and is related to the ability of x-rays to ionize air. The rad is the unit of absorbed dose and corresponds to energy absorption of 100erg/g. The International Commission on Radiological Units and Measurements (ICRU) recommended that the rad be replaced as a unit by the gray (Gy), which corresponds to an energy absorption of 1 J/kg. Consequently, 1 Gy=100 rad." (Hall and Giaccia, 2012, p.5)

Linear accelerators are one kind of high-energy machines that generate external X-rays of various energies, enabling the treatment of malignancies in various anatomic locations. External beam radiotherapy is usually delivered in several fractions daily to allow normal organs and tissues repair through sublethal damage (SLD) repair and repopulation between fractions (30). The other reason for fractionated x-rays treatment are reoxygenation and reassortment of cells into sensitive phases of the cell cycle between fractions. These classical "four Rs", repair, repopulation, reoxygenation, reassortment, and a newer member, radiosensitivity, illustrate the basic principles of radiobiology which will be discussed in the following sections (31, 32).

1.3.1.1 Repair

Cellular damage caused by radiation can operationally be classified as lethal damage, potentially lethal damage (PLD), and sublethal damage (SLD). Lethal damage is irreversible and irrepairable and can cause irrevocable cell death. PLD is a part of the radiation damage that can be affected by postirradiation environmental conditions. SLD can be repaired in hours under

normal circumstances, unless an additional sublethal damage, such as a second dose of radiation, is added, and then becomes a lethal damage (29). PLD is potentially lethal because it can induce cell death under ordinary circumstances. But PLD can be repaired, for example, when the cells are incubated in a balanced salt solution instead of a full growth medium for several hours after irradiation (29). SLD repair represents the increase in cell survival that is observed under fractionated radiation.

"By splitting radiation dose into small parts, cells are allowed to repair sublethal damage. The amount of damage that is repaired depends on the ability of the cell to recognize the damage and activate **a)** repair pathways and **b)** cell cycle arrest. Malignant cells have often suppressed these pathways, often through mutation or inhibition of TP53, preventing them from undergoing efficient repair. Normal tissue cells with intact repair pathways are able to repair the sublethal damage by the time the next fraction is delivered." (http://ozradonc.wikidot.com/the-5-r-s-of-fractionation)

1.3.1.2 Reassortment

Eukaryotic cells go through the cell cycle, which is composed of the G_0, G_1, S, G_2 and M phases. G_0 is when cells are in their senescence state; G_1 phase is a preparation phase in which cells become bigger and synthesize RNA and proteins that are needed for dividing. S phase is the synthetic phase in which DNA replication occurs. G_2 phase is another preparation phase in which cells will continue to grow and build apparatus needed for mitosis. M phase is the mitosis phase in which one cell divides into two progeny cells (33). Understanding the cell cycle is very important in that radiation usually kills fast-dividing cells while it is not effective in senescent cells. When cells were in different phases of cell cycle, they respond differently to radiation. Cells are most resistant to radiation when they are in S phase, less resistant when in G_1 phase, and most sensitive to radiation during mitosis and G_2 (34). Therefore, synchronizing cells to their radiosensitive phase, in the other word, reassortment, is an important principle in fractionated

radiation to enhance radiosensitivity, because the survivors after the first dose of radiation are predominantly in a resistant phase. If the time interval between two doses is appropriately selected and allows the progression of these resistant cells to sensitive phase, increased radiosensitivity can be observed (29).

1.3.1.3 Repopulation

When the time interval between two doses of radiation is longer than the cell cycle time which allows cells to divide, the surviving fraction will be increased for both normal and malignant cells. Fast repopulation of normal tissues is very important in early reduction of toxicity in these tissues. However, accelerated repopulation can be observed in tumors as well, especially at the later period of fractionated radiotherapy. Therefore, overall treatment time should be less than 5 weeks for fast-growing tumors (29, 35).

1.3.1.4 Reoxygenation

It has been demonstrated that cells become less sensitive to radiation with the decreasing amount of molecular oxygen level, mainly due to the absence of nearby blood vessels (101). Tumors are usually composed of hypoxic cells, normoxic cells and anoxic cells. Because of the difference in their sensitivity to radiation, oxygenated cells are killed first after radiation while hypoxic cells remain resistant. However, hypoxic cells can be reoxygenated at different speeds after exposed to a dose of radiation by a process called reoxygenation. The mechanism includes the reopening of temporarily closed blood vessel (several minutes), reduced respiration of lethally damaged cells (less than an hour), and the reduced distance between blood vessels and tumor cells due to

the death of oxygenated cells (days). Therefore, fractionated radiotherapy is crucial to increase treatment efficacy by reoxygenation (29, 36).

1.3.1.5 Radiosensitivity

Besides the classical "four Rs", the intrinsic radiosensitivity of the cells determines the overall sensitivity. There are mainly three factors that determine cellular radiosensitivity: cell proliferation rate, differentiation stage and metabolism rate (37, 38, 39). Specifically, fast growing cells tend to be more sensitive to radiation, while slow growing cells are resistant to radiation (37); stem cells are more sensitive to radiation while terminally differentiated cells are resistant to radiation (38); cells that have a longer mitotic future are more radiosensitive compared to those with a shorter mitotic future (39). Therefore, when characterizing potential chemotherapeutic agents that might have radiosensitive ability, it is important that they shouldn't change the intrinsic radiosensitivity of the cells.

1.3.2 Chemotherapy

After the first accidental discovery of chemotherapy in early 20th century, it has been widely used to treat different kinds of cancers in clinical oncology (40). Most chemotherapeutic drugs work by affecting DNA synthesis, therefore, they can effectively target the fast-growing cells while having little effect on senescent cells (41).

The combinational use of carboplatin and a taxane is the standard first-line therapeutics for ovarian cancer. Carboplatin forms association bonds with the platinum molecules that bind to GC rich sites in DNA, thereby producing intrastrand and interstrand DNA crosslinks, leading to

DNA strand breakage during replication (102). Paclitaxel can bind to tubulin and inhibit depolymerization of tubulin and therefore inhibit the disassembly of microtubules (103). As a result, cell division can be inhibited. It also has a very weak synergy with radiation therapy (29). Docetaxel has a similar function, in which it can form stable tubulin polymers, and thereby inhibiting the mitotic spindle apparatus, leading to final cell death (42). Although this combination serves as a standard adjuvant therapy for ovarian cancer, myelosuppression is the most common side effect. While carboplatin can cause thrombocytopenia, docetaxel can cause fluid accumulation, including pleural effusions and ascites (104, 105). Moreover, treatment with taxane can also cause neuropathy, which aggravates with increasing dose of paclitaxel (106). Besides these side effects, patients with recurrent and refractory epithelial ovarian cancer are very resistant to chemotherapy (107). The possible mechanisms include cancer cell specific abnormalities, such as increased tolerance to DNA damage due to the increased DNA damage repair, the overexpression of the ABCC transporter which can modulate platinum-drug efflux, decreased CTR1 (Copper transport protein) which is a platinum influx transporter protein, and a change in the tumor microenvironment (43). In order to overcome drug resistance, novel chemotherapeutic agents are under investigation.

Bevacizumab (Avastan) is an anti-VEGF (vascular endothelial growth factor) humanized-monoclonal antibody that can inhibit angiogenesis (29). Since blood vessels are the most important source of nutrients and oxygen to the nearby tumor cells, VEGF inhibition can make existing tumor vessel regression (108). Although some clinical trials in ovarian cancer patients have shown improvement in progression free survival (PFS) (44, 45), it has life-threatening side effects, including gastrointestinal (GI) perforation, bleeding, high blood pressure, headache, and

prevent wound healing from surgery (109). Doxorubicin is an intercalating agent which can intercalate between base pairs in the DNA helix and thereby preventing DNA replication (29). It is also a topoisomerase II inhibitor, which functions in preventing DNA ligation after DNA double strand break (DSB) (46). Common side effects include myelosuppression, cardiotoxicity and cardiomyopathy (47). Although it is an FDA approved drug for ovarian cancer, a recent clinical trial conducted in Norway and Sweden showed that as a consolidation therapy, radiation therapy can achieve better 5-year PFS compared to the combination of doxorubicin and cisplatin (48). Etoposide is another FDA approved topoisomerase II inhibitor to treat ovarian cancer. Although it is effective when combined with intraperitoneal cisplatin application in patients with platinum-sensitive recurrent ovarian cancer, the median survival is strongly correlated with the residual disease (49). Moreover, myelosuppression is also commonly observed in these patients. Gemcitabine belongs to the category of antimetabolites. It is a nucleotide analogue that inhibits DNA synthesis. It can also terminate DNA strand (29). Although gemcitabine is an FDA approved chemotherapeutic agent for ovarian cancer, it failed to prolong survival when used together with primary standard treatment (50). Myelosuppression is also observed in patients treated with gemcitabine (110).

1.3.3 Radiosensitizers.

Since the goal of our research is to find a way to maintain the therapeutic efficacy of radiation therapy while reducing the dose, and thereby reducing side effects, it is important to use radiosensitizers. There are usually two mechanisms of radiation sensitization: hyperthermia and the use of chemotherapeutic agents as an adjunct therapy, which will be discussed in the following sections.

1.3.3.1 Hyperthermia

Hyperthermia can damage and kill cancer cells when heating the body tissue (51) (usually 41 ℃ to 45 ℃). Since hyperthermia can severely change the tumor microenvironment, it can sensitize the tumors to radiation therapy (51). Specifically, the most important factor in hyperthermia-induced radiosensitization is the stimulation of vascular activity, which increases the level of oxygen delivered to the tumor, and therefore leads to oxygen-dependent radiosensitization (52). Moreover, hyperthermia can also affect pH, cellular metabolism and gene/protein expression (such as HSP family of protein) to enhance radiosensitization (53). Hyperthermia can also enhance immune system activity by activating immune effector cells to increase the amount of secreting immune factors and/or activating cytotoxic T cells (54).

Hyperthermia can also sensitize tumors to chemotherapy and/or combined with chemotherapy to achieve radiosensitization. The most important reason for hyperthermia-induced radiosensitization is that it can enhance DNA damage while inhibiting DNA damage repair pathways. Furthermore, it improves chemotherapeutic drug uptake by tumor cells, increases free radicals production and increases vascular delivery (55). Currently, hyperthermia also has some advantage in treating advanced stage EOC. The combination of aggressive cytoreductive surgery with intra-operative hyperthermic intraperitoneal chemotherapy (HIPEC) is an effective treatment for advanced EOC (56).

1.3.3.2 Chemotherapy as a radiosensitizer

The principle goal of integrating chemotherapy into radiation therapy in cancer treatment is to improve tumor control, recurrence-free survival and overall survival. Since most side-effects

caused by radiation therapy are dose-limiting, it is important to maintain the therapeutic efficacy of radiation while reducing its dose, which can be achieved by maximizing the recognition of tumor versus normal tissue based on their characteristics. For example, radiation can target fast-growing cells while chemotherapeutic drugs may target tumor cells that have aberrant gene expression. Moreover, since cancer is a heterogeneous disease, emerging evidence has shown that the lowest initial tumor burden together with the optimal dose of radiation and chemotherapy can achieve the best therapeutic result, based on the principle that different treatment can target at different subpopulation of the tumor (57, 58).

1.4 Fractalkine Receptor (CX_3CR1)

Despite the advances in the use of chemotherapeutic agents against ovarian cancer, it is still crucial to find novel targets to improve disease treatment. Identification of novel molecules that are involved in the progression of ovarian cancer might help to establish new treatments. Our lab has been focused on fractalkine receptor (CX_3CR1) and its role in ovarian carcinoma tumorigenesis and metastasis. Our group showed that while CX_3CR1 is seldom expressed in normal OSE and normal ovarian surface epithelial cells (HOSEpiC), it is expressed in immortalized EOC cell lines T1074, HOSE11-12, IOSE29, IOSE80, benign serous cystadenoma and primary and metastatic EOC specimens (59). The following sections will be a detailed background introduction to the fractalkine receptor and its role in EOC.

1.4.1 Fractalkine Receptor: Nomenclature, Structure and Function

1.4.1.1 Nomenclature of Chemokine Receptor and Fractalkine Receptor (CX_3CR1)

Fractalkine receptor (CX_3CR1) belongs to a chemokine family of G protein coupled receptors (60). GPCRs are seven trans-membrane receptors that are targets of approximately 30% of commercially available drugs, such as Salmeterol, Olanzapine and Clopidrogel (61). According to the sequence homology and functional similarity, human GPCRs can be grouped into five classes: rhodopsin, adhesion, secretin, metabotropic glutamate and frizzled/taste2. The rhodopsin-like receptor, which is the largest family of GPCRs, can be further sub-categorized into four families: α, β, γ and δ. Chemokine receptors belong to the γ rhodopsin family (62) and can be divided into four categories: CXCRs, CCRs, CX_3CRs, and XCRs based on the type of ligand that they bind (63). The ligand, which is a chemokine, can be accordingly sub-classified into four groups, and the classification is based on the local sequence of the first two closely paired cysteine residues. If there is no amino acid between these two cysteines, the chemokine is sub-classified as CC; when there is one non-cysteine amino acid in between, the chemokine is known as CXC; when there are three non-cysteine amino acids between the two cysteines, it is then CX_3C. Generally, there are four invariant cysteine residues localize on chemokine, in which the first and the third form a disulfide bond while the second and the fourth form the other disulfide bond. However, in the sub-category of C, the chemokine only possesses two of the four cysteines. Moreover, there are also chemokines that have six cysteines. The R after cysteine (C) stands for receptor and S is a number that is designated based on the chronological order in which it was identified (64). While all the other subfamilies of chemokines contain several different members, CX_3CL1 is the only member in the CX_3C subfamily. While most chemokine receptors can bind to multiple different chemokines, CX_3CR1 can only specifically interact with CX_3CL1 (65).

1.4.1.2 The Structure of Chemokine Receptor and Fractalkine Receptor (CX_3CR1)

Generally, chemokine receptors have approximately 350 amino acids and contain seven helical transmembrane (7TM) regions that are embedded in the lipid bilayer of the cell membrane, three extracellular loops (ECLs) composed of hydrophilic amino acids, extracellular acidic N-terminus that contain N-linked glycosylation sites which are important for ligand specificity, three intracellular hydrophilic loops, and intracellular C-terminus, which is usually coupled with G-proteins, that can conduct signal transduction in cytoplasm through the phosphorylation of serine and threonine. (Figure 1.2) There are two cysteines located in extracellular loop 1 and 2, with a disulfide bond in between (67). Fractalkine receptor, CX_3CR1, is also a 7TM GPCR and it contains several functionally important motifs that are present in other chemokine receptors as well. For example, the DRY (Asp-Arg-Tyr) motif is present for G protein interactions and signal transduction (68).

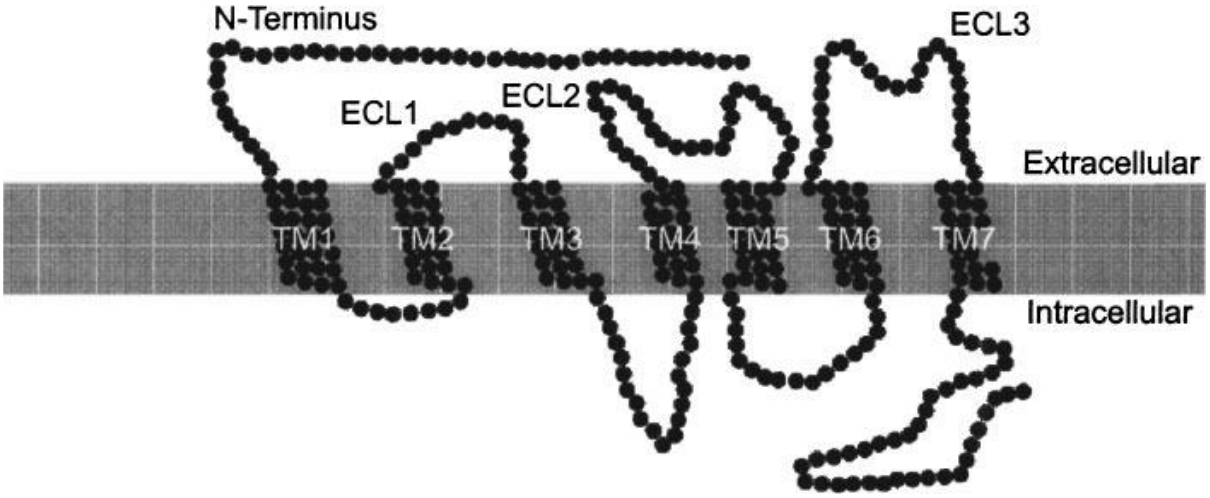

Figure 1.2 Topology of a typical chemokine receptor. (Permission not required) (STRUCTURE, FUNCTION, AND INHIBITION OF CHEMOKINES, Annual Review of Pharmacology and Toxicology. Vol. 42: 469-499 (Volume publication date April 2002) DOI: 10.1146/annurev.pharmtox.42.091901.115838)

1.4.1.3 Function of Chemokine Receptor

The intracellular signaling of the chemokine receptors is activated upon binding of the chemokine ligand. After the ligand anchoring to the N-terminus of the receptor which allows for a conformational change of the ligand, together with the specific interaction between acidic residues in the receptor and basic residues on the ligand, the flexible N-terminus of the ligand will then further bind to the ECLs and the trans-membrane regions of the receptor and then lead to receptor activation (69). The following intracellular signal transduction depends on coupling to Bordetella pertussis toxin (PT)-sensitive (α β γ) heterotrimeric G-proteins that bound to the intracellular loops (70). Upon receptor activation, the receptor will act as a guanine nucleotide exchange factor (GEF) to activate the associated G-protein by facilitating the exchange of GDP, which binds to the Gα subunit, for GTP. The Gα subunit, as well as the associated GTP, can then detach from the receptor and the leftover Gβγ subunits to further activate downstream effectors (71, 72). Besides the Gα subunit, the Gβγ heterodimer can also activate downstream effectors to regulate the amount of secondary messenger and ultimately results in diverse physiological responses, such as leukocyte migration, cell differentiation and angiogenesis (73, 74). After activation, GTP will be hydrolyzed by the GTPase, and the Gα and the Gβγ subunits will then reassociate and bind to the receptor for desensitization (72).

1.4.1.4 Function of Fractalkine Receptor (CX_3CR1)

CX_3CR1 is widely known for its function in regulating peripheral immune and inflammatory response and central nervous system (CNS) due to its expression in T lymphocytes, monocytes/macrophages, leukocytes, natural killer (NK) cells, neutrophils and microglia, and its interaction with fractalkine (CX_3CL1) that expressed in endothelial, epithelial and dendritic cells

(75). For example, Fone *et al.* reported that CX_3CL1 expressed in endothelium can interact with CX_3CR1 expressed in leukocytes, and thereby mediating the initial capture, firm adhesion, and activation of circulating leukocytes to activate an inflammatory response (76). Harrison *et al.* showed that CX_3CL1 expressing neurons can communicate with CX_3CR1 expressing microglia to regulate physiological and pathological process such as cerebral ischemia, stroke and neurodegenerative diseases (77).

Besides these findings, fractalkine receptor also plays an important role in various cancers. Shulby *et al.* demonstrated the expression of CX_3CL1 in both human bone marrow endothelial cells and osteoblasts and the expression of CX_3CR1 in human prostate cancer cells. The interaction between the fractalkine and its receptor can guide the circulating prostate cancer cells to the bone marrow, which migrate and survive in the bone tissue (78). Erreni *et al.* showed that the cancer stem cells and progenitor cells isolated from glioblastoma multiforme specimens express the CX_3CL1 and CX_3CR1, indicating their involvement in the glioblastoma tumorigenesis. Moreover, the immunohistochemistry staining results suggested that the amount of CX_3CL1 is positively correlated with the stage of the tumor and overall survival (79). Marchesi *et al.* reported that CX_3CR1 is expressed in pancreatic ductal adenocarcinoma (PDAC) cells and can migrate to neural cells that express CX_3CL1 which indicates tumor neurotropism (80). Moreover, high expression of CX_3CR1 is also related to early tumor recurrence (80). Jaminson-Gladney *et al.* illustrated that the ability of breast adenocarcinoma cells to metastasize to the skeleton is based on the interaction between CX_3CL1 expressed in endothelial and stromal cells of the bone marrow and CX_3CR1 expressed in the breast cancer cells (81). Together with the direct role that fractalkine-fractalkine receptor chemotaxis plays in mediating multiple cancer

distant dissemination, soluble CX_3CL1 existed in tumor microenvironment can promote antitumor activity by recruiting NK cells (82).

1.4.2 Fractalkine Receptor and Epithelial Ovarian Carcinoma

Recently, there has been growing interest in the area of the role fractalkine and its receptor plays in EOC. Due to the impact the tumor microenvironment exerts on cancer progression, Hart *et al.* showed that CX_3CR1+ leukocytes infiltration into the ovarian tumor microenvironment can induce immunosuppressive activity by inhibiting naïve T cell responses (83). Moreover, Gaudin *et al.* reported that CX_3CL1 is present in healthy OSE, the surface of fallopian tube, and malignant ovarian epithelial cells, and its production can accelerate tumor cell proliferation partially due to the autocrine effect of the interaction between CX_3CL1 and CX_3CR1, which are also expressed in EOC cells (84).

Our lab is also interested in the role the fractalkine axis plays in regulating ovarian cancer. Together with the specific expression of CX_3CR1 in the primary and malignant EOC, we also validated the finding that CX_3CL1 is present in the ascites of EOC patients, and its presence is required for tumor cell proliferation (59). Moreover, we also reported that EOC cells that express CX_3CR1 can functionally interact with CX_3CL1 expressed in peritoneal mesothelial cells and therefore mediate cancer cell migration inside the peritoneal cavity. The EOC cells can adhere to tissues and organs covered by the mesothelial linings and thus promote metastasis (59). Furthermore, since our previous work has also demonstrated the expression of CX_3CR1 in ovarian teratoma, which is an abnormally differentiated keratinocyte, and CX_3CR1 is also present in normally developing skin, we further demonstrated that CX_3CR1 is required for

epidermal lineage differentiation (85). Therefore, skin toxicity might be a side effect when applying anti-fractalkine treatment against ovarian cancer (85).

1.4.3 Fractalkine Receptor Antagonist

Due to the involvement of the chemokine axis in the pathogenesis of multiple diseases such as AIDS, multiple sclerosis (MS), endometriosis, ovarian cancer, etc., a huge effort has been exerted on the discovery and development of chemokine receptor antagonist, including chemokine mutants/analogues, small molecule inhibitors and neutralizing monoclonal antibodies. In 2009, Dorgham *et al.* established a modified phage display selection strategy to select CX_3CL1 analogues that can bind to CX_3CR1 without inducing receptor internalization (86). The selected CX_3CR1 antagonist-F1 can inhibit calcium responses, chemotactic function and adhesion mediated by fractalkine axis (86). Moreover, F1 can also inhibit the recruitment of monocyte/macrophage to the site of inflammation in an *in vivo* model. In 2010, White *et al.* described a specific CX_3CR1 antagonist AZ12201182 that can inhibit the pro-survival effect of CX_3CL1 on CX_3CR1 expressing human coronary artery smooth muscle cells (CASMC) (66). Moreover, AZ12201182 inhibits DNA synthesis, and can decrease epiregulin mRNA levels that are usually induced by CX_3CL1 (66). In 2012, AstraZeneca in Sweden produced the first potent and selective, orally available CX_3CR1 antagonists----substituted 7-amino-5-thio-thiazolo [4, 5-d] pyrimidines (AZD8797) which are now commercially available at Axon Medchem (87). Later on, this drug was proved to be potent in treating MS by blocking the infiltration of CX_3CR1+ leukocytes (88) and alleviating chemotherapy-induced pain (89).

1.5 Dissertation Objectives and Outline

The main goal of this dissertation research is to understand how loss of CX_3CR1 can sensitize EOC cells to radiation therapy, and therefore develop novel approaches to the treatment of EOC. In particular, transient downregulation of CX_3CR1 achieved by introducing CX_3CR1 siRNA to EOC cells originally derived from patients with HGSC can lead to radiosensitization as determined by *in vitro* clonogenic assay. A major possible mechanism is related to the impaired DNA damage repair pathway. Another possible mechanism, such as aberrant reactive oxygen species (ROS) accumulation may also contribute to the fractalkine receptor dependent radiosensitization. This dissertation consists of four major chapters: (1) Transient downregulation of fractalkine receptor in epithelial ovarian cancer cell lines can lead to radiosensitization; (2): Transient downregulation of fractalkine receptor in epithelial ovarian cancer cell lines lead to less DNA damage repair; (3): Loss of CX_3CR1 leads to persistent oxidative DNA damage. (4): CX_3CR1 stable knockdown reduces overall tumor burden and inhibits metastasis *in vivo*.

Chapter 2, the first part of this dissertation, includes transfecting different EOC cell lines originally derived from HGSC patients and other commonly used EOC cell lines with either CX_3CR1 siRNA to establish transient downregulation or CX_3CR1 shRNA to establish stable downregulation; Treating non-transfected, the control siRNA transfected/pvector shRNA transfected, and CX_3CR1 siRNA/shRNA/overexpressor transfected cells with x-ray radiation; and conducting clonogenic assay to assess the surviving fraction from each cell line under different conditions to evaluate the radiosensitization effect. While transient downregulation of CX_3CR1 in EOC cells that have specific p53 mutation status can lead to radiosensitization, stable

downregulation or upregulation of CX_3CR1 cannot alter ovarian cancer cells' sensitivity to x-ray radiation mainly due to the change in intrinsic radiosensitivity.

Chapter 3 describes the major mechanism behind CX_3CR1 dependent radiosensitization. DNA damage repair related proteins were measured using immunofluorescence staining and western blot in different cell lines; clonogenic assays were further utilized to evaluate cellular radiosensitivity upon addition of the ATM inhibitor (KU55933) and the PARP inhibitor (Olaparib). Based on the results obtained, we concluded that impaired DNA damage repair is one of the pathways contributing to radiosensitization.

Chapter 4 describes how CX_3CR1 status affects the cellular redox system. ROS levels were measured by flow cytometry. Our results indicated that loss of CX_3CR1 induces persistent oxidative damage which also contribute to the overall radiosensitization.

Chapter 5 describes loss of CX_3CR1 as being potent in abrogating ovarian carcinoma metastasis *in vivo*. Cancer cell adhesion to the omentum was evaluated by short-term adhesion assay *in vivo*; overall tumor burden was evaluated by long-term overall survival assay. Our results confirmed our previous published findings that CX_3CR1 is a promising cellular target in the treatment against metastatic ovarian carcinoma.

This dissertation will present a novel combinational therapy against EOC with a mechanistic understanding. By introducing fractalkine receptor downregulation to alter cancer cells'

sensitivity to radiation, x-ray radiation might be more commonly used in the treatment against EOC.

CHAPTER 2.

TRANSIENT DOWNREGULATION OF FRACTALKINE RECEPTOR IN EPITHELIAL OVARIAN CANCER CELL LINES CAN LEAD TO RADIOSENSITIZATION

2.1 Introduction

The cells we used in this study are SKOV3 (monolayer), SKOV3 (spheroids), CAOV3 (monolayer), OVCAR4 (monolayer), OVSAHO (monolayer), IGROV1 (monolayer) and A2780 (monolayer). SKOV3, CAOV3, OVCAR4 and OVSAHO are originally derived from HGSC patients whose genomes contain mutated p53 (111). Spheroids are multicellular aggregates that are present in the peritoneal fluid of patients. They are believed to facilitate intraperitoneal spread of cancer cells and are more resistant to chemotherapeutic agents compared to the same cells that grow as monolayers due to the decrease in drug penetration, increase in drug efflux pumps, hypoxic environment, etc. (112). Studying both monolayers and spheroids could offer insight into the radiosensitivity change upon fractalkine receptor downregulation.

IGROV1 is a human ovarian adenocarcinoma cell line (113), and is found to originate from either the endometrioid or the clear cell instead of the serous histotype. A2780 was established from tissue obtained from an untreated ovarian cancer patient (114). Both IGROV1 and A2780 have wild-type p53 which differs from the common feature of high grade serous histotype. Due to the important role p53 plays in regulating the ionizing radiation-induced DNA damage response, evaluating the CX_3CR1-dependent radiosensitization in these p53 wildtype models

could enable the use of p53 status as a predictive marker to define the response of ovarian cancer patients to radiation and CX_3CR1 inhibition.

Variations in cellular sensitivity to ionizing radiation are correlated to p53 mutation location (115). The p53 contains 393 amino acids and consists of three functional domains, an N-terminus activation domain, DNA binding domain and C-terminal oligomerization domain. (Figure 2.1) The N-terminus includes a transactivation domain and a proline-rich domain. The central core is the DNA-binding domain, and the C-terminus contains a nuclear localization signal sequence, a tetramerization domain, a nuclear export signal sequence, and a regulatory domain (116). The positions of p53 mutations spread throughout the TP53 gene, and the mutations are extremely heterogeneous. The position of mutation in TP53 could affect cellular sensitivity to chemotherapy and radiotherapy (115, 153). Besides, Brachova P, *et al*. showed that the ovarian cancer patients with TP53 mutations that abolish the wild-type p53 function have a shorter progression-free survival and a greater risk of recurrence (158). Therefore, it is important to determine the p53 mutation in order to predict each patient's response to anti-cancer drugs and ionizing radiation.

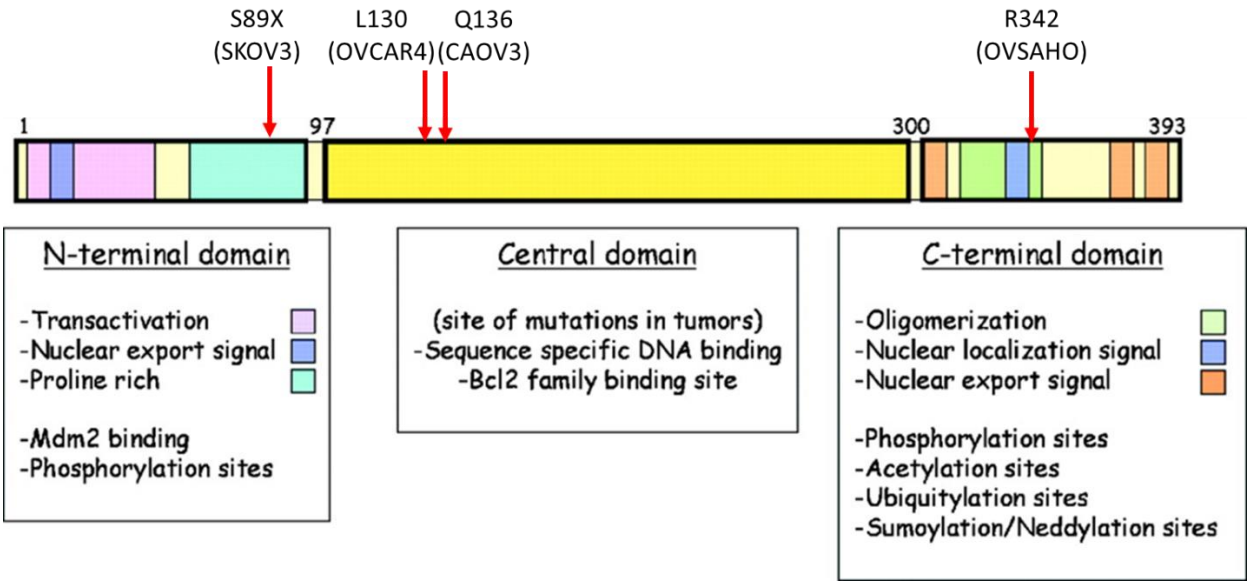

Figure 2.1 Diagram showing the domain structure of the p53 protein. The p53 protein is a transcription factor that contains several well-defined domains. At the N-terminus are the transactivation domain and a proline-rich region, which is required for apoptotic function. Within the N-terminus are the interaction sites of p53 with components of the transcriptional machinery as well as ubiquitin ligase Mdm2. The central domain harbors the sequence specific DNA binding region, where most of the tumor associated mutations occur. This central region also contains binding sites for interaction with members of the Bcl2 protein family. The C-terminal region contains the oligomerization domain as well as nuclear localization and export signals. Several sites within the N-terminal region have been shown to be phosphorylated and the C-terminal region contains numerous sites of modification which influence stability, localization and activity of p53. Modified from Yee KS and Vousden KH. 2005. Reprinted with permission from *Carcinogenesis*, 2005, 26(8): 1317-1322. Copyright (2005) Oxford University Press.

The way to evaluate radiosensitivity is based on the shape of the survival curve. In the context of radiobiology, loss of the reproductive integrity, which defines the loss of the capability of a single cell to divide indefinitely and produce a colony that contains more than 50 cells, is the opinion to evaluate reproductive cell death (117). Since mitotic cell death is the dominant mechanism of irradiation-induced cell death, clonogenic assay can most accurately define cellular growth after radiation. The survival fraction can be calculated based on the

quantification of the clonogenic assay, and the survival curves can then be plotted based on the survival fraction under each treatment condition.

In the early years of radiotherapy, target theory pioneered the survival curve theory. There are four simple target models used to describe the correlation between the survival fraction (S) and the radiation dose (D). They are the single hit single target model, the single hit multi-target model, the multi-hit single target model and the multi-hit multi-target model (118, 119). Single hit multi-target model (Figure 2.2 A) is the most commonly used, and it is based on the following assumptions: 1), there are n targets in the cell; 2), one hit on a target is sufficient to cause inactivation of that target; 3), when all n targets are inactivated, the cell dies (120). Therefore, the shape of the curve is sigmoid, and can be plotted using the following equation:

$$S=1-(1-e^{-D/D0})^{n}$$

with n being the back extrapolation of the exponential portion of the survival curve to zero dose, D_0 being the dose required to reduce 63% surviving fraction. Another parameter, Dq, describes the width of the shoulder, and mathematically, $Dq=D_0\log^{n}$ (121). These parameters are widely used to assess the sensitivity of cells to radiation: n reflects cellular damage repair ability. When n increases, cells become more resistant to radiation, due to the increased damage repair ability. Dq reflects the capacity of the cells to accumulate sublethal damage. If Dq increases, cells are more resistant to radiation. D_0 reflects the average lethal dose, the larger the D_0, the more resistant the cells (122, 123). The sensitizing enhancement ratio (SER) is defined by D_0control/D_0treatment, which is crucial in deciding the extent of radiosensitization (124, 125).

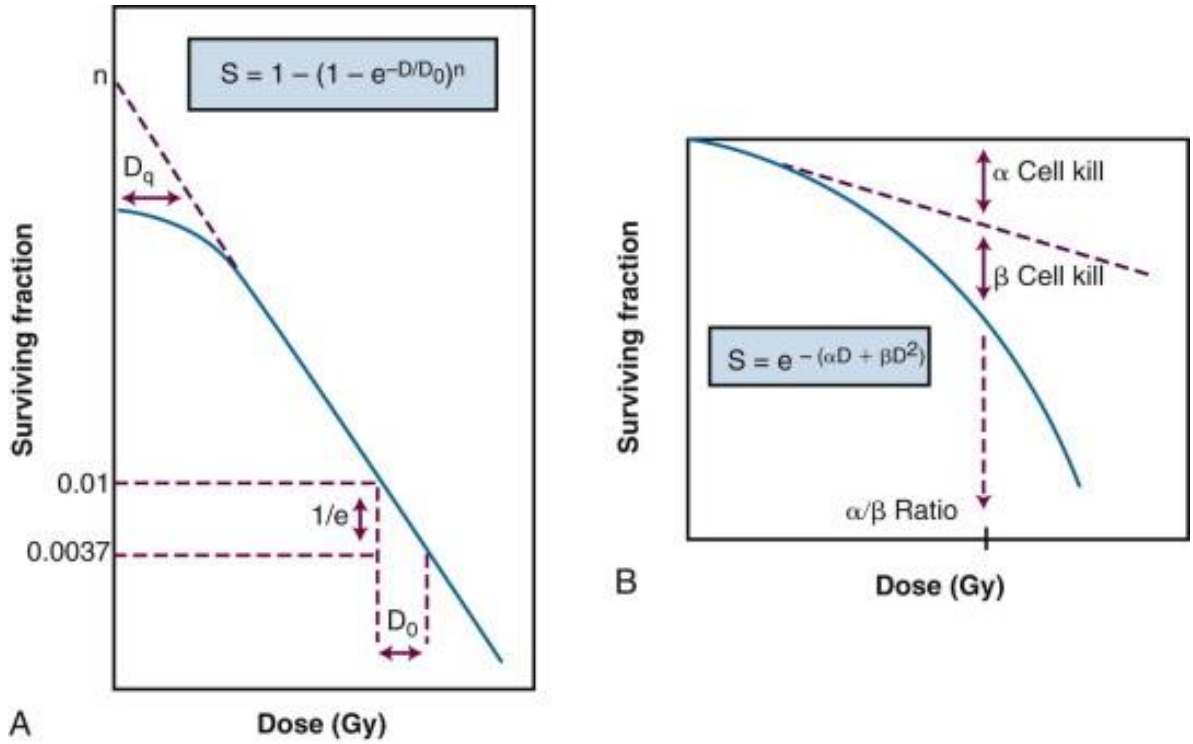

Figure 2.2 Comparison of two mathematical models commonly used to fit cell survival curve data. A, The single-hit, multitarget model is shown with its associated parameters, D_0, n, and Dq. Although this model has since been invalidated, values for its parameters are still used for comparative purposes. D_0, dose increment that reduces the cell survival to 37% (1/e) of some initial value on the exponential portion of the curve (i.e., a measure of the reciprocal of the slope); Dq, a measure of the width of the shoulder; n, back extrapolation of the exponential portion of the survival curve to zero dose (i.e., a measure of the steepness of the shoulder). B, The linear-quadratic model and its associated parameters, α and β, form the basis for current isoeffect formulas used in radiation therapy treatment planning. Reprinted with permission from *Clinical Radiation Oncology*, Chapter 1: Biologic Basis of Radiation Oncology. Copyright (2012) Elsevier Inc.

However, this model has been invalidated due to the unsatisfied representation to some mammalian cell survival curves and some curves inferred from clinical studies (126, 154, 155, 156, 157). Moreover, the interaction between the radiation and the biological object is not described molecularly (126). Therefore, a different interpretation of cell survival, the linear

quadratic model (Figure 2.2 B), was proposed. It can fit survival data much better, especially when the radiation damage was on cells. The mathematical expression of the curve is:

$$S=\exp(-\alpha D-\beta D^2)$$

which describes the radiation damage molecularly. The assumption of this expression is that the DNA double strand break is the determinant lethal lesion, and α is the probability of two sublesions in both DNA polynucleotide strands caused by a single hit break while β is the probability of two sublesions caused by two separate events. In fractionated radiation, α and β are usually used in the clinic to calculate the dose per fraction and the number of fractions (121, 126). To compare the radiosensitivity between the control group and the treatment group, radiation enhancement factor (REF) and dose modifying factor (DMF) are used. REF is defined by the surviving fraction of the control group compared to that of the treatment group when the dose is 2 gray (SF_2control/SF_2treatment), and DMF is defined as the dose that is required to kill 90% of the population in the control group compared to that in the treatment group (DMF_{10}control/DMF_{10}treatment). When both REF_2 and DMF_{10} are larger than 1.1, the treatment group can then be considered radiosensitized (127, 128, 129). Although the multi-target single hit model has been invalidated, values for its parameters were still used to compare radiosensitivity. These values of the parameters can only be utilized for comparative purpose when they are in a statistically meaningful range (126).

The extent of radiosensitivity is positively correlated to the cell proliferation rate because radiation works by damaging DNA. Since cancer cells might lack the appropriate genes to repair

the damaged DNA, the lesions will accumulate with the proliferation of cells and finally lead to reproductive cell death. Therefore, to compare the radiosensitivity upon the addition of a treatment, such as chemotherapeutic drug, gene silencing, etc., it is important to consider that the cells' initial intrinsic radiosensitivity should be similar before and after the treatment, so that the function of the treatment is the single factor that affects cellular radiosensitivity.

2.2 Materials and Methods

2.2.1 Cell Lines and Cell Cultures

Human ovarian carcinoma cell lines SKOV3 and OVCAR4 with serous histotype that originated from malignant cells in the ascites fluid were purchased from the National Cancer Institute (NCI) Tumor Cell Repository (Detrick, MD). Another human ovarian carcinoma cell line, CAOV3, that originated from malignant cells in the ascites of HGSC patients was obtained from Dr. M. S. Stack (University of Notre Dame, IN). IGROV1 and A2780 were also purchased from NCI Tumor Cell Repository (Detrick, MD). OVSAHO were obtained from the Japanese Collection of Research Bioresources Cell Bank (Osaka, Japan). SKOV3, CAOV3, IGROV1 and A2780 were cultured according to manufacturer's instructions using minimal essential media (MEM) (Corning) supplemented with 10% fetal bovine serum (FBS) (SIGMA-ALDRICH), 0.5% penicillin/streptomycin (Corning), 0.4% amphotericin B (Corning) and 0.22% g/ml sodium bicarbonate (Santa Cruz Biotechnology) for less than 20 consecutive passages. OVCAR4 and OVSAHO were grown in RPMI (Corning) containing 10% FBS, 0.5% penicillin/streptomycin, 0.4% amphotericin B and 0.2% g/ml sodium bicarbonate. All cells were kept at 37℃ and 5% CO_2 in a humidified incubator, and were routinely tested for Mycoplasma.

2.2.2 Reagents and Antibodies

Antibodies used in this research are: β-tubulin, β-actin (University of Iowa, E7, 1:200), CX_3CR1 (Abcam, ab51668, 1:2000), GAPDH (Santa Cruz Biotechnology, sc-137179, 1:200), anti-rabbit IgG, HRP-linked antibody (Cell Signaling Technology, 1:1000-1:5000), anti-mouse IgG, HRP-linked antibody (Santa Cruz Biotechnology, sc-2005, 1:500-1:3000), ECL reagents were purchased from GE Healthcare and Thermo Scientific. Control siRNA and CX_3CR1 siRNA were purchased from Santa Cruz Biotechnology, CX_3CR1 cDNA clone, PRS Vector shRNA negative control and CX_3CR1 shRNA plasmids were all purchased from Origene.

2.2.3 siRNA-Mediated Silencing

Cells were plated in six well plates (Celltreat) one day before transfection. CX_3CR1 siRNA and control siRNA were lyophilized according to the manufacturer's instructions prior to use, and then cells were transfected using DharmaFECT (Thermo Scientific). The transfected cells were cultured in their growth media for 72 hrs and then either harvested for analysis or subjected to x-ray radiation. CX_3CR1 siRNA is a pool of 3 different siRNA duplexes that were designed to target the following sequences: sc-39904A: 5'-CCCAGUUCAUGUUCACAAA-3', sc-39904B: 5'-CCCUGCUCAUUAUGAGUUAtt-3', sc-39904C: 5'-CCUACUGCAUCGAGUCAAAtt-3'

2.2.4 Stable Cell Lines Generation

SKOV3 cells were plated in six well plates one day before transfection. At the day of transfection, plasmids (CX_3CR1 cDNA clones, PRS vector shRNA and CX_3CR1 shRNA plasmids) were resuspended in DNA/RNase free water according to the manufacturer's instructions prior to use, and SKOV3 cells were transfected by DharmaFECT. One day post-

transfection, the cells were split into 48 well plates (SIGMA-ALDRICH) and were either treated with 1 mg/ml G418 (Corning) or treated with 4 μg/ml puromycin (Enzo Life Sciences) for the selection of the control clones or CX_3CR1-shRNA clones. After 2-6 weeks, resistant clones were isolated, CX_3CR1-overexpressing clones were maintained in regular complete MEM with 0.2mg/ml G418, and CX_3CR1-shRNA/pvector clones were maintained in regular complete MEM with 1-2 μg/ml puromycin. Clones were screened for CX_3CR1 expression by western blot. The CX_3CR1 shRNA constructs contain 4 unique sequences: 5'-TAGCCATTGTTGCCTGAATCCTCTCATCT-3', 5'-TATTCTACTCCGTCATCTTTGCCATTGGC-3', 5'-CATCGTCCTGGCCGCCAACTCCATGAACA-3', 5'-CCTCATCTGAATCACAAAGGAGCAGGCAT-3'.

Stable CX_3CR1 expression: the cDNA clones used in the study are the full-length gene with the following sequence: (158)

ATGGATCAGTTCCCTGAATCAGTGACAGAAAACTTTGAGTACGATGATTTGGCTGAG
GCCTGTTATATTGGGGACATCGTGGTCTTTGGGACTGTGTTCCTGTCCATATTCTACT
CCGTCATCTTTGCCATTGGCCTGGTGGGAAATTTGTTGGTAGTGTTTGCCCTCACCAA
CAGCAAGAAGCCCAAGAGTGTCACCGACATTTACCTCCTGAACCTGGCCTTGTCTGA
TCTGCTGTTTGTAGCCACTTTGCCCTTCTGGACTCACTATTTGATAAATGAAAAGGGC
CTCCACAATGCCATGTGCAAATTCACTACCGCCTTCTTCTTCATCGGCTTTTTTGGAA
GCATATTCTTCATCACCGTCATCAGCATTGATAGGTACCTGGCCATCGTCCTGGCCG
CCAACTCCATGAACAACCGGACCGTGCAGCATGGCGTCACCATCAGCCTAGGCGTC
TGGGCAGCAGCCATTTTGGTGGCAGCACCCCAGTTCATGTTCACAAAGCAGAAAGA

AAATGAATGCCTTGGTGACTACCCCGAGGTCCTCCAGGAAATCTGGCCCGTGCTCCG
CAATGTGGAAACAAATTTTCTTGGCTTCCTACTCCCCCTGCTCATTATGAGTTATTGC
TACTTCAGAATCATCCAGACGCTGTTTTCCTGCAAGAACCACAAGAAAGCCAAAGC
CATTAAACTGATCCTTCTGGTGGTCATCGTGTTTTTCCTCTTCTGGACACCCTACAAC
GTTATGATTTTCCTGGAGACGCTTAAGCTCTATGACTTCTTTCCCAGTTGTGACATGA
GGAAGGATCTGAGGCTGGCCCTCAGTGTGACTGAGACGGTTGCATTTAGCCATTGTT
GCCTGAATCCTCTCATCTATGCATTTGCTGGGGAGAAGTTCAGAAGATACCTTTACC
ACCTGTATGGGAAATGCCTGGCTGTCCTGTGTGGGCGCTCAGTCCACGTTGATTTCT
CCTCATCTGAATCACAAAGGAGCAGGCATGGAAGTGTTCTGAGCAGCAATTTTACTT
ACCACACGAGTGATGGAGATGCATTGCTCCTTCTCTGA

2.2.5 Spheroids Formation Assay

Six well plates were coated with 0.5% agarose which was allowed to solidify and cool at room temperature for at least 30 min. 1 million cells were resuspended and transferred on top of the agarose and incubated in the humidified incubator with 5% CO_2 at 37 ℃ for at least 24 hrs for spheroids formation. The formed spheroids were then identified and evaluated using microscopy (Zeiss) and an example is shown in Figure 2.3.

A B

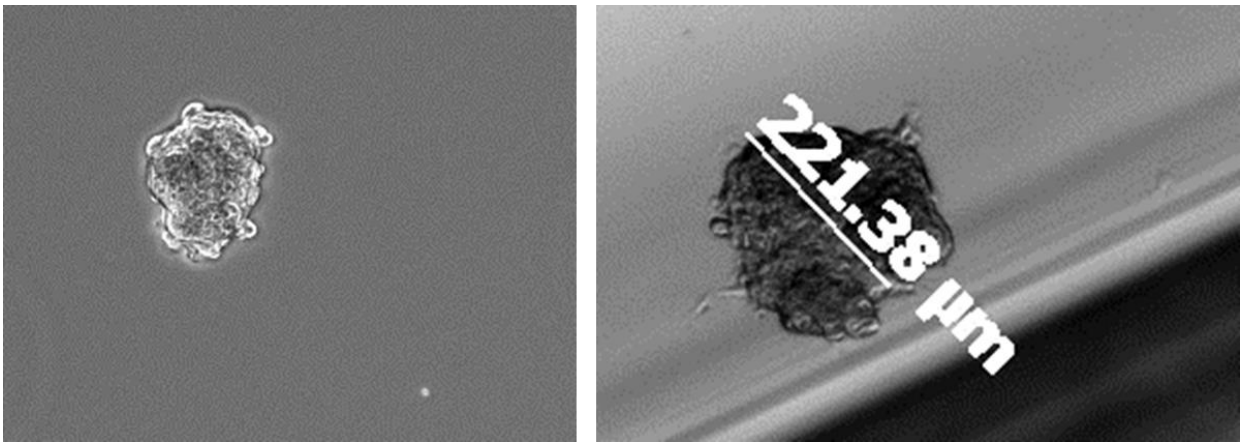

Figure 2.3 Spheroids Formation Assay. SKOV3 monolayer cells were plated on top of the agarose gel as described above. A) The regular shape of a spheroid. B) The diameter of spheroids ranges between 60 to 300 µm.

2.2.6 Clonogenic Assay

After radiation, a certain number of the cells in six well plates from each treatment condition were re-plated onto p100 plates (Thermo Scientific) and allowed to grow for 1-2 weeks until visible colonies formed. These colonies were then fixed with 4% para-formaldehyde (Santa Cruz Biotechnology) and stained with 0.05% crystal violet (SIGMA-ALDRICH). The stained colonies were then quantitatively analyzed to calculate surviving fraction. The survival curve was then plotted using SigmaPlot 12.5 (SigmaPlot).

2.2.7 Western Blot

For the detection of CX_3CR1, the cells were lysed in lysis buffer (50mM Tris pH8, 150mM NaCl, 1% NP40, and phosphatase inhibitor cocktail tablets [Roche]) and centrifuged for 15 min at 13,200 rpm at 4 ℃. The supernatants were quantified using the Bradford method (Bio-Rad Laboratories). The desired amount of protein was then mixed with sample loading buffer (65.8

mM Tris-HCl pH6.8, 2.1% SDS, 26.3% glycerol, 0.01% bromophenol blue and 0.5% β-mercaptoethanol right before use.) and boiled for 5min. 20 µg of protein from each treatment condition was loaded on 10% SDS-PAGE, and proteins were electro-transferred onto PVDF (Millipore). The membrane was then blocked with 3% BSA for 1hr at room temperature (RT), incubated with primary antibody for 3 hr at RT, washed with Tris-buffered saline with 0.1% Tween (TBST) 3 times, followed by incubation with secondary antibody for 1 hr at RT, and developed by enhanced chemiluminescence. The densitometric values were determined by Quantity One 1-D Analysis Software (Bio-Rad Laboratories).

2.2.8 Statistical Analyses

Statistical significance was determined by two-way ANOVA test using SigmaPlot software. For each test, p values of <0.05 was considered significant.

2.3 Results

2.3.1 Transient Downregulation of CX_3CR1 in Different EOC Cell Lines

Our lab has shown that CX_3CR1 is expressed in EOC cell lines originated from HGSC patients (SKOV3, CAOV3, and OVCAR4), and CX_3CR1 is downregulated in the presence of CX_3CR1 siRNA as determined by western blot (Figure 2.4). Compared to the control siRNA treated group, the reduction of the total CX_3CR1 expression is approximately 80% in SKOV3, 85% in CAOV3 and 55% in OVCAR4.

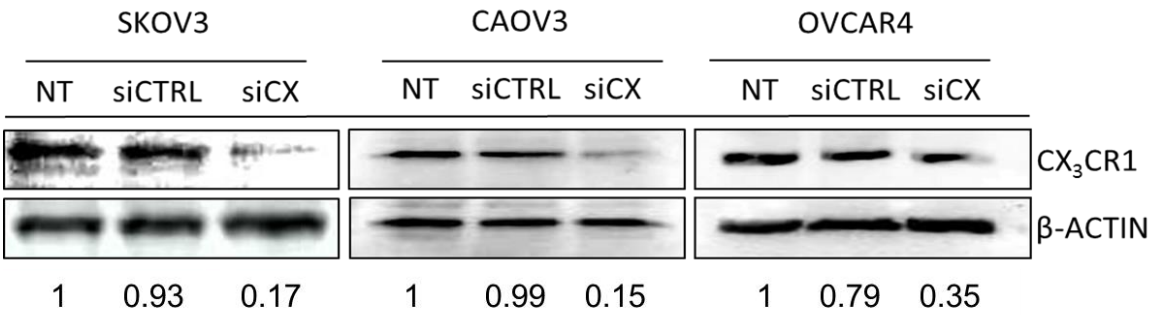

Figure 2.4 CX_3CR1 Downregulation Level in SKOV3, CAOV3 and OVCAR4
Protein levels of CX_3CR1 in SKOV3, CAOV3 and OVCAR4. 72 hours after transfection with the control or specific siRNA. (NT: non-transfected, siCTRL: transfected with the control siRNA; siCX: transfected with CX_3CR1 siRNA.) CX_3CR1 was detected using anti-CX_3CR1 antibodies by western blot analysis. Numbers below the bands are densitometry results. The western blot shown is the representative result from 3 independent experiments.

2.3.2 CX_3CR1 siRNA Treatment Induces Radiosensitization in SKOV3, CAOV3 and OVCAR4

To investigate the role of CX_3CR1 in regulating cellular sensitivity to radiation, clonogenic assays were done to assess cell survival after each treatment condition. As shown in Figure 2.5, 2.6, 2.7, 2.8 and Table 2.1, cells that were transfected with CX_3CR1 siRNA were more sensitive to ionizing radiation than the cells that were treated with the control siRNA and non-treated cells. One common trait of these cell lines is that the position of the mutated p53 amino acid is in close proximity, with CAOV3 mutated at pQ136 in the DNA binding domain, OVCAR4 mutated at pL130 in the DNA binding domain and SKOV3 mutated at pS89X in the proline-rich domain (130). The differences in the surviving fraction between CX_3CR1 siRNA treated cells and the control siRNA treated cells were significantly different, as determined by two-way ANOVA test. The surviving fraction of the control siRNA treated SKOV3 monolayers after 2 Gy was reduced to 0.89, whereas the surviving fraction of CX_3CR1 siRNA treated SKOV3 monolayers was 0.56. The treatment with CX_3CR1 siRNA in SKOV3 resulted in increased radiosensitivity by a factor

of 1.59, calculated at the dose of 2 Gy by dividing the surviving fraction of the control siRNA transfected SKOV3 curve with that of the corresponding CX_3CR1 siRNA transfected SKOV3. Moreover, the dose needed to achieve a 10% surviving fraction in the control siRNA treated SKOV3 monolayers was 9.81 Gy, whereas the dose needed in CX_3CR1 siRNA treated SKOV3 monolayers was 7.4 Gy. The treatment with CX_3CR1 siRNA resulted in increased radiosensitivity by a factor of 1.33, calculated by dividing the dose of the control siRNA transfected SKOV3 with that of the corresponding CX_3CR1 siRNA transfected SKOV3. Radiosensitization was scored positive (+) as shown in table I, when the value for the control/CX_3CR1 siRNA exceeded 1.1 at both 2 Gy and at 10% cell survival. Similar findings were also observed in SKOV3 spheroids, CAOV3, and OVCAR4, with the results shown in Table 2.1.

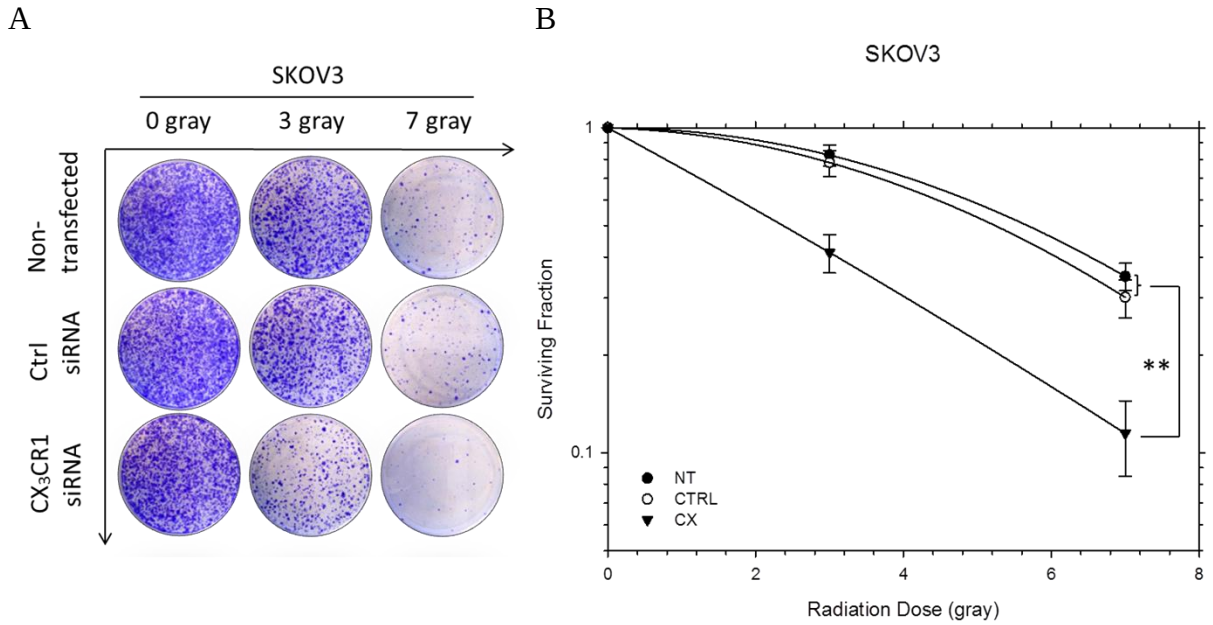

Figure 2.5 CX_3CR1 Transient Knockdown Radiosensitizes SKOV3. SKOV3 were either non-transfected or transfected with the control siRNA or CX_3CR1 siRNA. Cellular radiosensitivity was measured using clonogenic assay. A) Pictures of clonogenic assay results of SKOV3 stained with crystal violet. B) Clonogenic survival assays quantification results after transfection and administration of ionizing radiation at increasing doses from 0 gray to 7 gray. Surviving fractions for CX_3CR1 siRNA transfected SKOV3 were calculated after normalizing to the surviving fraction obtained for cells transfected with the control siRNA. Values shown represent the mean ± SD for 5 independent experiments. **$p<0.001$ according to two-way ANOVA test.

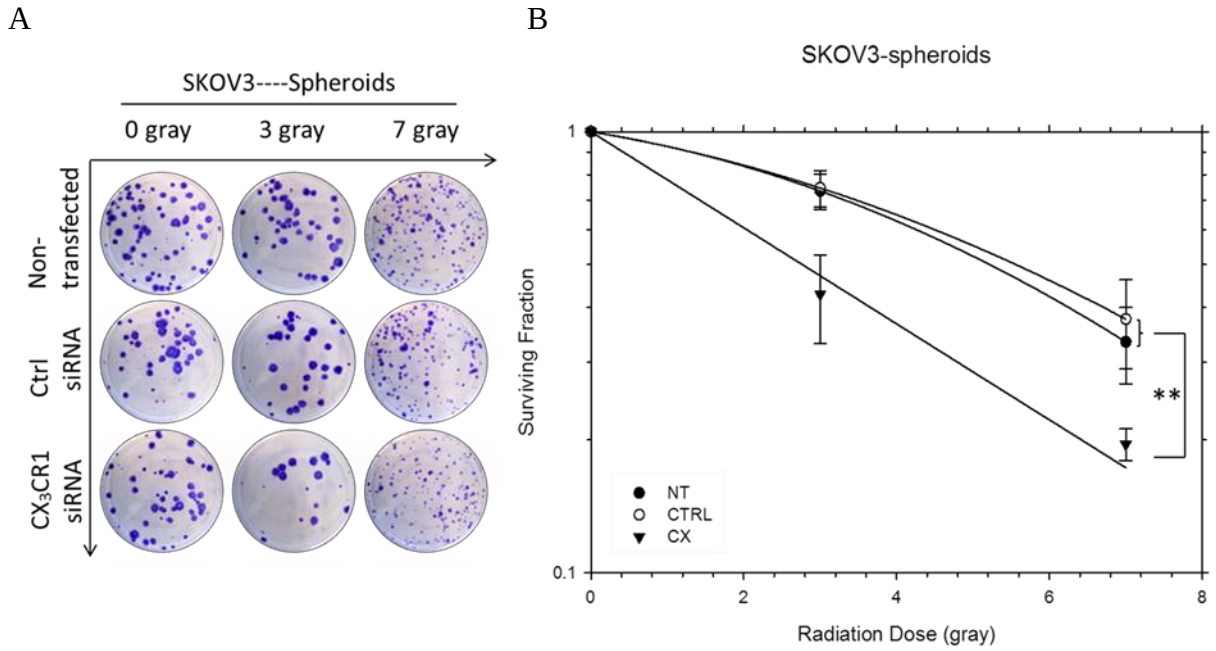

Figure 2.6 CX_3CR1 Transient Knockdown Radiosensitizes SKOV3 (spheroids). SKOV3 were either non-transfected or transfected with the control siRNA or CX_3CR1 siRNA before the formation of spheroids. Cellular radiosensitivity was measured using clonogenic assay. A) Pictures of clonogenic assay results of SKOV3 (spheroids) stained with crystal violet. B) Clonogenic survival assays quantification results after transfection and administration of ionizing radiation at increasing doses from 0 gray to 7 gray. Surviving fractions for CX_3CR1 siRNA transfected SKOV3 were calculated after normalizing to the surviving fraction obtained for cells transfected with the control siRNA. Values shown represent the mean ± SD for 5 independent experiments. **$p<0.001$ according to two-way ANOVA test.

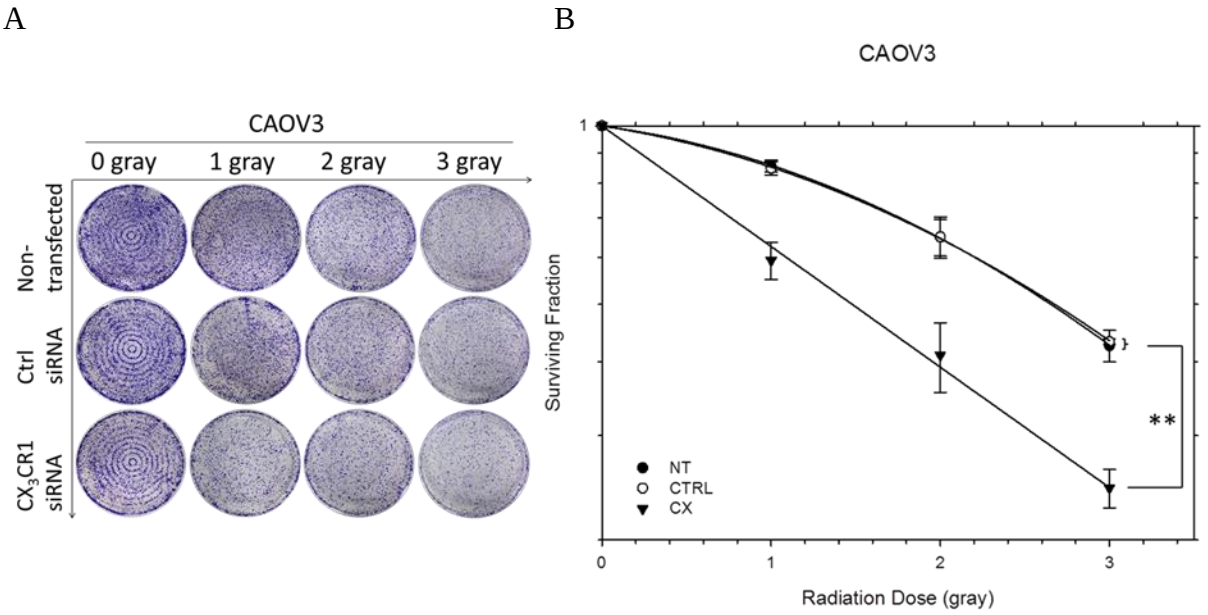

Figure 2.7 CX_3CR1 Transient Knockdown Radiosensitizes CAOV3. CAOV3 were either non-transfected or transfected with the control siRNA or CX_3CR1 siRNA. Cellular radiosensitivity was measured using clonogenic assay. A) Pictures of clonogenic assay results of CAOV3 stained with crystal violet. B) Clonogenic survival assays quantification results after transfection and administration of ionizing radiation at increasing doses from 0 gray to 3 gray. Surviving fractions for CX_3CR1 siRNA transfected CAOV3 were calculated after normalizing to the surviving fraction obtained for cells transfected with the control siRNA. Values shown represent the mean $\pm$SD for 3 independent experiments. **$p<0.001$ according to two-way ANOVA test.

A B

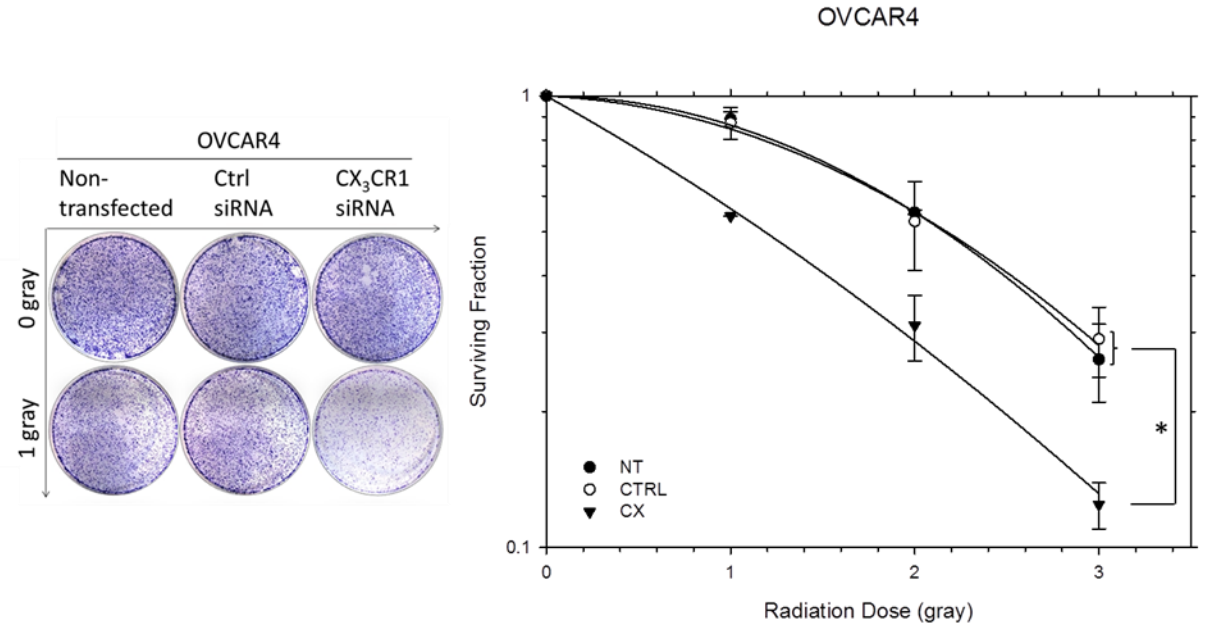

Figure 2.8 CX_3CR1 Transient Knockdown Radiosensitizes OVCAR4. OVCAR4 were either non-transfected or transfected with the control siRNA or CX_3CR1. Cellular radiosensitivity was measured using clonogenic assay. A) Pictures of clonogenic assay results of OVCAR4 stained with crystal violet. B) Clonogenic survival assays quantification results after transfection and administration of ionizing radiation at increasing doses from 0 gray to 3 gray. Surviving fractions for CX_3CR1 siRNA transfected OVCAR4 were calculated after normalizing to the surviving fraction obtained for cells transfected with the control siRNA. Values shown represent the mean ± SD for 3 independent experiments. *$p<0.05$ according to two-way ANOVA test.

Table 2.1 CX_3CR1 Transient Knockdown Radiosensitizes Epithelial Ovarian Carcinoma Cells.

Cell Line	$SF2_{control}/SF2_{CX3CR1}$	$D10_{control}/D10_{CX3CR1}$	Radiosensitization[a]
SKOV3	1.59	1.33	+
SKOV3 (spheroids)	1.38	1.2	+
CAOV3	1.65	1.11	+
OVCAR4	1.93	1.23	+

[a] Radiosensitization was scored positive (+) if the value for control/CX_3CR1 siRNA was larger than 1.1 at both 2 Gy and at 10% clonogenic cell survival.

2.3.3 Transient Downregulation of CX_3CR1 in OVSAHO

OVSAHO was originally derived from serous papillary adenocarcinoma and has a p53 mutation in the tetramerization domain (p.R342) (130). Our lab has shown that CX_3CR1 is expressed on OVSAHO, and the CX_3CR1 downregulation was determined by western blot analysis (Figure 2.9). Compared to the control siRNA transfected group, the reduction of CX_3CR1 in OVSAHO is approximately 81%.

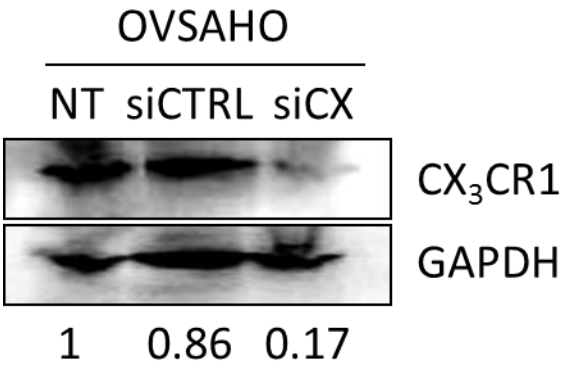

Figure 2.9 CX_3CR1 Downregulation Level in OVSAHO. Cells were collected 72 hours after transfection and CX_3CR1 expression level was detected using anti-CX_3CR1 antibodies by western blot analysis. Numbers below the bands are densitometry results. The western blot shown is the representative result from 3 independent experiments.

2.3.4 CX_3CR1 siRNA cannot Induce Radiosensitization in OVSAHO

Unlike SKOV3, CAOV3 and OVCAR4, OVSAHO has a mutation of p53 at the oligomerization domain which inhibits the interaction of p53 monomers (130, 159). As shown in Figure 2.10 and Table 2.2, CX_3CR1 has no effect on sensitizing OVSAHO to x-ray radiation as assessed by clonogenic survival assay. Therefore, the result indicated that OVSAHO cannot be radiosensitized upon CX_3CR1 downregulation.

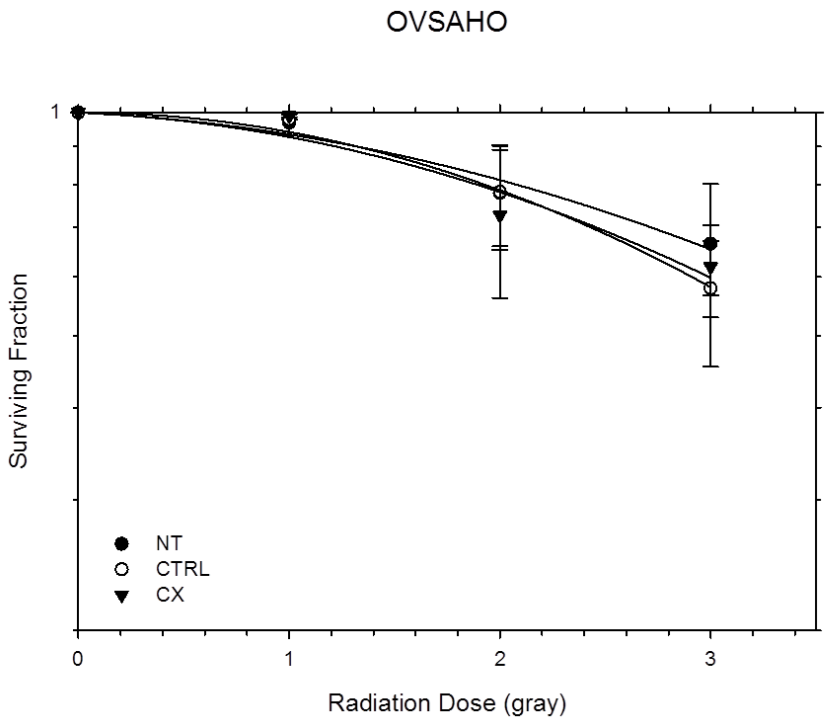

Figure 2.10 Loss of CX_3CR1 Failed to Sensitize OVSAHO to Ionizing Radiation. OVSAHO were transfected accordingly as described in Materials and Methods. Clonogenic survival assay were used to evaluate the radiosensitization level. Surviving fractions for CX_3CR1 siRNA transfected OVSAHO were calculated after normalizing to the surviving fraction obtained for cells transfected with the control siRNA. Values shown represent the mean ± SD for 3 independent experiments.

Table 2.2 CX_3CR1 Transient Knockdown Failed to Radiosensitizes OVSAHO

Cell Line	$SF2_{control}/SF2_{CX3CR1}$	$D10_{control}/D10_{CX3CR1}$	Radiosensitization
OVSAHO	1.01	0.92	-

2.3.5 Transient Downregulation of CX_3CR1 in IGROV1 and A2780

CX_3CR1 is expressed in both IGROV1 and A2780 (32). The level of CX_3CR1 downregulation by CX_3CR1 siRNA was determined by western blot analysis (Figure 2.11). Compared to the control siRNA transfected group, the reduction of CX_3CR1 in IGROV1 is approximately 58% and A2780 is approximately 59%.

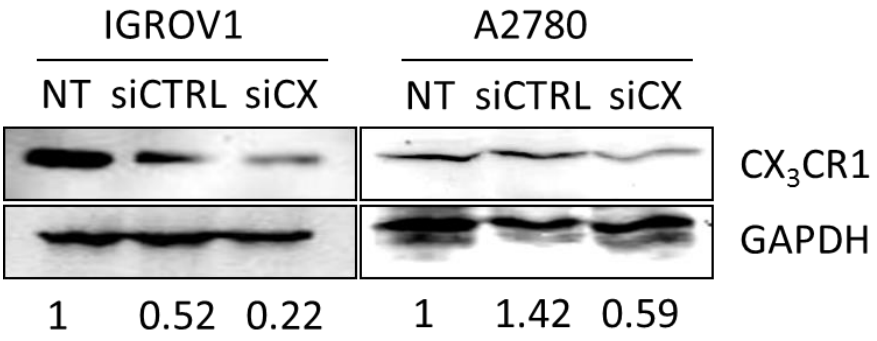

Figure 2.11 CX_3CR1 Downregulation Level in IGROV1 and A2780. Cells were collected 72 hours after transfection and CX_3CR1 was detected using anti-CX_3CR1 antibodies by western blot analysis. Numbers below the bands are densitometry results. The western blot shown is the representative result from 3 independent experiments.

2.3.6 CX_3CR1 siRNA cannot Induce Radiosensitization in P53 Wildtype Human Ovarian Cancer Cell Lines

Due to the cytoprotective role TP53 plays in mediating cell-cycle arrest, apoptosis and DNA damage repair (131), we examined the extent of CX_3CR1 inhibition-mediated radiosensitization in p53 wildtype cell lines IGROV1 and A2780 to. As shown in Figure 2.12, 2.13 and Table 2.3, CX_3CR1 downregulation failed to radiosensitize IGROV1 and A2780 as evaluated by clonogenic assays, which is in contrast to the responses of those p53 null and mutated cell lines.

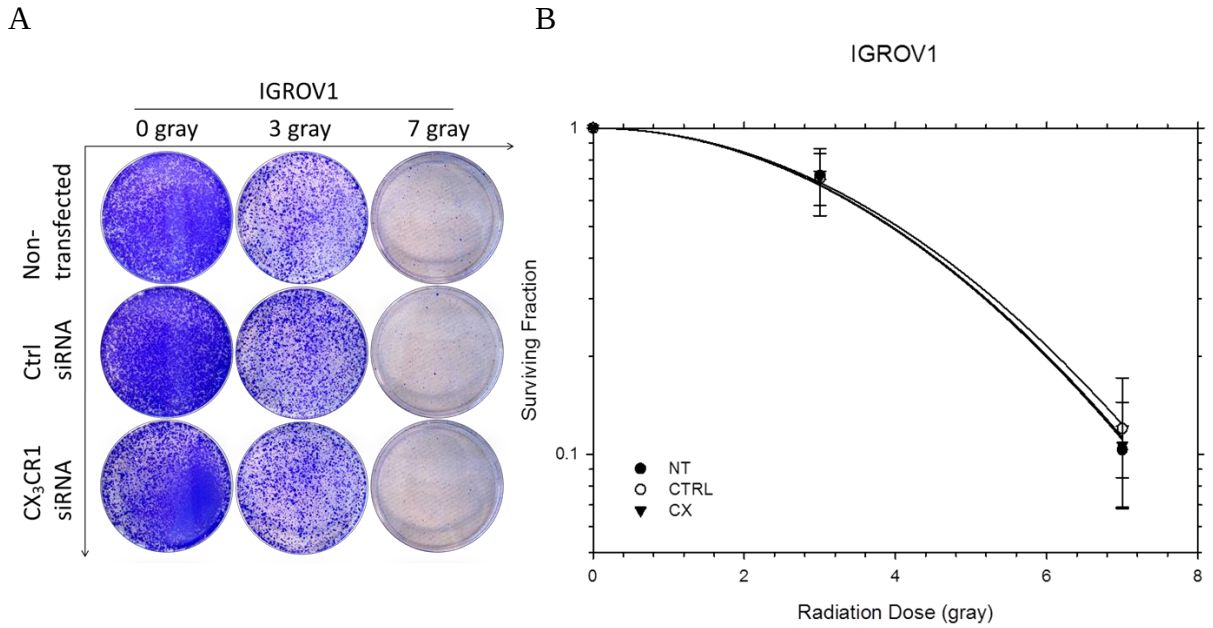

Figure 2.12 Loss of CX_3CR1 Failed in Sensitizing p53 Wildtype IGROV1 to Ionizing Radiation. IGROV1 were transfected as described in the Materials and Methods. Clonogenic survival assays were used to evaluate the radiosensitization. A) Pictures of the clonogenic assay results stained with crystal violet. B) Clonogenic survival assay were used to evaluate radiosensitization. Surviving fractions for CX_3CR1 siRNA transfected IGROV1 were calculated after normalizing to the surviving fraction obtained for cells transfected with the control siRNA. Values shown represent the mean $\pm$ SD for 3 independent experiments.

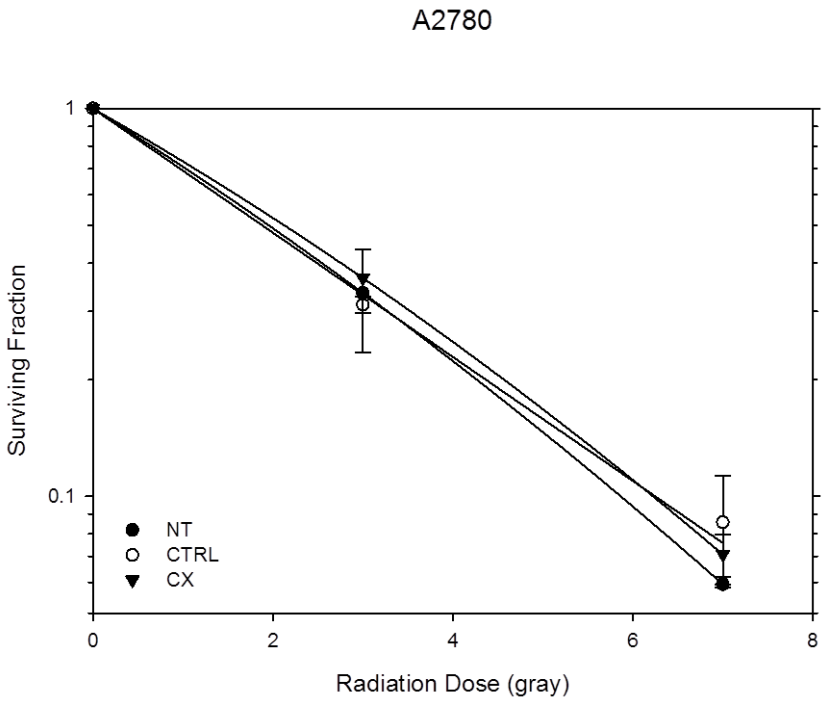

Figure 2.13 Loss of CX_3CR1 Failed in Sensitizing p53 Wildtype A2780 to Ionizing Radiation. A2780 were transfected as described in the Materials and Methods. Clonogenic survival assays were used to evaluate the radiosensitization level. Surviving fractions for CX_3CR1 siRNA transfected A2780 were calculated after normalizing to the surviving fraction obtained for cells transfected with the control siRNA. Values shown represent the mean ± SD for 3 independent experiments.

Table 2.3 CX_3CR1 Transient Knockdown Failed to Radiosensitizes IGROV1 and A2780

Cell Line	$SF2_{control}/SF2_{CX3CR1}$	$D10_{control}/D10_{CX3CR1}$	Radiosensitization
IGROV1	1.01	1.02	-
A2780	0.92	1.003	-

2.3.7 Stable Downregulation or Upregulation of CX_3CR1 in SKOV3

The level of CX_3CR1 expression in different stable clones were determined by the quantification of western blots (Figure 2.14). Clone1 (CX1) and clone6 (CX6) are two representative clones

selected with different levels of CX_3CR1 downregulation. Compared to the cells transfected with pVector clone, the increase of CX_3CR1 is approximately 129% in overexpressor (OE), and the reduction is approximately 95% in CX1 and 98% in CX6, respectively. Notably, stable transfection changed the cellular proliferation rate, with the doubling time approximately 18 hours in OE, 24 hours in pVector, 36 hours in CX1 and 48 hours in CX6.

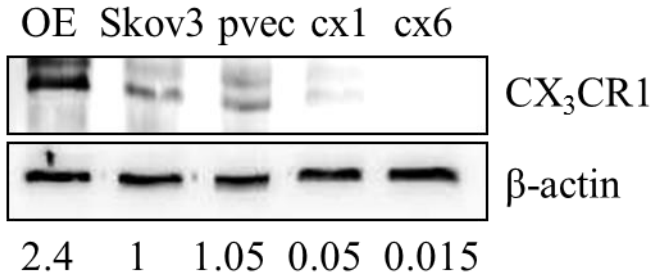

Figure 2.14 CX_3CR1 Levels in Stable Clones. Protein level of CX_3CR1 in OE, pVector, parental SKOV3, CX1 and CX6. The establishment of these clones were described in Materials and Methods. (Clones established by Hilal Gurler) (OE [overexpressor]: SKOV3 transfected with CX_3CR1 cDNA clones; pvec[pVector]: SKOV3 transfected with PRS vector shRNA; CX1, CX6: SKOV3 transfected with CX_3CR1 shRNA plasmids) CX_3CR1 was detected using anti-CX_3CR1 antibodies by Western Blot analysis. Numbers below the bands are densitometry results. (Western Blot done by Hilal Gurler)

2.3.8 Stable Downregulation or Upregulation of CX_3CR1 cannot Change Ovarian Cancer Cells' Sensitivity to X-Ray Radiation

Based on the result that transient downregulation of CX_3CR1 promotes radiosensitivity in EOC cells, we examined whether stable increase and decrease of CX_3CR1 could affect cellular radiosensitivity. After the establishment of the clones, cells were subjected to x-ray radiation,

followed by clonogenic survival assay. Due to the changes in growth rate, fast growing cells become more sensitive to radiation while slow growing cells are more resistant to radiation. The difference in initial intrinsic radiosensitivity affects the accurate evaluation of cellular radiosensitivity changed upon CX_3CR1. As shown in Figure 2.15, increased expression of CX_3CR1 failed to induce radioresistance while downregulation of CX_3CR1 failed to induce radiosensitization. Specifically, CX_3CR1 overexpression accelerates cellular proliferation, therefore they become more sensitive to radiation, which complicates the possible evolution of radioresistance induced by CX_3CR1 overexpression. Meanwhile, CX_3CR1 stable downregulation decelerates cell growth, thus they become more resistant to radiation, which complicates the possible evolution of radiosensitization caused by loss of CX_3CR1.

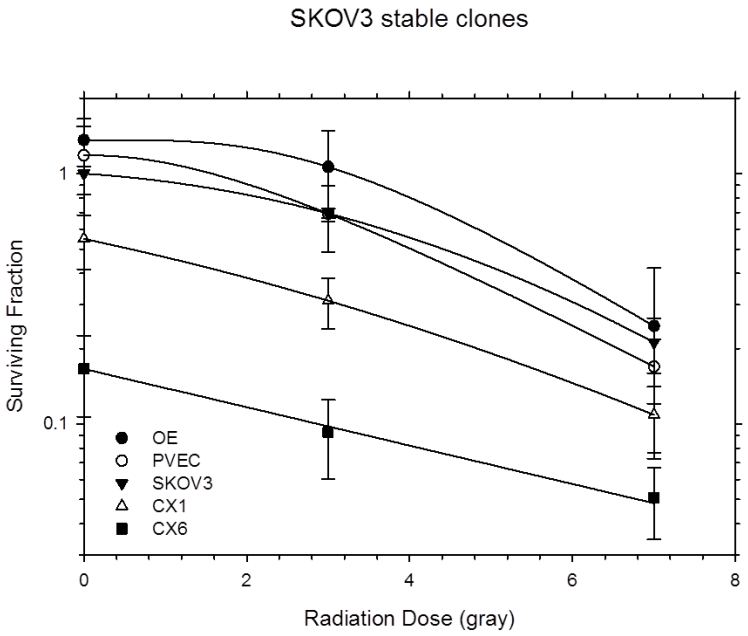

Figure 2.15 Stable Alteration of CX_3CR1 in SKOV3 Failed to Affect Cellular Radiosensitivity. Stable clones from SKOV3 were established as described in Materials and Methods. Clonogenic survival assay were used to evaluate radiosensitivity. Values shown represent the mean ± SD for 3 independent experiments.

2.4 Discussion

The majority of EOC patients respond to paclitaxel and platinum-based adjuvant chemotherapy initially, but most of them, especially patients with advanced stage disease, develop recurrent EOC that were platinum-refractory (132). Therefore, it is important to adjust the treatment of advanced stage EOC patients that were resistant to platinum-based chemotherapy. Radiation therapy has survival advantages over chemotherapy, especially in patients with minimal residual disease (133, 134). However, radiation therapy is not commonly used for the therapy against EOC due to severe dose-related toxicities, such as small bowel obstruction (135). Thus, modification to the radiation treatment needs to be investigated to decrease the toxicity while still

maintaining the therapeutic efficacy. There are multiple ways to modify radiation treatment, including the development of novel chemotherapeutic drugs as radiation sensitizing agents (136) and the improvement of the radiation delivery technology (137, 138, 139).

Our group has been interested in chemokines and chemokine receptors and their role in regulating ovarian cancer metastasis. CX_3CR1 is expressed in EOC cells and mediates their motility and adhesion to peritoneal mesothelial cells (140). The lymphotactin receptor XCR1 is also expressed on EOC cells and contributes to cell migration and proliferation (141). Due to the possible role that chemokine signaling plays in changing radiosensitivity (142), we hypothesized that CX_3CR1 might also participate in regulating radiosensitivity. In order to test this, our study began with transiently knocking down CX_3CR1 with specific siRNAs in multiple EOC cell lines and evaluating survival by clonogenic assay. As shown in Figure 2.4-2.8 and Table 2.1, CX_3CR1 is capable of affecting EOC cells' sensitivity to x-ray radiation. Moreover, p53 status may play an important role in CX_3CR1-dependent radiosensitization, due to loss of CX_3CR1 was unable to increase OVSAHO cells' sensitivity to ionizing radiation. Furthermore, cellular sensitivity was also not changed in p53 wild-type cells. This phenomenon possibly resulted from the cytoprotective action of p53. When cells are exposed to ionizing radiation and other DNA damaging agents, activated p53 can induce cell cycle arrest at G_1 phase to repair the damaged DNA (143). Therefore, in cell lines with defective p53, their ability to repair damaged DNA completely relies on the G_2 checkpoint. If the G_2 checkpoint can be abrogated by other modifications, which in our case by inhibiting CX_3CR1, these cancer cells can be significantly sensitized when exposed to ionizing radiation. Similarly, our data also indicated that the downregulation of CX_3CR1 could selectively damage tumor cells while leaving the normal cells

intact. The G_1 checkpoint activation in normal cells by activating p53 can protect them from ionizing radiation-induced DNA damage. Our observations are consistent with previous reports that p53 mutated cell lines can be selectively radiosensitized. Vance *et al*. reported that the combined inhibition of PARP1 and Chk1 can radiosensitize p53 mutant pancreatic cancer cells (144). Powell *et al*. described that caffeine can selectively sensitize p53 (-) cells to DNA damaging agents (145). Lee YJ *et al.* demonstrated that oleamide can enhance radiosensitization of p53 mutant cells (146).

P53 can regulate and be regulated by a complex network of proteins, mRNAs and microRNAs. The differences in the location of the p53 mutation point can affect the p53-related network, so that the degree of cellular radiosensitivity caused by CX_3CR1 downregulation would vary (147). For example, missense mutations in the DNA-binding domain can directly affect the proper folding of loops and helixes that form the DNA-binding interface and therefore disrupt the following trans-activating of some genes that may correlate with CX_3CR1-dependent radiosensitization. However, mutations in the tetramerization domain may lead to no effect on DNA-binding and thus trans-activate some other genes that may be related to radioresistance (148). Therefore, it is important to determine the p53 mutation and examine the regulation of overall transcriptional control in individuals before the designation of an overall therapeutic approach (149).

Due to the fact that the downregulation caused by siRNA transfection is only transient, the protein level would finally increase after several days. We next investigated if we could also observe a similar effect by stably increasing and decreasing CX_3CR1 by introducing shRNA. As

shown in Figure 2.15, the shRNA transfection failed to change the overall cellular sensitivity to radiation, as the shRNA integration into genome alone changed cellular proliferation rate, which compensated the possible change in sensitivity brought by CX_3CR1. Radiation is more effective in fast growing cells compared to slower growing cells, and the way radiation affects cellular reproductive integrity is by targeting DNA backbone and thereby causes damage. In the fast-duplicating cells, they tend to accumulate DNA damage faster and they have less time to repair the damaged DNA as compared to the cells with low reproductive efficiency (121). Therefore, the CX_3CR1 shRNA transfection, which might sensitize the cells to radiation, failed eventually due to the observation that these cells divided slower compared to the control shRNA transfected cells. So shRNA transfection, in our case, is not an appropriate approach to evaluate how stable CX_3CR1 expression alteration could affect overall cellular radiosensitivity.

One of the possible reasons leads to the inaccurate evaluation of the radiosensitization in the stable clones is the off-target effects caused by shRNA transfection, which might result from the unintended hybridization between the RNAi molecules and the non-target transcripts. These effects usually arise from a perfect sequence complementarity between the “seed” hexamers at the 5’ end of the antisense strand and a target site in the 3’UTR of a transcript (150). The unpredictable off-target effects might also change the growth-related gene expression and therefore lead to the change in intrinsic radiosensitivity.

Recently, site-specific genomic editing technology has been evolved into a new era with the development of a novel tool called Clustered, Regularly Interspaced Short Palindromic Repeat Associated (CRISPR-Cas) proteins (151, 152). This technique enables the specific knockout of

any human loci and knockin a functional cassette containing the clone selection gene such as GFP and puromycin resistant gene. There are two distinct components in this system: the Cas nuclease Cas9 (a double-stranded DNA endonuclease) and a guide RNA with target specificity. The base-pairing between the guide RNA and the complementary target sequence in the genomic DNA enable the recruitment of the gRNA/cas9 complex. In order to activate the endonuclease activity, the target sequence must follow by a Protospacer Adjacent Motif (PAM) sequence. Then the activated endonuclease would cut the double stranded DNA and cause a DNA double strand break. There are usually two mechanisms to repair the DSB, homologous recombination (HR) and non-homologous end joining (NHEJ). The NHEJ repair pathway which is an error-prone repair pathway (will be discussed in detail in chapter 3) would result in deletions, and HR is a sequence predictable repair pathway (will also be discussed in detail in chapter 3) that requires the presence of a repair template. Currently we have the CX_3CR1 sequence cloned in pCas Guide Vector and a non-coding template DNA containing homologous arms and the puromycin-resistant gene containing cassette. The co-transfection of these two will allow the specific knockout of CX_3CR1 while incorporating the selective cassette. In the future, after we obtain these CX_3CR1-specific knockout clones, the radiosensitization in stable clones will be re-conducted and re-evaluated.

2.5 Conclusion

Collectively, the results demonstrated that transient downregulation of CX_3CR1 can effectively sensitize the p53 mutant and null EOC cells to radiation as evaluated by *in vitro* clonogenic assay. The combination of radiation and CX_3CR1 knockdown provides a novel approach against EOC.

CHAPTER 3.

TRANSIENT DOWNREGULATION OF FRACTALKINE RECEPTOR IN EPITHELIAL OVARIAN CANCER CELL LINES LEAD TO LESS DNA DAMAGE REPAIR AND ACCUMULATED DNA DOUBLE STRAND BREAK

3.1 Introduction

DNA is the principal target for radiation-induced damage (161). The double helical DNA (deoxyribonucleic acid) consists of two strands, and the backbone of each strand consists of deoxyribose and phosphate groups. There are four bases attached to this backbone: thymine (T), cytosine (C), adenine (A) and guanine (G). Based on the structural similarity, thymine and cytosine belong to pyrimidines, adenine and guanine belong to purines. The two complementary strands are held together by hydrogen bonds: adenine pairs with thymine and guanine pairs with cytosine (183). When cells are exposed to ionizing radiation, the damage to DNA can either be direct or indirect. Direct DNA damage is dominant when the source of radiation has high linear energy transfer. When sparsely ionizing radiations, such as x-ray, is the source of radiation, the damage is usually indirect, that is, the radiation interacts with the water molecules in the cell to produce free radicals such as hydrogen (H+) and hydroxyls (OH-) ions. These ions can then be turned into other substances such as hydrogen peroxide (H_2O_2) to damage the DNA and result in single-strand and double-strand breaks (161).

In order to repair ionizing radiation-induced damage, there are specialized pathways developed in cells to sense, respond and repair the damaged DNA. Base excision repair (BER) repair pathway is activated when a single nucleotide base is damaged (Figure 3.1). A DNA glycosylase

would first cleave the bond between the damaged base and ribose, and thus remove the base. This step is followed by the removal of the ribose phosphate by the action of an apurinic endonuclease I (APE1), and then followed by the insertion of the correct nucleotide by DNA polymerase β (Polβ). Finally, x-ray repair cross-complementing group 1 (XRCC1) would mediate the ligation by forming a heterodimer with DNA ligase III (LIG3). LIG3 would then connect the repaired nucleotide to the backbone (161, 162).

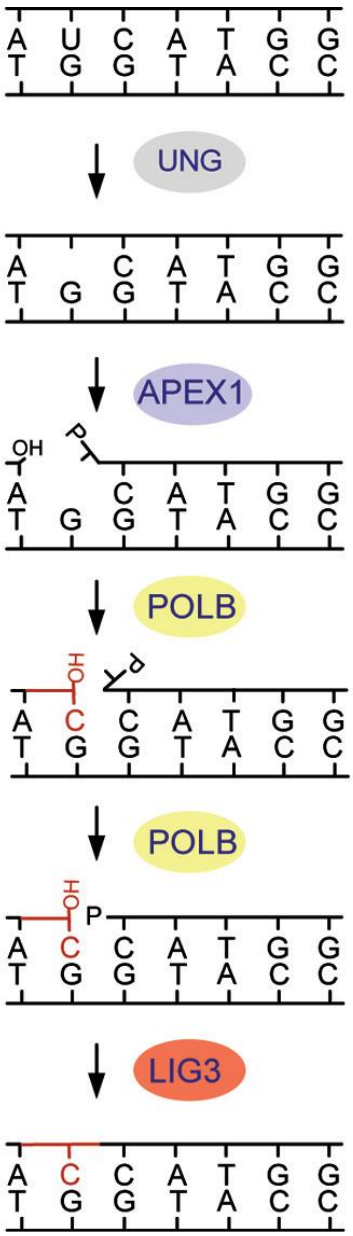

Figure 3.1 The core BER pathway. In this pathway, the UNG glycosylase catalyzes the excision of the damaged uracil base, creating an abasic (AP) site. The APEX1 endonuclease catalyzes the incision of the DNA backbone 5' to the AP site. POLB displaces the AP site and polymerizes DNA to fill in the gap. POLB then catalyzes the removal of the displaced AP site. Finally, LIG3 catalyzes the formation of a phosphodiester bond, completing the repair pathway. Reprinted with permission from *Cellular and Molecular Life Sciences*, 2009, Volume 66, Issue 6: 981-993. Copyright (2009), Birkhauser Verlag, Basel.

Nucleotide excision repair (NER) repairs damage such as bulky adducts in the DNA and the damage caused by UV radiation (Figure 3.2). NER can be further divided into two pathways: global genomic NER (GGR) and transcription-coupled repair (TCR). While the former one is capable of repairing damage that is genome-wide, the latter one can only repair the genes that are actively transcribed. The other difference between the two pathways is the damage recognition step. In GGR, XPC-XPE protein complexes are recruited at the damaged site while in TCR, RNA polymerase I/II together with CSA, CSB gets recruited at the damaged site to prevent the further transcription of the genome. There are over 20 proteins involved in the pathway. Following the damage recognition step, TFIIH complex helicase is recruited to unwind the DNA and facilitates the excised oligomer to release. Eventually, the resulting gap is filled with the assistance of Polymerase-PCNA complex followed by the ligation of the strand (161, 163). Since NER is a dominant mechanism for UV induced DNA damage, mutations in NER-related gene have little contribution to cellular radiosensitivity.

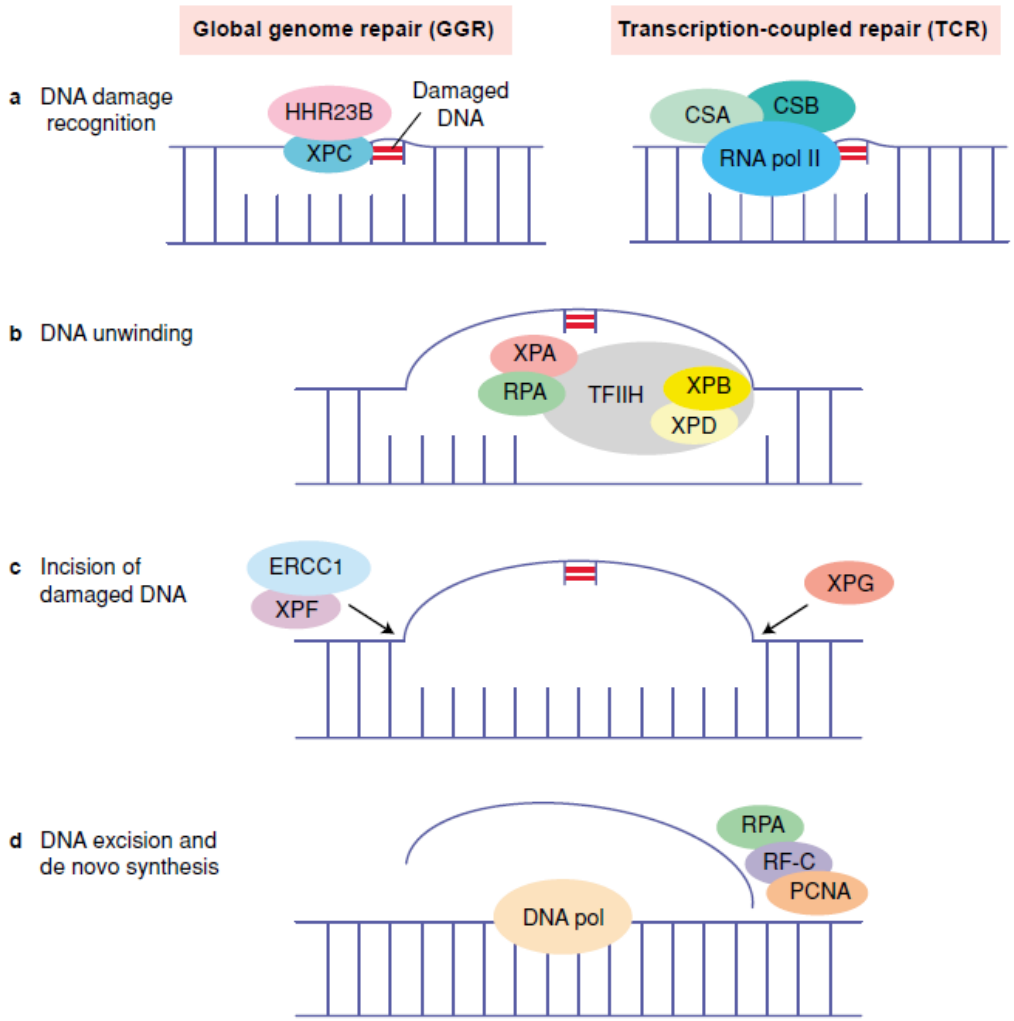

Figure 3.2 Proposed model for mammalian nucleotide excision repair (NER). NER consists of two sub-pathways: global genome repair (GGR) and transcription-coupled repair (TCR). (a) The two sub-pathways differ only in the first step, DNA damage recognition. In GGR, the protein complex XPC/HHR23B binds to the damaged DNA site, recruiting the entire repair protein apparatus to the injury. By contrast, in TCR, a stalled RNA polymerase II fulfils this function at the site of the DNA lesion, facilitated by the Cockayne syndrome proteins CSA and CSB. (b) In the second step, DNA unwinding, the lesions are opened by the concerted action of XPA, replication protein A (RPA), and the bi-directional XPB/XPD helicase subunits of the transcription factor IIH (TFIIH) complex. (c) During incision of the damaged DNA, the exchange repair cross complementing (ERCC1)/XPF complex cuts at the single-strand to double-strand transition on the 5' side of the damage, and XPG cuts at the 3' side of the open complex. (d) Finally, DNA excision and de novo synthesis is accomplished by mammalian DNA replication factors such as the heterotrimeric replication protein A (RPA), replication factor C (RF-C), proliferating cell nuclear antigen (PCNA), and DNA polymerase δ and ε. The reaction is completed by ligation of the newly synthesized DNA. Reprinted with permission from *Expert Reviews in Molecular Medicine*, 2002, Volume 4: 1-22. Copyright (2002), Cambridge University Press.

In eukaryotic cells, there are two mechanisms, homologous recombination (HR) and non-homologous end joining (NHEJ), to repair DNA DSBs. The homologous recombination is a less used mechanism to repair the damaged DNA, because its activation requires the presence of sister chromatid to be used as a template and when the cell is in late S/G_2 phase. For all the other time points in the cell cycle together with S/G_2 phase, NHEJ is used to repair the damaged DNA. (Figure 3.3) Classical NHEJ is initiated with the break ends recognized by Ku70/80 heterodimer, followed by the recruitment and auto-phosphorylation of DNA-dependent protein kinase catalytic subunit (DNA-PKcs). The Ku/DNA-PKcs complex can hold the two DNA DSB ends in close proximity and recruit Artemis, which is an end-processing enzyme with endonuclease activity. The phosphorylated and activated Artemis then helps to recruit XRCC4 (x-ray repair cross-complementing protein 4) – XLF (XRCC4-like factor) – LIG4 (DNA ligase 4) complexes for DNA strand ligation. Besides the classical NHEJ, alternative-NHEJ (alt-NHEJ) is also used to repair the damaged DNA. Unlike classic NHEJ, alt-NHEJ is independent of the core classic NHEJ components, such as Ku80 and XRCC4. Alt-NHEJ is initiated with the involvement of PARP1, and then Mre11 and CtIP are recruited to create a single-strand DNA resection. Most of these single-strand DNA has short complementary microhomologies (5-25 nucleotides) that can conduct the strand annealing process. Therefore, alt-NHEJ sometimes can be also called as microhomology-mediated end joining (MMEJ). Eventually, the break ends would be joined together by XRCC1 and ligase III. This is an exclusively mutagenic process with long strand deletions (161, 164, 165).

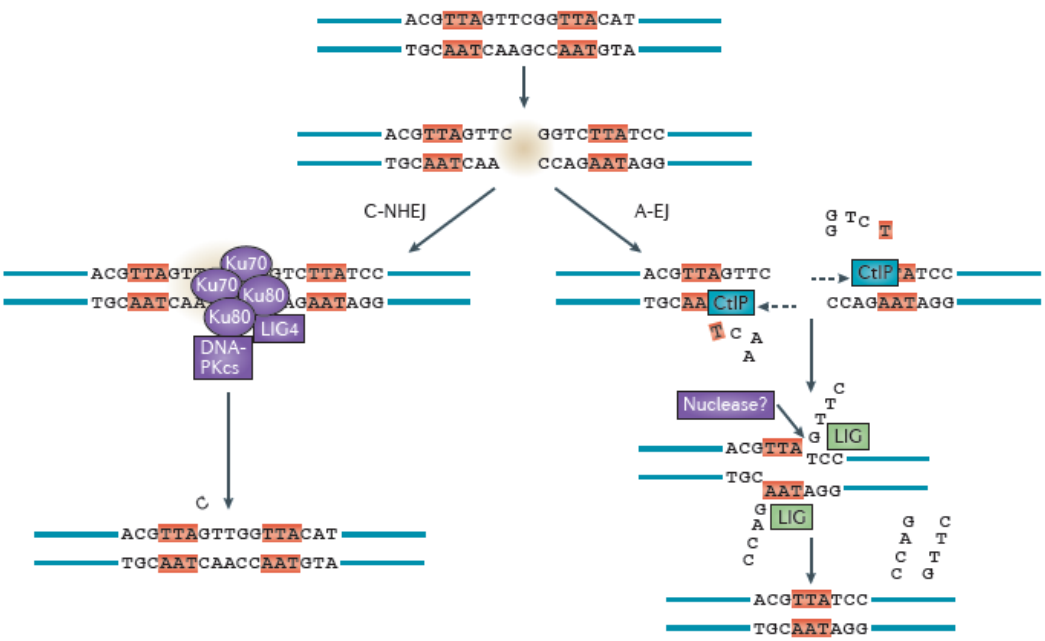

Figure 3.3 Steps in classical and alternative end-joining. On the appearance of a DNA double-strand break, two pathways can be active. Classical non-homologous end-joining (C-NHEJ) involves the binding of Ku70–Ku80 to the DNA break, followed by the recruitment of DNA-dependent protein kinase catalytic subunit (DNA-PKcs) and several other factors that mediate blunt-end ligation of the break by DNA ligase 4 (LIG4). This process has no sequence requirements and may cause small-scale mutation, such as the addition or the deletion of a small number of nucleotides at the break junction. Alternative end-joining (A-EJ) involves exonucleolytic processing of the double-strand break to reveal stretches of potentially complementary sequence (microhomology; indicated in red) on either side of the break. This resection process may be mediated by the exonuclease CtBP-interacting protein (CtIP). Following base pairing at regions of microhomology, the ends are joined by an undetermined ligase enzyme (LIG). Reprinted with permission from *Nature Reviews Cancer*, 2013, 13: 443-453. Copyright (2013), Nature Publishing Group.

When the undamaged sister chromatid is present, DSBs can be repaired by homologous recombination pathway (Figure 3.4). After ionizing radiation exposure, the initial step in HR is the damage recognition by the MRE11-RAD50-NBS1 (MRN) complex, which has nuclease

activities (endonuclease and exonuclease) that can help process the DNA end resection. Additionally, this nuclease activity is required for ATM activation (ATR activation if the damage is caused by UV radiation and replication stress), which can then activate numerous downstream signaling proteins, such as chk2 (chk1 when ATR is phosphorylated), p53, etc. The formed 3' DNA single strand tails are then coated by RPA which is a heterotrimeric complex (RPA1, RPA2, RPA3). Then, specific HR proteins are recruited to the RPA-coated single-strand overhangs, such as BRCA1/2 and Rad51. Rad51 is a crucial protein due to its role in mediating strand invasion of the single strand DNA (ssDNA) 3' overhang into the homologous sequence of the sister chromatid and facilitating the formation of D-loop. The invading ssDNA could be extended to facilitate the formation of the Holliday junction (HJ). The resolution of the HJ can occur in two ways: crossover and non-crossover models, depend on the recruited proteins to fill the gap and finish the repair (161, 166, 167, 168). In addition, at the beginning of the process, histone variant H2A.X is phosphorylated by ATM at Ser139, lead to the formation of γH2A.X. Phosphorylated H2A.X can then promote the recruitment of its decoder, MDC1 (mediator of DNA damage checkpoint protein 1) and its counterpart (169). Once bound to γH2A.X, MDC1 in turn recruits more DNA damage repair related proteins, such as the downstream signaling proteins and MRN complexes based on the MDC1-NBS1 interaction. This would allow the further phosphorylation of ATM and lead to the amplification and foci formation of γH2A.X. Once the damaged DNA gets repaired, several γH2A.X phosphatases, which can dephosphorylate γH2A.X, are recruited and terminate the signaling. Therefore, the formation of γH2A.X foci is considered as a marker of DSB formation and repair (169, 170).

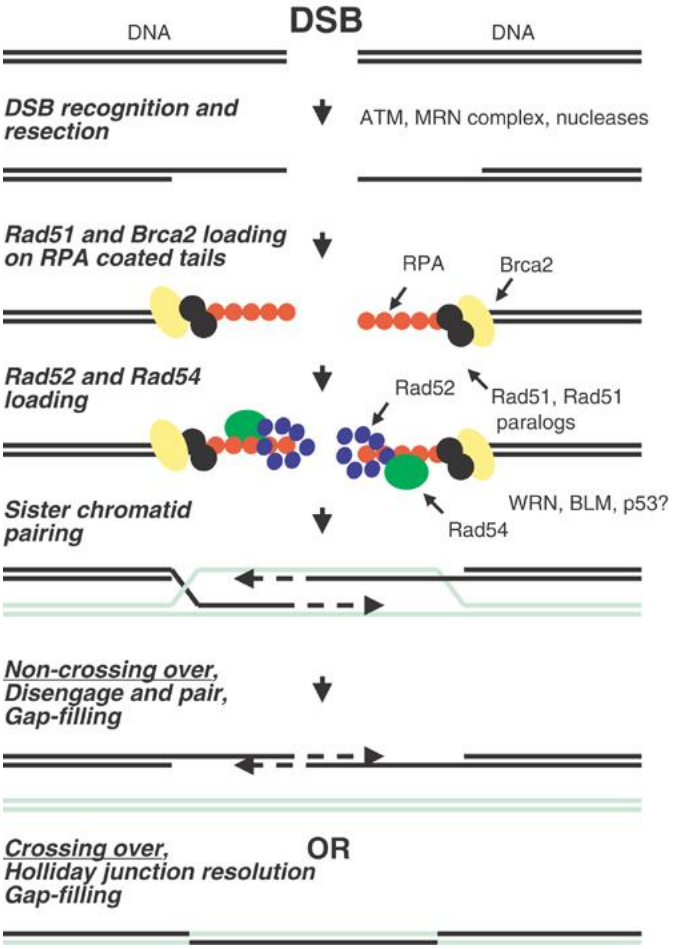

Figure 3.4 Homologous recombination. In the earliest stages of DSB repair by HRR, ATM senses and perhaps binds to the DSB, and phosphorylates H2AX, which would then attract BRCA1 and NBS1, also phosphorylated by ATM. BRCA1 may help serve as an anchor and coordinator of the repair events that follow. The MRN complex, most likely with the help of other nucleases, resects the DNA to provide ssDNA overhangs necessary for DNA pairing and strand exchange. Since the MRN complex is only known to possess 3' to 5' but not 5' to 3' exonuclease activity, other nucleases might be involved. The 5' to 3' resection shown in the figure is based on the yeast HRR model, in which 3' overhangs are essential intermediates. BRCA2, attracted to the DSB by BRCA1, facilitates the loading of RAD51 onto RPA-coated DNA overhangs with the help of RAD51 paralogs that in turn attract RAD52 and RAD54, perhaps with the help of the BLM and/or WRN helicases. The tumor suppressor P53, known to interact with BRCA1, RAD51, BLM and WRN, is also likely found in this DNA–protein complex. BLM and WRN interact with Holliday junctions. From this point, there are two possibilities to finish HRR: (1) either by non-crossing-over in which case the Holliday junctions disengage and DNA strands pair followed by gap filling, or (2) by a crossing-over resulting from Holliday junction resolution and gap filling. It is not known as to which DNA polymerase and ligase are involved in the polymerization and ligation steps. Reprinted with permission from *Oncogene*, 2003, 22: 5792-5812. Copyright (2003), Nature Publishing Group.

Many tumors harbor mutations in DNA damage repair related genes, while in normal cells, these genes are functional and redundant, providing the rationale that targeting the remaining DNA damage repair pathways in the tumor cells is a promising approach for the selective radiosensitization. For example, most high grade serous ovarian carcinomas are associated with BRCA mutation, 2% of the cases have an ATM/ATR mutation and 3% of them harbor a Rad51c mutation. Targeting the single strand break repair pathway using poly (ADP-ribose) polymerase (PARP) inhibitors can effectively sensitize tumors with mutations in DNA double strand repair related genes to ionizing radiation (171). PARP1 can be rapidly recruited to the damaged DNA and facilitate the formation of poly (ADP) ribose (pADPr) by transferring ADP-ribose subunits from NAD+ to acceptor proteins. pADPr can then recruit XRCC1, which is an important protein in base excision repair. Therefore, PARP inhibition may lead to inefficient DNA single-strand break repair and also increase DSB (172, 173). Since BRCA1/2 functions are required for homologous recombination, which is an error-free damage repair pathway, tumor cells with BRCA1/2 mutations are more susceptible to ionizing radiation when treated with PARP inhibitor compared to normal tissues. With the same concept, genes that participate in DNA damage repair pathway are the promising targets for radiosensitization. Moreover, instead of using PARP inhibitors only in patients with BRCA abnormalities, targeting both PARP and the proteins that can regulate DNA DSB repair potentially benefits more patients.

3.2 Materials and Methods

3.2.1 Materials

Antibodies used in this research are: p-ATM (Santa Cruz Biotechnology, sc-47739, 1:50 for immunofluorescence staining; Abcam, ab81292, 1:5000 for western blot), p-Chk2 (Cell Signaling Technology, #2197, 1:1000), total Chk2 (Santa Cruz Biotechnology, sc-5278, 1:200), α-tubulin (University of Iowa, AA4.3, 1:200), β-tubulin (University of Iowa, E7, 1:200), DNA-PKcs (Abcam, ab32566, 1:1000), p-DNA-PKcs (phospho T2609) (Abcam, ab18356, 1:500), total ATM (Abcam, ab78, 1:2000), p-Chk1 (Cell Signaling Technology, #8191, 1:1000), total Chk1 (Cell Signaling Technology, #2360), GAPDH (Santa Cruz Biotechnology, sc-137179, 1:200), γH2A.X (Abcam, ab18311, 1:50 for immunofluorescence staining; Santa Cruz Biotechnology, sc-101696, 1:200 for western blot), anti-rabbit IgG, HRP-linked antibody (Cell Signaling Technology, 1:1000-1:5000), anti-mouse IgG, HRP-linked antibody (Santa Cruz Biotechnology, sc-2005, 1:500-1:3000), Alexa Fluor 488 goat anti mouse IgG (green) (Life Technologies, A11029), Alexa Fluor 546 goat anti rabbit IgG (red) (Life Technologies, A11035), DAPI (Life Technologies), ATM kinase inhibitor (Santa Cruz Biotechnology, sc-202963), Olaparib (Selleckchem), ECL reagents were purchased from GE Healthcare and Thermo Scientific. DMSO (Sigma, D4540), 4% paraformaldehyde (Santa Cruz Biotechnology, sc-281392), Triton X-100 (Sigma, T8787), goat serum (GIBCO, 16210-064), ProLong Gold antifade reagent (Life Technologies, P36930), Poly-D-Lysine (MP Biomedicals, 102694), collagen (Corning, Ref354236).

3.2.2 Western Blotting

Cells were harvested and lysed in RIPA buffer (1.25ml 1M Tris buffer, pH7.4, 7.5ml 1M NaCl, 0.5ml NP-40, 0.5g Sodium Deoxycholate, 0.5ml SDS, 5 tablets of complete mini EDTA-free phosphatase inhibitor, protease inhibitor). Same amount of protein separated by SDS-PAGE

were electro-transferred onto PVDF membranes, with background reduction using 5% BSA (w/v) at room temperature for 60 minutes (or without blocking, but immerse the membrane in pure methanol for 10 seconds and dry on filter paper for 15 minutes), and incubated with primary antibodies at 4 ℃ overnight. After incubation with secondary antibody at room temperature for 2 hours, the membranes were developed with enhanced chemiluminescence (ECL) reagents.

3.2.3 Immunofluorescence Staining

Cells were seeded on coverslips, followed by transfection and radiation. Then cells were fixed with 4% PFA. Before blocking with 5% BSA, the samples were permeabilized using 0.1% Triton X-100, and stained with primary antibody in 2% goat serum at room temperature for 2 hours, followed by incubation with secondary antibody in 2% goat serum at room temperature in dark for 1 hour, and DAPI incubation for 10 minutes. Slides were mounted using ProLong Gold antifade reagent, and images were taken with a Carl Zeiss microscope using an AxioCam camera. Images were taken with x 50 (numerical aperture, 0.75) objectives. Monochrome pictures taken with DAPI, GFP, and DsRed filter sets were merged using the AxioVision software. The exposures were identical among each group.

3.2.4 Cellular Colony Formation Assay

Epithelial Ovarian Carcinoma cells were seeded in 6-well plates and subjected to transfection, ATM inhibitor (KU55933, 5 μM) and PARP inhibitor (Olaparib, 5 μM) treatment and radiation. After the cells were seeded onto p100 cell culture plates, the media (DMSO/KU55933/Olaparib containing) were changed every two days, and the colonies were quantified at day 14 after staining with 0.05% crystal violet, and the survival curves were plotted using SigmaPlot.

3.2.5 Statistical Analysis

The Student *t* test was performed by Excel and two-way ANOVA test was performed using Sigmaplot. The results represent the mean of at least triplicate experiments with error bars corresponding to standard deviation. For each test, p values of <0.05 were considered significant.

3.3 Results

3.3.1 Loss of CX_3CR1 Lead to Less DNA Damage Repair

Since the DNA damage response signaling plays a core role after cells exposed to ionizing radiation, we investigated whether CX_3CR1 modulates the DNA damage response by looking at the phosphorylation status of ATM, DNA-PKcs, Chk1 and Chk2. To test this, SKOV3, CAOV3, and OVCAR4 cells were either non-transfected or subjected to CX_3CR1 siRNA or the control siRNA followed by ionizing radiation, and cells were either prepared for immunofluorescence staining or western blot. S1981 of ATM, T2609 of DNA-PKcs, S317 of Chk1, and T68 of Chk2 are well-established radiation-induced auto-phosphorylation sites. Whereas all three cell lines showed an increase phosphorylation level of these DNA damage repair proteins after exposure to ionizing radiation, upon CX_3CR1 downregulation, the DDR protein activation was impaired as shown in Figure 3.5 and 3.6, with a reduced number and decreased intensity of p-ATM foci and in Figure 3.7-3.9 as indicated by western blot and the quantitative analysis. Therefore, CX_3CR1 dependent DNA damage repair response impairment is one of the mechanisms that contributes to radiosensitization.

A

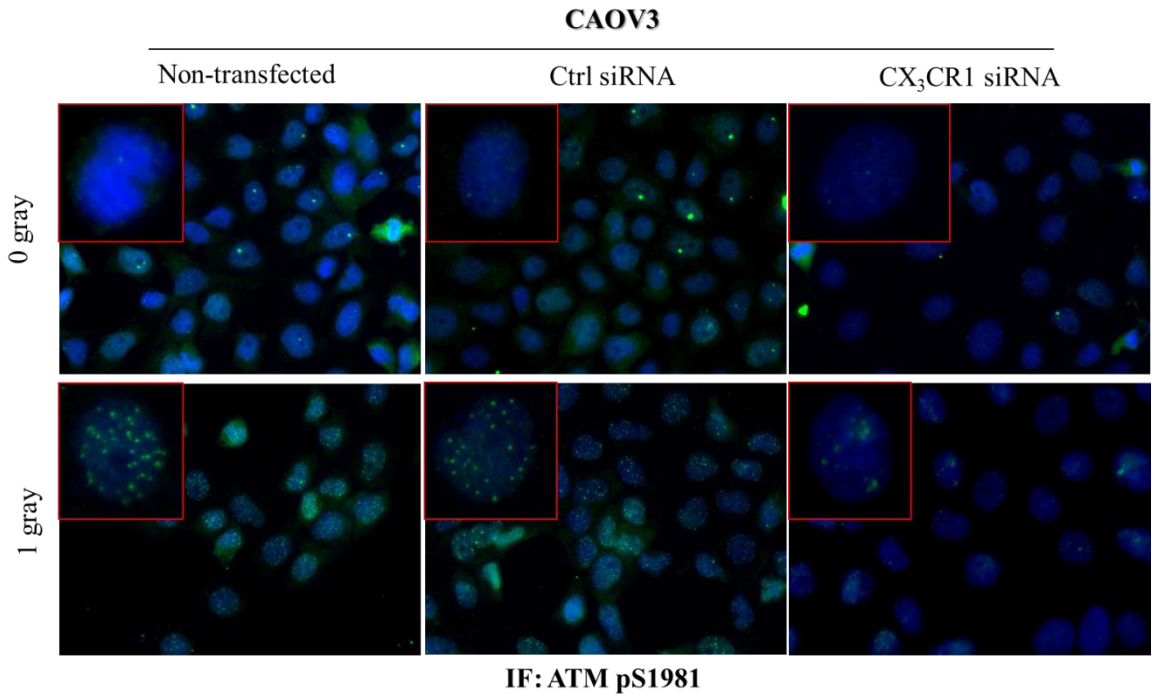

B

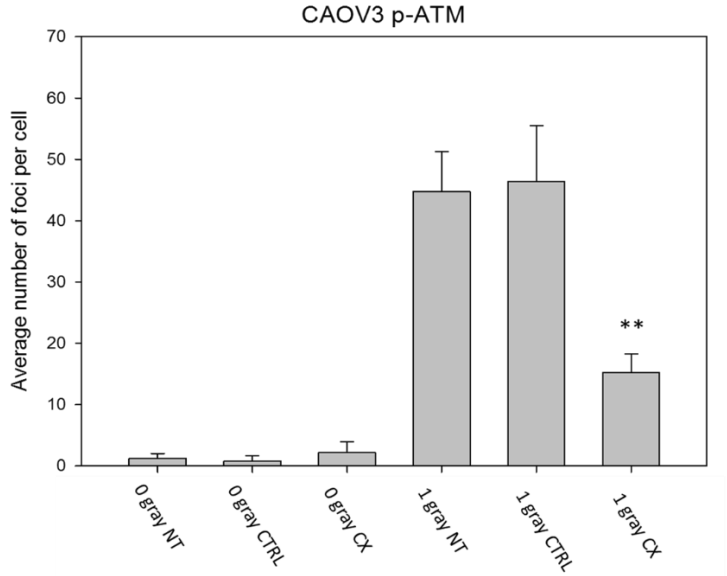

Figure 3.5 Loss of CX_3CR1 Decreases Ionizing Radiation-Induced ATM phosphorylation in CAOV3. Phosphorylated ATM foci formation is inhibited upon CX_3CR1 downregulation in human epithelial ovarian carcinoma cell line CAOV3. A) Cells were stained with anti-p-(S1981)-ATM antibody followed by goat anti-mouse Alexa Fluor 488 (green), counterstained with DAPI (blue). Insets show individual nuclei. B) Immunofluorescence quantification results of CAOV3. Quantification analysis was conducted by Image J (National Institutes of Health) and the one-way ANOVA test was conducted by SigmaPlot. Values shown represent the mean ± SD from 3 independent experiments. The asterisk indicated a significant difference from the non-transfected group (1 gray) and the control siRNA-transfected group (1 gray). **$p<0.001$.

A

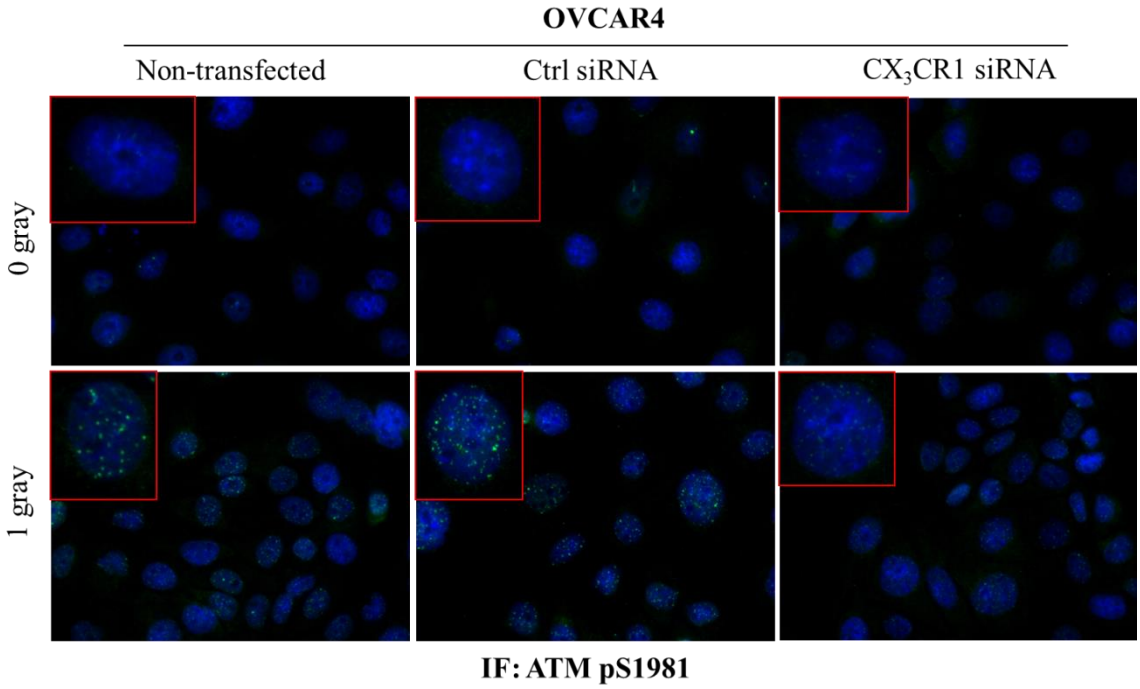

B

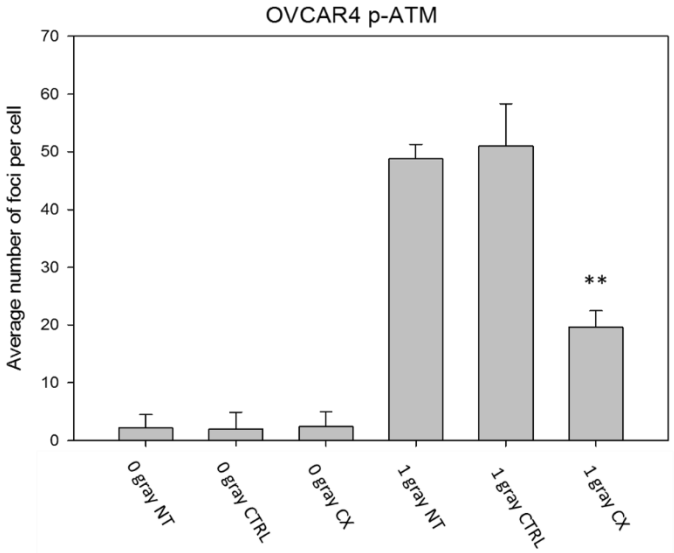

Figure 3.6 Loss of CX_3CR1 Decreases Ionizing Radiation-Induced ATM phosphorylation in OVCAR4. Phosphorylated ATM foci formation is inhibited upon CX_3CR1 downregulation in human epithelial ovarian carcinoma cell line OVCAR4. A) Cells were stained with anti-p-(S1981)-ATM antibody followed by goat anti-mouse Alexa Fluor 488 (green), counterstained with DAPI (blue). Insets show individual nuclei. B) Immunofluorescence quantification results of OVCAR4. Quantification analysis was conducted by Image J (National Institutes of Health) and the one-way ANOVA test was conducted by SigmaPlot. Values shown represent the mean ± SD from 3 independent experiments. The asterisk indicated a significant difference from the non-transfected group (1 gray) and the control siRNA-transfected group (1 gray). **$p<0.001$.

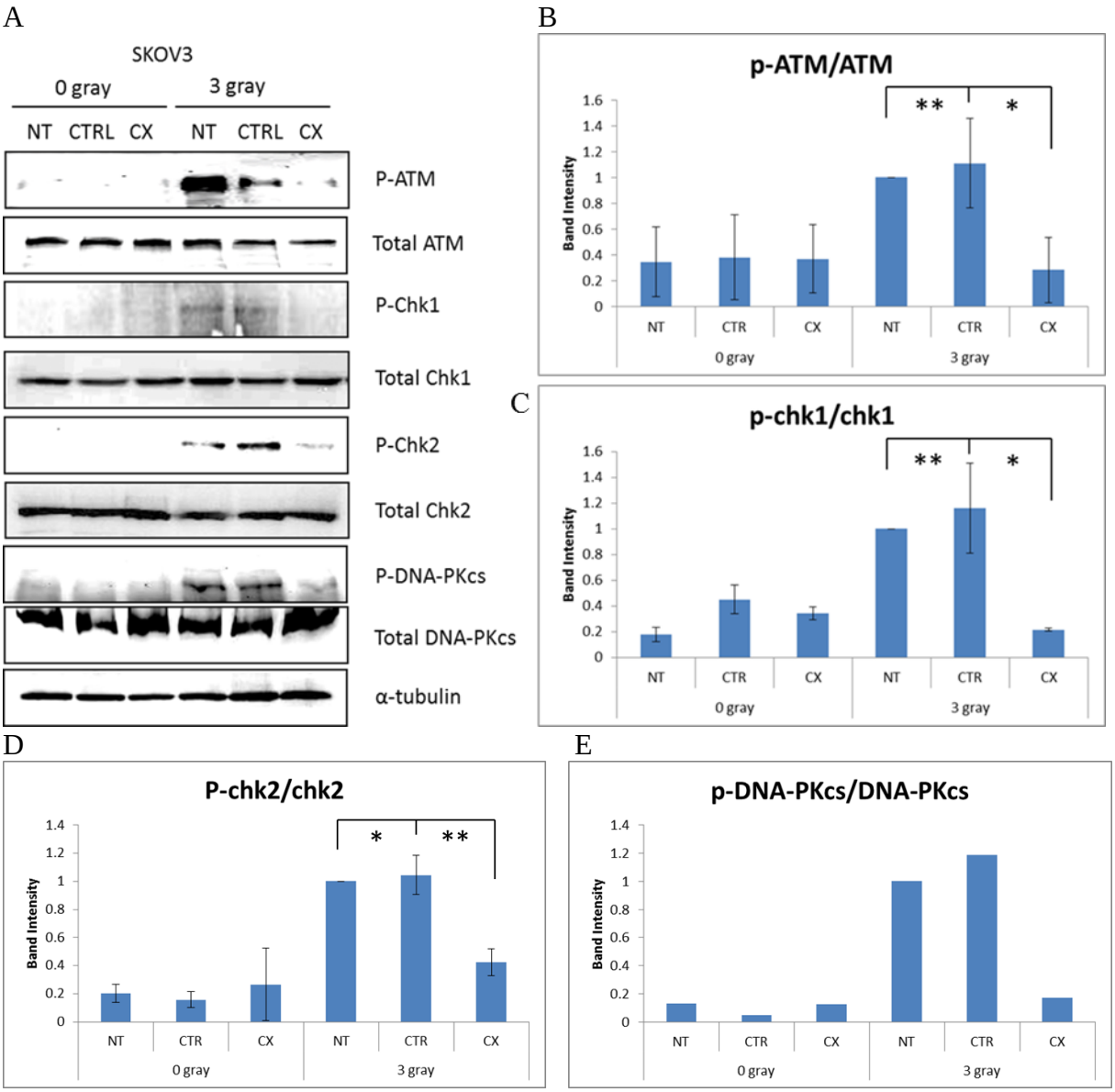

Figure 3.7 CX_3CR1 Downregulation Impairs Ionizing Radiation-Induced DDR Protein Activation in SKOV3. ATM, Chk1, Chk2 and DNA-PKcs phosphorylation are inhibited upon CX_3CR1 downregulation in human ovarian carcinoma cell lines SKOV3. A) Cells were transfected accordingly and were either radiated or left untreated, followed by western blot detection. B-E) Western blot quantification results. Quantitative measurements were conducted by Quantity One. The quantification of each phosphorylated protein was normalized to its total protein. The measurements were taken from at least three independent experiments and the student *t* test was conducted by Excel. *$p<0.05$ and **$p<0.001$ according to student *t* test.

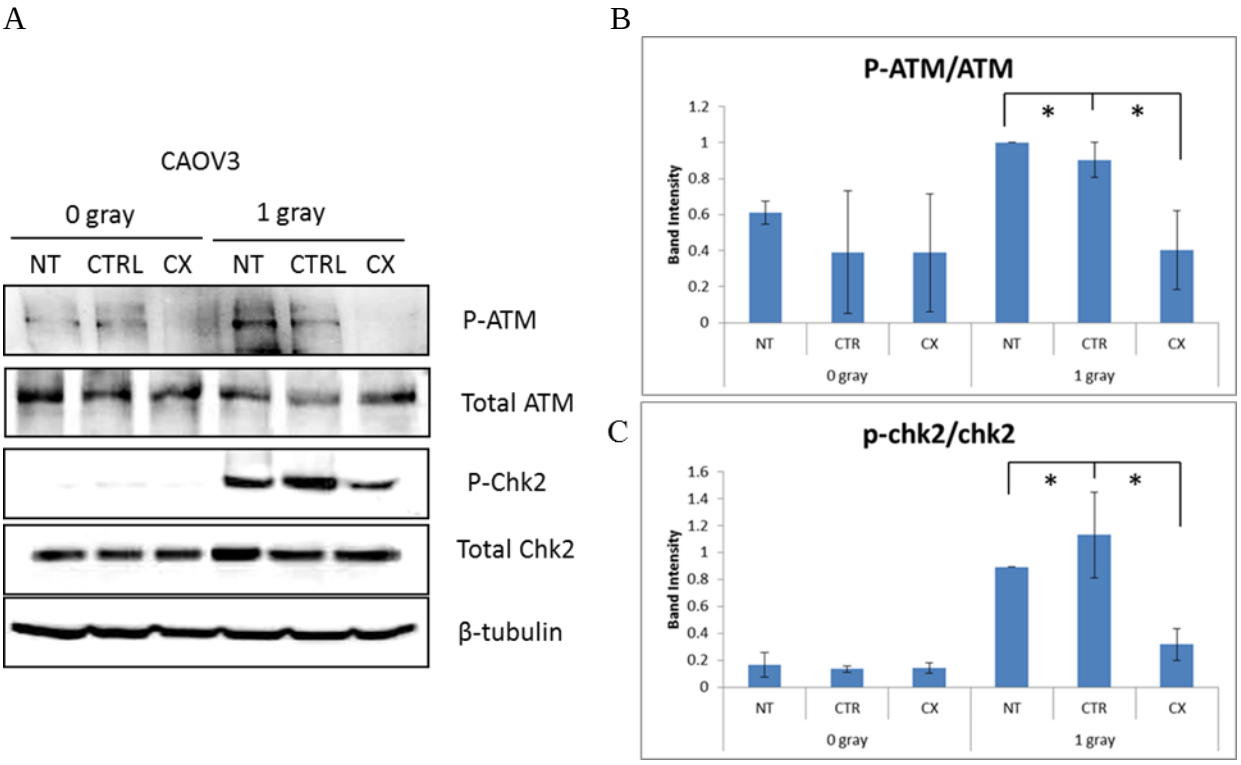

Figure 3.8 CX_3CR1 Downregulation Impairs Ionizing Radiation-Induced DDR Protein Activation in CAOV3. ATM and Chk2 phosphorylation are inhibited upon CX_3CR1 downregulation in human ovarian carcinoma cell lines CAOV3. A) Cells were transfected accordingly and were either radiated or left untreated, followed by western blot detection. B-C) Western blot quantification results. Quantitative measurements were conducted by Quantity One. The quantification of each phosphorylated protein was normalized to its total protein. The measurements were taken from at least three independent experiments and the student *t* test was conducted by Excel. *$p<0.05$ according to student *t* test.

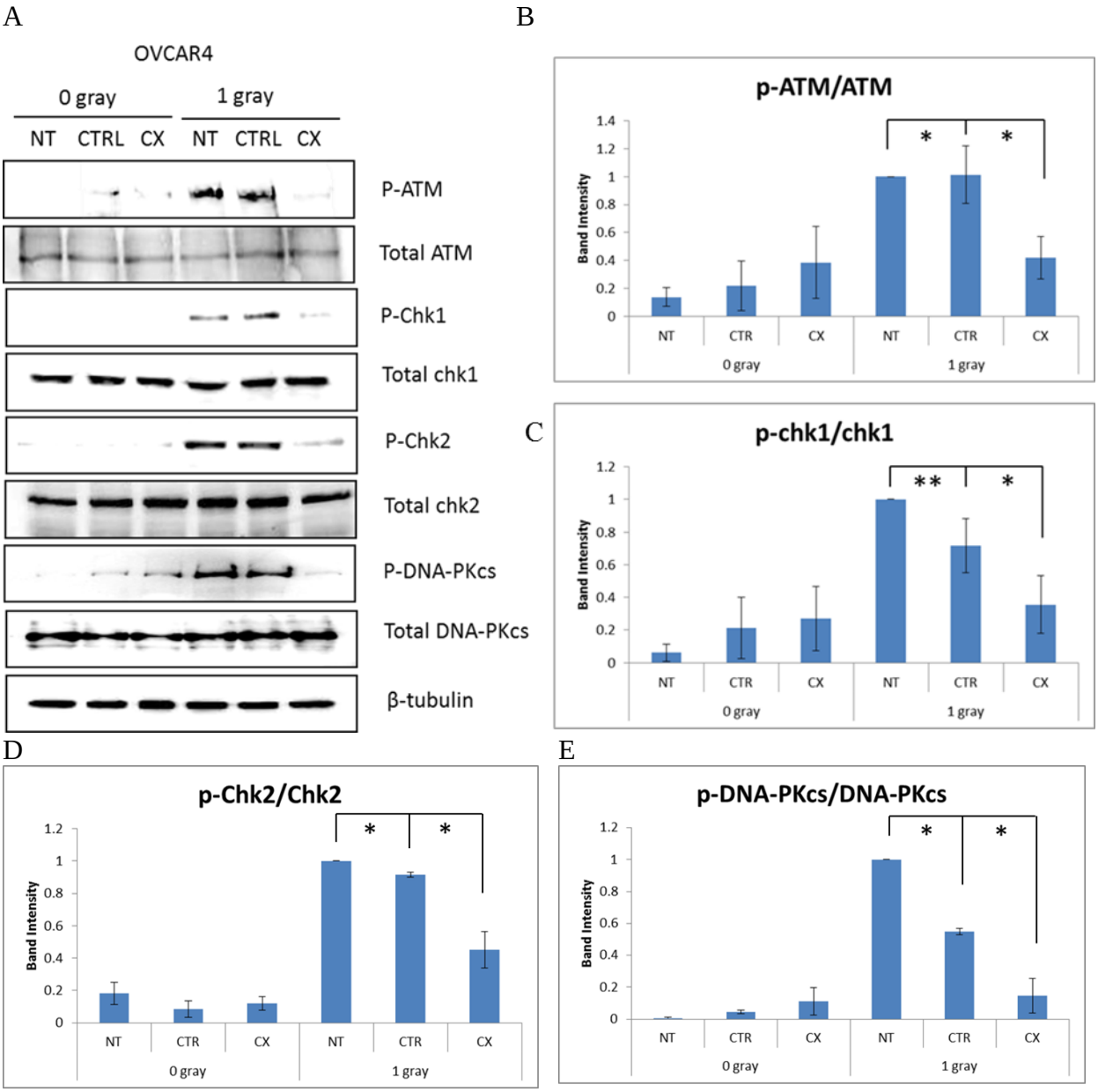

Figure 3.9 CX_3CR1 Downregulation Impairs Ionizing Radiation-Induced DDR Protein Activation in OVCAR4. ATM, Chk1, Chk2 and DNA-PKcs phosphorylation are inhibited upon CX_3CR1 downregulation in human ovarian carcinoma cell lines OVCAR4. A) Cells were transfected accordingly and were either radiated or left untreated, followed by western blot detection. B-E) Western blot quantification results. Quantitative measurements were conducted by Quantity One. The quantification of each phosphorylated protein was normalized to its total protein. The measurements were taken from at least three independent experiments and the student *t* test was conducted by Excel. *$p<0.05$ and **$p<0.001$ according to student *t* test.

3.3.2 Addition of ATM Inhibitor Further Reduces Clonogenic Ability and Induces Similar Level of Radiosensitization with Loss of CX_3CR1

Next, we are interested in whether CX_3CR1 knockdown and ATM inhibitor have similar effects in radiosensitization. CAOV3 were transfected accordingly and treated either with ATM inhibitor KU55933 at the concentration of 5 μM or the vehicle control DMSO 30min before radiation. Western blots were conducted to confirm the ATM inhibition upon KU55933 and transfection with CX_3CR1 siRNA. Clonogenic survival assay was conducted to evaluate the radiosensitivity under each condition and cells were continually exposed to either DMSO or KU55933 during the clonogenic assay. As shown in Figure 3.10 A and B, while CX_3CR1 downregulation inactivates p-ATM, the addition of ATM inhibitor further abrogates the phosphorylation of ATM. Moreover, as shown in Figure 3.11 and Table 3.1, the control siRNA transfected cells that were treated with ATM inhibitor showed a less clonogenic ability compared to the DMSO treated group, and CX_3CR1 siRNA transfected cells that were treated with ATM inhibitor displayed the lowest clonogenic ability among the groups. Furthermore, the radiosensitization caused by CX_3CR1 siRNA transfection is similar to the one caused by ATM inhibitor treatment.

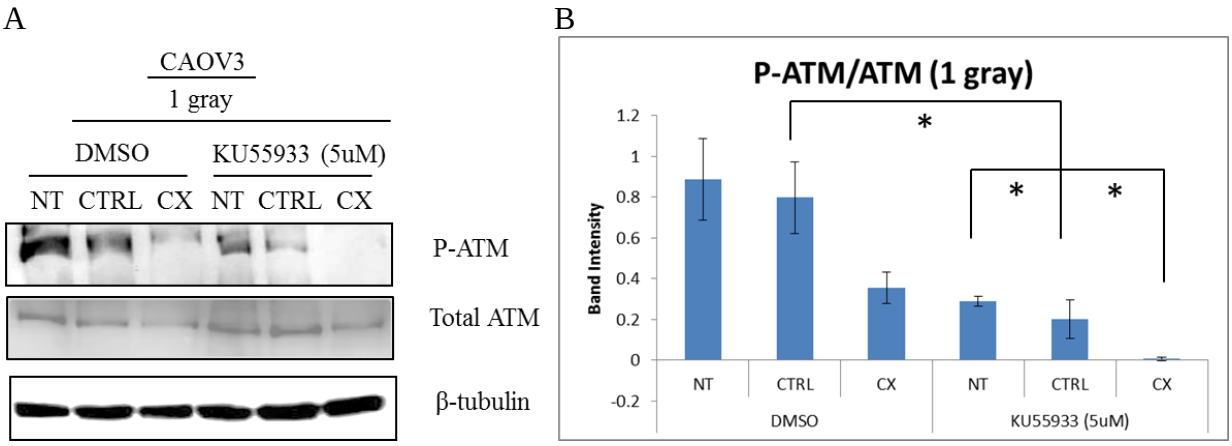

Figure 3.10 KU55933 Inhibits the ATM Kinase Activity. A) ATM phosphorylation is further inhibited upon 5 µM KU55933 treatment after radiation as evaluated by western blot. B) Western blot quantification results. Quantitative measurements were conducted by Quantity One. The quantification of each phosphorylated protein was normalized to its total protein. The measurements were taken from at least three independent experiments and the student *t* test was conducted by Excel. *$p<0.05$ according to student *t* test.

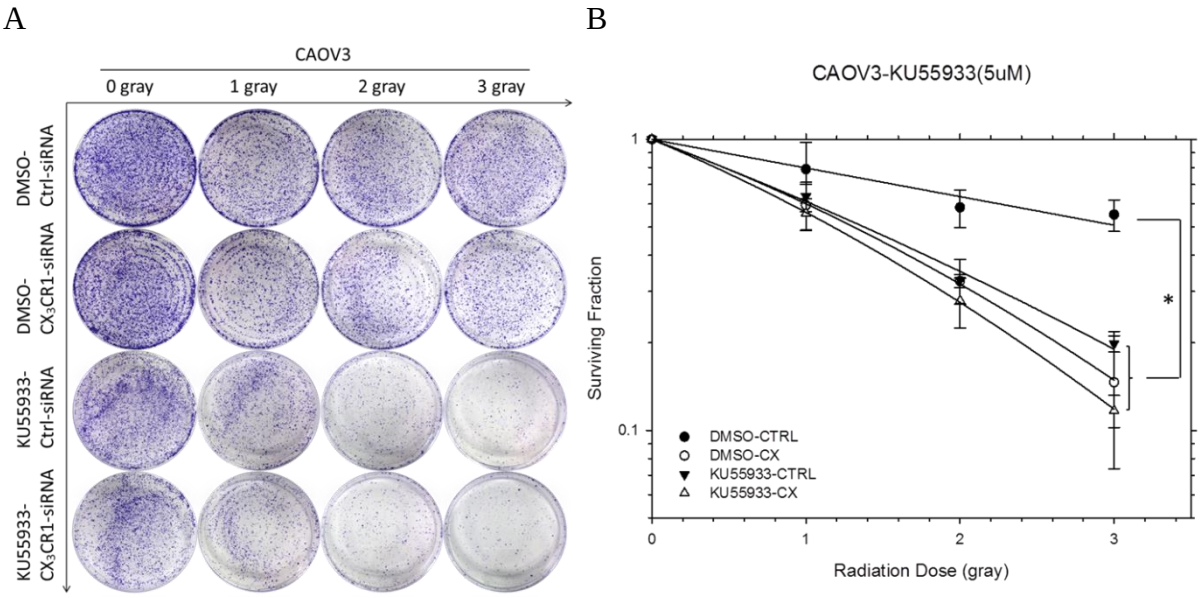

Figure 3.11 KU55933 can further Reduce the Clonogenic Ability and CX_3CR1 Transient Knockdown Induces Similar Level of Radiosensitization in CAOV3 as Compared to KU55933. CAOV3 were either transfected with the control siRNA or CX_3CR1 siRNA, and then exposed to 5 µM KU55933 for 30min before radiation. Cellular radiosensitivity was measured using the clonogenic assay. During the clonogenic assay, cells were either cultured in complete MEM, or complete MEM with DMSO (1/1000 v/v) or complete MEM with 5 µM KU55933. A) Pictures of clonogenic assay results of CAOV3 stained with crystal violet. B) Clonogenic survival assays quantification results after the transfection and the administration of ionizing radiation at increasing doses from 0 gray to 3 gray. Surviving fractions for CX_3CR1 siRNA transfected CAOV3 (with DMSO or KU55933) and the control siRNA transfected KU55933 treated CAOV3 were calculated after normalizing to the surviving fraction obtained from cells transfected with the control siRNA and treated with DMSO. Values shown represent the mean ± SD from 5 independent experiments. *$p<0.05$ according to two-way ANOVA test.

Table 3.1 Loss of CX_3CR1 and KU55933 can Radiosensitize CAOV3 to a Similar Level

Treatment	$SF2_{DMSO+control}/SF2_{treatment}$	$D10_{DMSO+control}/D10_{treatment}$	Radiosensitization
DMSO+ CX_3CR1	2	2.94	+
KU55933(5μM)+ control	1.81	2.57	+
KU55933(5μM)+ CX_3CR1	2.31	3.2	+

3.3.3 Loss of CX_3CR1 Lead to the Persistence of γ H2A.X Foci

H2A.X can be phosphorylated on serine 139 in early response to ionizing radiation. This phosphorylated H2A.X which is called γH2A.X, is considered to be the marker of IR induced DNA double strand breaks. In order to assess the effects of CX_3CR1 downregulation on the response to ionizing radiation, CAOV3 and OVCAR4 were either non-transfected or transfected with CX_3CR1 siRNA and the control siRNA followed by 1 gray of ionizing radiation. Cells were immunofluorescently stained 30 minutes after radiation. As shown in Figure 3.12 and 3.13, irradiation of CAOV3 and OVCAR4 in the control groups leads to the formation of γH2A.X, whereas the downregulation of CX_3CR1 caused a marked reduction in the intensity of γH2A.X foci. This is because γH2A.X can be phosphorylated by PIKKs family members, such as ATM, ATR, and DNA-PKcs. Since the loss of CX_3CR1 can lead to the inactivation of ATM and DNA-PKcs, formation of γH2A.X foci was impaired. However, when the cells were collected 16 hours after radiation, as shown in Figure 3.14-3.15, the radiated and CX_3CR1 downregulated group exhibits the highest amount of γH2A.X formation compared to the control groups. One of the possible explanations is that the majority of the DNA damage would be repaired in the control

groups 16 hours after radiation. DDR machinery is then switched off, which involves the activation of several γH2A.X phosphatases. These phosphatases, especially PP2A (protein phosphatase 2A) are directly activated by ATM, and then dephosphorylate γH2A.X (169). However, in the CX_3CR1 downregulated group, because the majority of the DNA damage are unrepaired due to the impaired DNA damage repair pathways, the rest of the unaffected DNA damage repair proteins can then activate γH2A.X. Therefore, even though loss of CX_3CR1 can transiently inactivate γH2A.X, it will eventually lead to foci persistence.

A

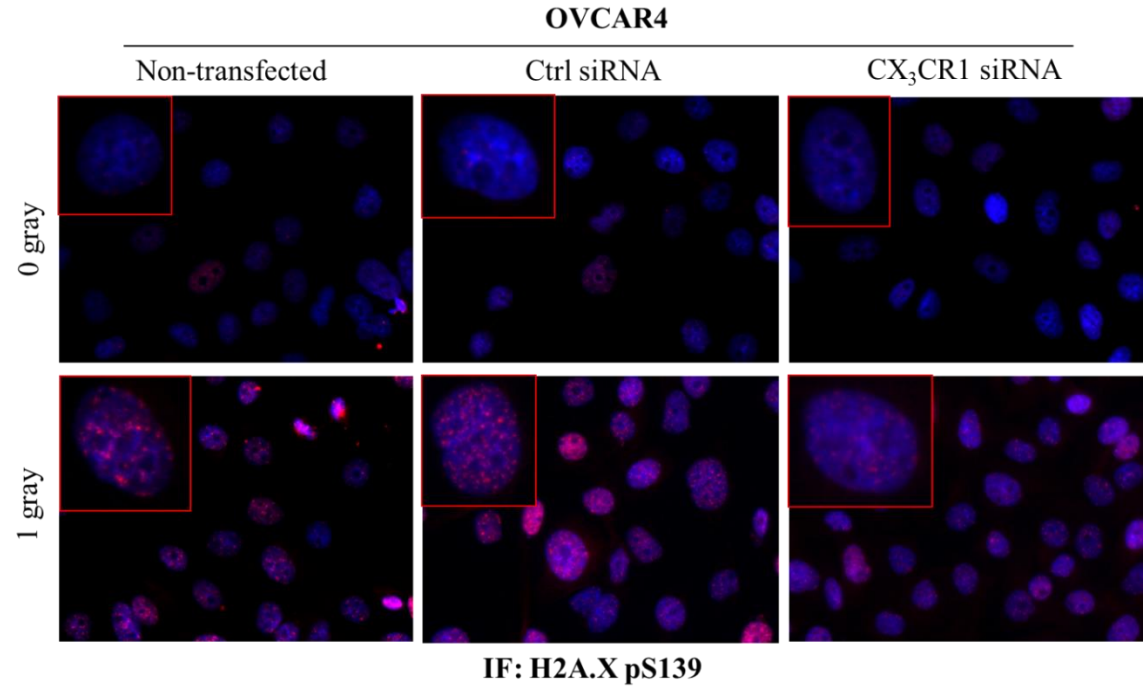

B

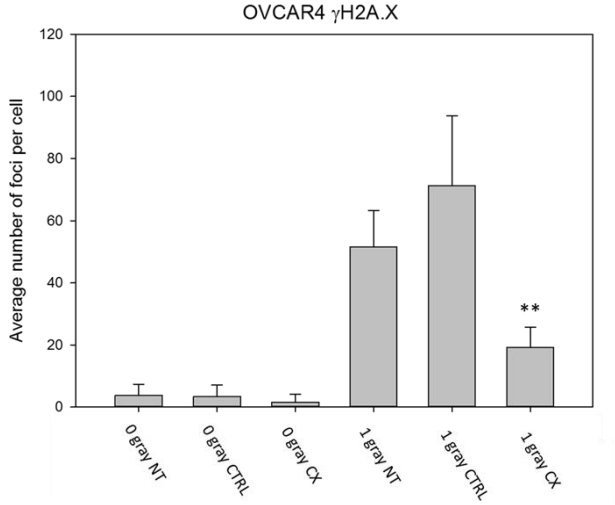

C

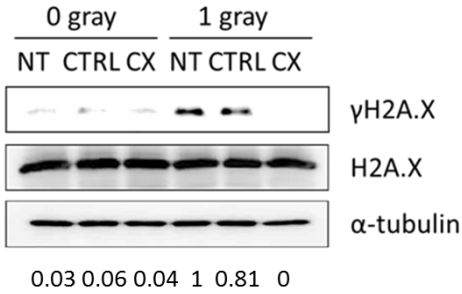

Figure 3.12 Loss of CX_3CR1 Decreases Ionizing Radiation-Induced γ-H2A.X Foci Formation in OVCAR4. A) Immunofluorescence staining of γ-H2A.X 30 minutes after radiation. OVCAR4 cells were deposited onto collagen pre-coated coverslips and stained with anti-p-(S139)-H2A.X antibody followed by goat anti-rabbit Alexa Fluor 546 (red), counterstained with DAPI (blue). Microscopy was performed by Zeiss with the magnifications: x50. Inserts show individual nuclei. B) Quantification of the immunofluorescence staining of OVCAR4. Quantification analysis was conducted by Image J (National Institutes of Health) and the one-way ANOVA test was conducted by SigmaPlot. Values shown represent the mean ± SD from 3 independent experiments. The asterisk indicated a significant difference from the non-transfected group (1 gray) and the control siRNA-transfected group (1 gray). **$p<0.001$. C) γ-H2A.X formation was inhibited upon CX_3CR1 downregulation as assessed by western blot.

A

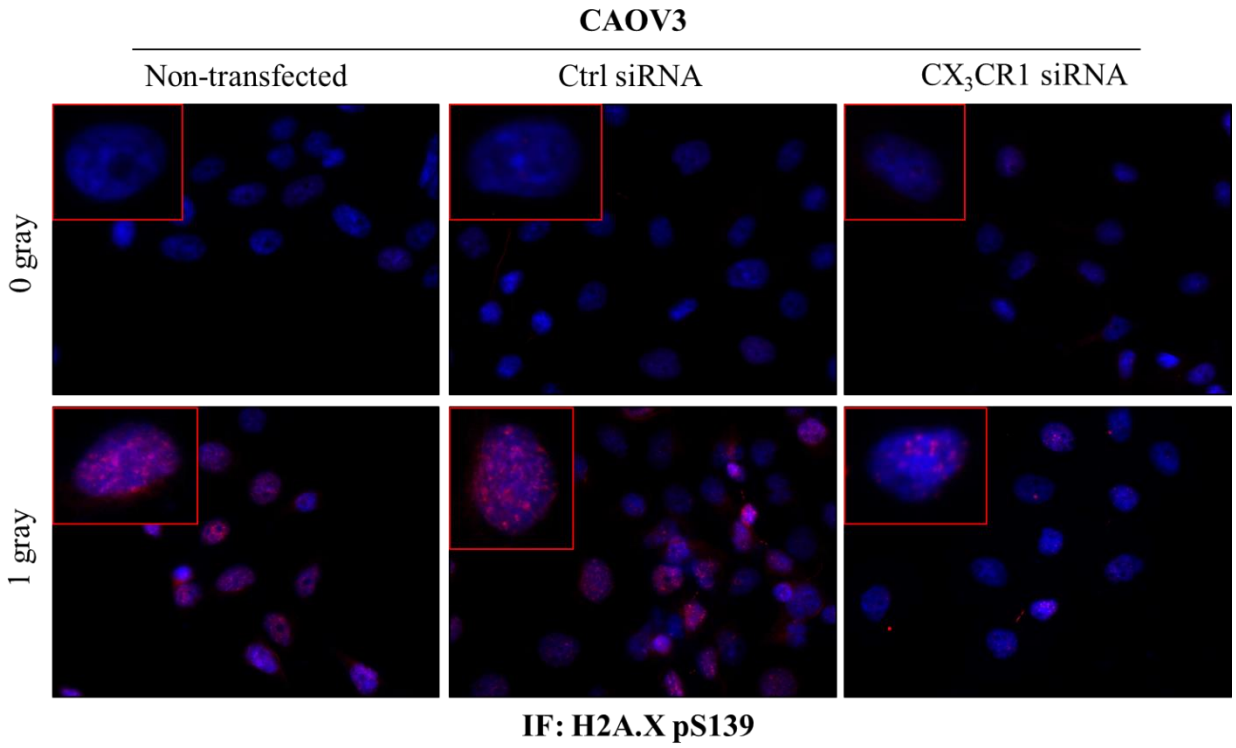

B

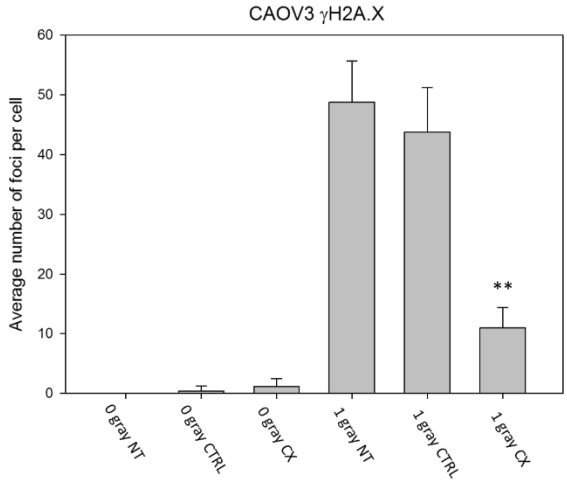

Figure 3.13 Loss of CX_3CR1 Decreases Ionizing Radiation-Induced γ-H2A.X Foci Formation in CAOV3. A) Immunofluorescence staining of γ-H2A.X 30 minutes after radiation. CAOV3 cells were deposited onto poly-D-lysine pre-coated coverslips and stained with anti-p-(S139)-H2A.X antibody followed by goat anti-rabbit Alexa Fluor 546 (red), counterstained with DAPI (blue). Microscopy was performed by Zeiss with the magnifications: x50. Inserts show individual nuclei. B) Quantification analysis was conducted by Image J (National Institutes of Health) and the one-way ANOVA test was conducted by SigmaPlot. Values shown represent the mean ± SD from 3 independent experiments. The asterisk indicated a significant difference from the non-transfected group (1 gray) and control siRNA-transfected group (1 gray). **$p<0.001$.

A

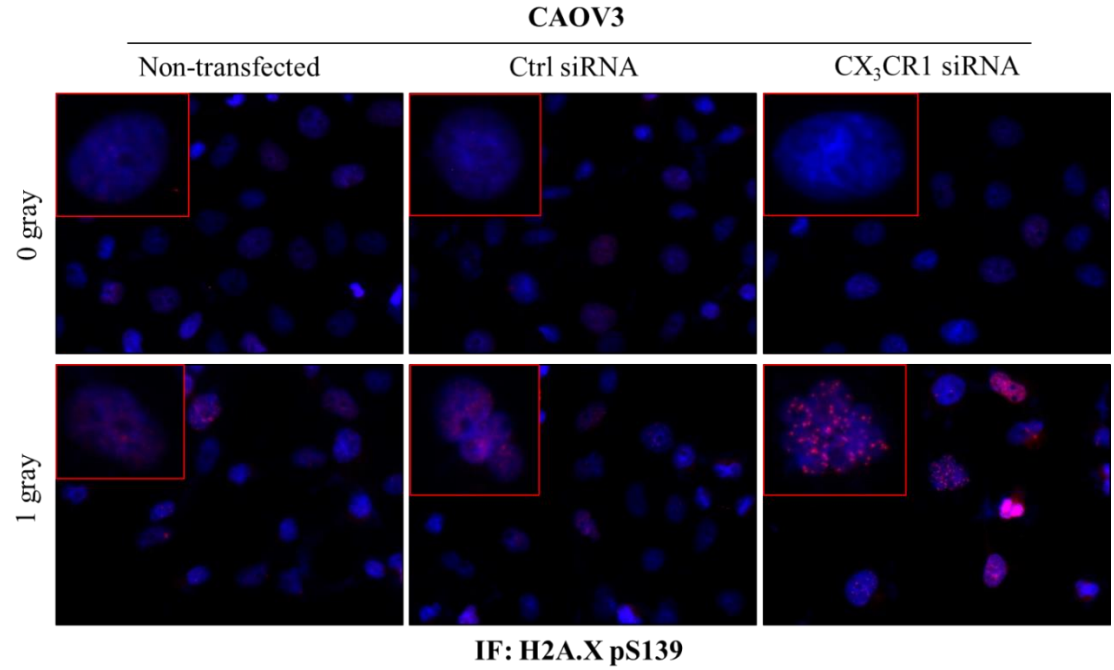

B

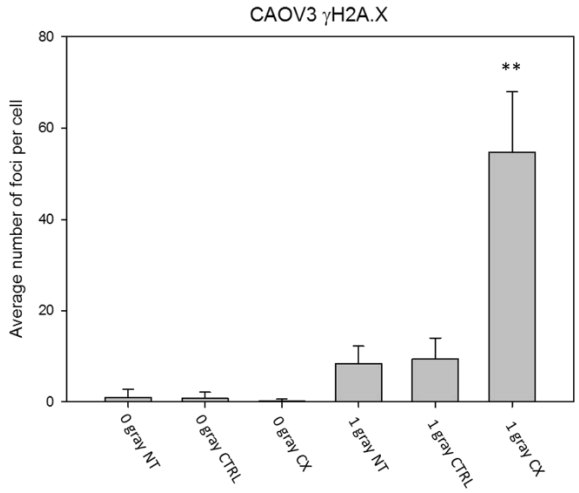

C

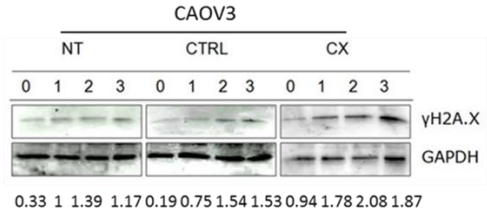

Figure 3.14 Loss of CX_3CR1 Leads to γ-H2A.X Foci Persistence in CAOV3. A) Immunofluorescence staining of γ-H2A.X 16 hours after radiation. CAOV3 cells were deposited onto poly-D-lysine pre-coated coverslips and stained with anti-p-(S139)-H2A.X antibody followed by goat anti-rabbit Alexa Fluor 546 (red), counterstained with DAPI (blue). Microscopy was performed by Zeiss with the magnifications: x50. Inserts show individual nuclei. B) Quantification of the immunofluorescence staining of CAOV3. Quantification analysis was conducted by Image J (National Institutes of Health) and the one-way ANOVA test was conducted by SigmaPlot. Values shown represent the mean ± SD from 3 independent experiments. The asterisk indicated a significant difference from the non-transfected group (1 gray) and the control siRNA-transfected group (1 gray). **$p<0.001$. C) γ-H2A.X expression persisted upon CX_3CR1 downregulation as assessed by western blot. Numbers below the bands are the corresponding densitometry analysis.

A

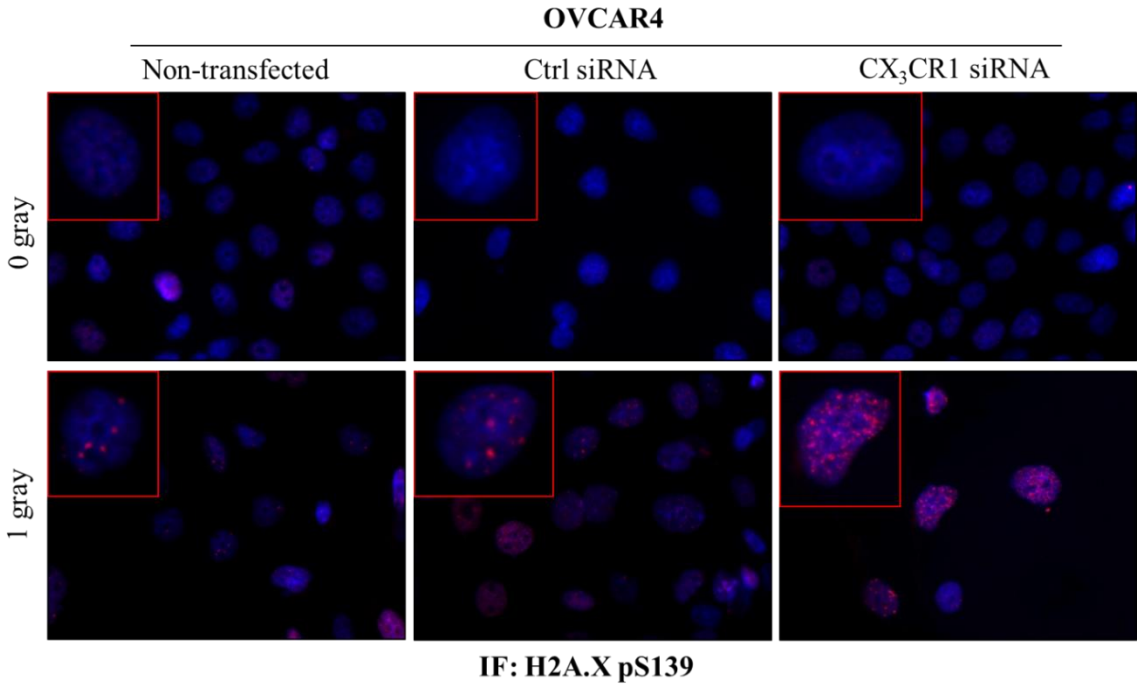

B

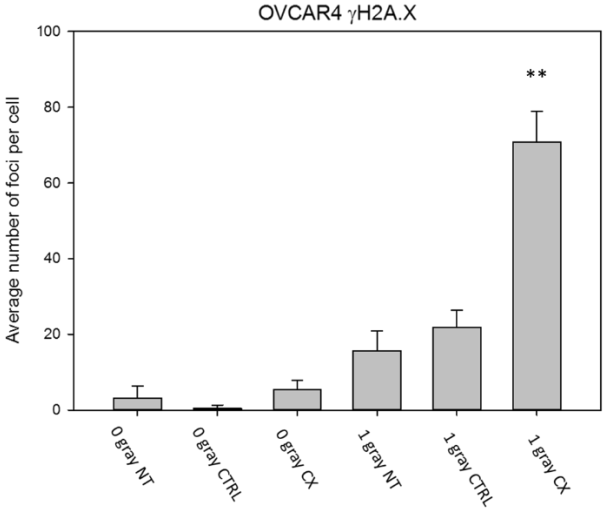

Figure 3.15 Loss of CX_3CR1 Leads to γ-H2A.X Foci Persistence in OVCAR4. A) Immunofluorescence staining of γ-H2A.X 16 hours after radiation. OVCAR4 cells were deposited onto collagen pre-coated coverslips and stained with anti-p-(S139)-H2A.X antibody followed by goat anti-rabbit Alexa Fluor 546 (red), counterstained with DAPI (blue). Microscopy was performed by Zeiss with the magnifications: x50. Inserts show individual nuclei. B) Quantification of the immunofluorescence staining of OVCAR4. Quantification analysis was conducted by Image J (National Institutes of Health) and the one-way ANOVA test was conducted by SigmaPlot. Values shown represent the mean ± SD from 3 independent experiments. The asterisk indicated a significant difference from the non-transfected group (1 gray) and the control siRNA-transfected group (1 gray). **$p<0.001$.

3.3.4 CX_3CR1 Inhibition can Sensitize Olaparib Treated CAOV3 to Ionizing Radiation

Since olaparib has been reported to enhance the susceptibility of homologous recombination-defective cells to ionizing radiation (172), and CX_3CR1 knockdown can inhibit the DNA double strand break repair pathway, olaparib may increase the cytotoxic effects of ionizing radiation in CX_3CR1-deficient cells. To test this hypothesis, CAOV3 were transfected accordingly and treated either with PARP inhibitor Olaparib at the concentration of 5 μM or the vehicle control DMSO 30min before radiation. Clonogenic assay was conducted after radiation to assess cellular response to ionizing radiation. The doses of the radiation are 1 gray, 2 gray and 3 gray. During the clonogenic assay, cells were continually exposed to either DMSO or Olaparib at the concentration of 5 μM. As shown in Figure 3.17 and Table 3.2, although Olaparib alone induced extensive cell death, it failed to sensitize CAOV3 to ionizing radiation, however, when combined with CX_3CR1 knockdown, Olaparib treated cells were significantly radiosensitized.

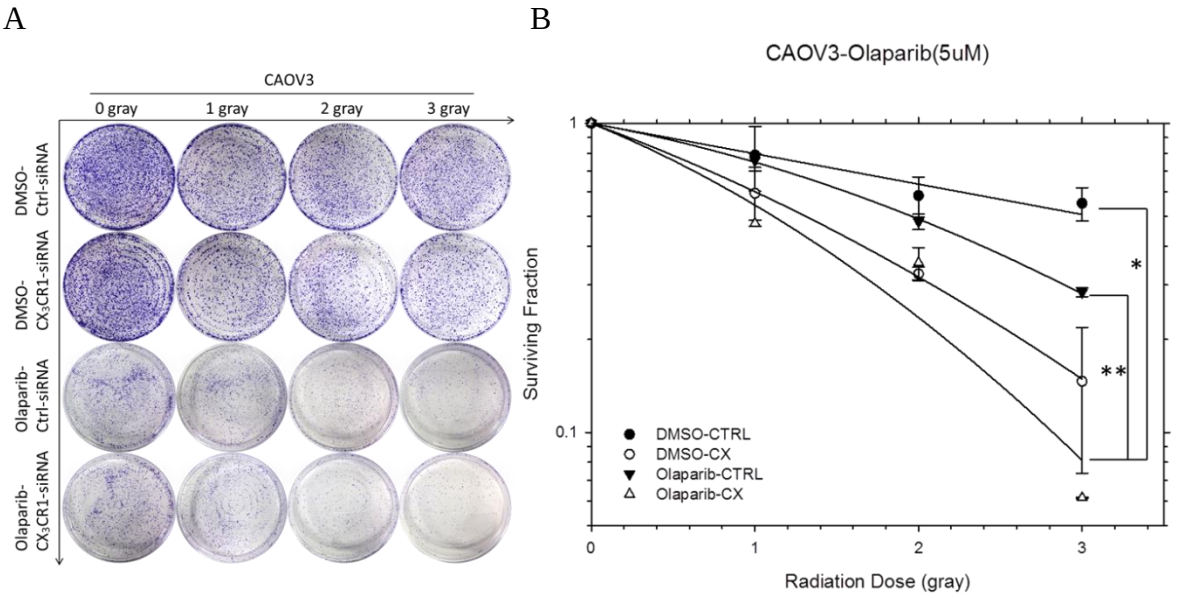

Figure 3.16 CX_3CR1 Knockdown Further Promotes the Radiosensitization Level in Olaparib Treated CAOV3. CAOV3 were either transfected with the control siRNA or CX_3CR1 siRNA, and then exposed to 5 µM Olaparib for 30min before radiation. Cellular radiosensitivity was measured using the clonogenic assay. During the clonogenic assay, cells were either cultured in complete MEM, or complete MEM with DMSO (1/1000 v/v) or complete MEM with 5 µM Olaparib. A) Pictures of the clonogenic assay results of CAOV3 stained with crystal violet. B) Clonogenic survival assays quantification results after the transfection and the administration of ionizing radiation at increasing doses from 0 gray to 3 gray. Surviving fractions for CX_3CR1 siRNA transfected CAOV3 (with DMSO or Olaparib) and the control siRNA transfected Olaparib treated CAOV3 were calculated after normalizing to the surviving fraction obtained from cells transfected with the control siRNA and treated with DMSO. Values shown represent the mean ± SD from 5 independent experiments. *$p<0.05$, **$p<0.001$ according to two-way ANOVA test.

Table 3.2 CX_3CR1 Knockdown can Further Sensitize Olaparib treated CAOV3 to Ionizing Radiation

Treatment	$SF2_{DMSO+control}/SF2_{treatment}$	$D10_{DMSO+control}/D10_{treatment}$	Radiosensitization
DMSO +CX_3CR1	2	2.94	+
Olaparib(5μM) +control	1.3	2.3	- (n.s.)[a]
Olaparib(5μM) +CX_3CR1	2.71	3.61	+
Treatment	$SF2_{Olaparib+control}/SF2_{treatment}$	$D10_{Olaparib+control}/D10_{treatment}$	Radiosensitization
Olaparib(5μM) +CX_3CR1	2.09	1.57	+

[a]Non-statistically significant differences were labeled as n.s.

3.4 Discussion

DNA double strand break is a deleterious lesion that can be caused by ionizing radiation. In order to survive from the harmful attack, cells develop several kinds of DNA damage response, such as the DNA damage repair pathways to escape from the catastrophic cell death. Since radiation can affect both normal tissue and tumors, high dose of radiation can lead to dose-related complications while low dose of radiation is not able to kill cancer cells. Moreover, cancer cells are also capable of developing resistance to radiation by altering some key cell survival gene expression; therefore, it is important to discover radiosensitizers that can increase cancer cell radiosensitivity with high selectivity to cancer cells.

The definition of radiosensitizers is that the chemotherapeutic agent is relatively nontoxic while it can increase the toxicity caused by ionizing radiation. Based on the DNA double strand break repair mechanism, the master regulator genes/proteins are the major targets of radiosensitizers,

such as the PI3K-like kinases: ATM, ATR and DNA-PKcs, because downregulation or function inhibition of these proteins can sensitize cancer cells to radiation (174). ATM is first characterized due to a rare autosomal recessive disorder, ataxia telangiectasia. Patients with this disease show extreme sensitivity to environmental radiation and a predisposition to cancer (175). Similarly, Seckel syndrome, due to the mutation of ATR, is an A-T like disorder that can lead to hypersensitivity to radiation therapy. Recently, a lot of selective inhibitors have been developed to sensitize human cancer cell lines to ionizing radiation. Hickson *et al*. identified and characterized ATM inhibitor KU55933 for sensitizing HeLa cells to ionizing radiation (176). Biddlestone-Thorpe *et al*. showed a more potent ATM inhibitor KU-60019 for preferentially sensitize p53-mutant glioma to ionizing radiation (177). Rainey *et al.* showed transient inhibition of ATM kinase by CP46672 is sufficient to sensitize HeLa cells to ionizing radiation (178). Zhao *et al*. characterized a novel DNA-PK inhibitor NU744, for sensitizing human colon cancer cells to ionizing radiation (179).

Similarly, as shown in Figure 3.5 and 3.6, transient CX_3CR1 downregulation is also capable of inactivating ATM after ionizing radiation as evaluated by immunofluorescence staining. Moreover, as shown in Figure 3.7-3.15 and Table 3.1, DNA-PKcs, Chk1, Chk2 and γH2A.X also cannot be phosphorylated after ionizing radiation upon CX_3CR1 downregulation in three ovarian cancer cell lines. ATM inhibitor KU55933 which can abrogate ATM kinase activity can induce a similar level of radiosensitization as compared to CX_3CR1 knockdown. After cells collected 16 hours after radiation, the DNA damage in CX_3CR1 downregulated and radiated group cannot be repaired, as indicated by persistent γH2A.X foci. Furthermore, as shown in Figure 3.16 and Table 3.2, loss of CX_3CR1 can also induce radiosensitization in Olaparib treated CAOV3, while

Olaparib alone failed to do so. Taken together, our data suggested that CX_3CR1 inhibition can sensitize ovarian cancer cells from HGSOC tumors to ionizing radiation, by inhibiting the DDR protein activity. Although ATM inhibitor might work with PARP inhibitor and lead to a similar result (184), it is possible that this approach could also induce a lethal response in normal cells. Therefore, CX_3CR1 downregulation, compared to a direct ATM inhibition, could be potentially better in terms of specificity.

Since CX_3CR1 is a seven-transmembrane protein and ATM, ATR, DNA-PKcs locate in nuclei, there should be a cytoplasmic signaling cascade to conduct the signal transduction from CX_3CR1 to these DDR proteins. One of the possible components in this cytoplasmic pathway could be ERK. G.E. White *et al*. demonstrated that ERK is directly downstream of CX_3CR1. When CX_3CR1 is activated upon CX_3CL1 binding, it can phosphorylate ERK and affects cellular proliferation (180). Moreover, ERK1/2 is critical in mediating IR-induced ATM phosphorylation. Golding *et al.* illustrated that ERK1/2 signaling is important in phosphor-(S1981) ATM foci formation and the localization of ATM to repair foci (181). Wei *et al.* validated that knockdown of ERK1 or ERK2 reduces the formation of ATM S1981 phosphorylation (182). Therefore, ERK1/2 is an interesting target and needs further investigation.

3.5 Conclusion

Taking together, our data demonstrated that loss of CX_3CR1 sensitizes EOC cells to radiation by inhibiting the activity of DNA damage repair related proteins. This mechanistic understanding indicated that loss of CX_3CR1 can be used as a radiosensitizer in the therapy toward high-grade serous ovarian malignancies.

CHAPTER 4.

LOSS OF CX_3CR1 LEAD TO PERSISTENT OXIDATIVE DNA DAMAGE

4.1 Introduction

When the cells are exposed to ionizing radiation, water molecules in the cells can be radiolyzed into highly reactive free radicals such as hydroxyl radical (.OH). It can be further converted into a series of highly reactive combinations such as hydrogen peroxide and superoxide. All these free radicals produce oxidative damage within the cell (185). The unpaired electrons from the free radicals can abstract the hydrogen atoms from the DNA to acquire new electrons and therefore lead to base damage, DNA single and double strand breaks, interstrand and intrastrand cross-links, and DNA-protein cross-links (186).

High level of ROS (reactive oxygen species) can lead to persistent oxidative DNA damage. However, cancer cells can usually develop antioxidant systems to defend against the production of reactive species. In mammalian cells, the antioxidants can be classified as non-enzymatic antioxidants and enzymatic antioxidants. The non-enzymatic subtype includes vitamin C, vitamin E, glutathione, coenzyme Q, etc., which can directly interact and detoxify ROS (3). The enzymatic antioxidants include superoxide dismutases (SOD), catalase, glutathione peroxidase (GPx), glutathione S-transferase (GST) (187). SOD can convert superoxide anion into hydrogen peroxide, which can be further converted into hydroxyl radical (188) and water by catalase and GPx (189). GST catalyzes the conjugation of reduced GSH to electrophilic centers in various substrates, including lipid peroxides (190). Additionally, small thiol-containing peptides, such as thioredoxin (Trx) can act as a reductase to directly repair the oxidized protein into its reduced

state (191). When the antioxidant systems are inhibited, the overproduced ROS can contribute to extensive DNA damage which can further enhance the ionizing radiation-induced DNA damage.

Besides the antioxidant systems, several intracellular signaling pathways are also activated to protect the cells from oxidative damage. NF-kB pathways (transcriptional factors), protein tyrosine kinases mediated pathways, MAPK pathways, etc. can be activated upon oxidative damage to further control cell proliferation, apoptosis, migration, metastasis, etc. (192, 193). Among these pathways, the mitogen-activated protein kinases (MAPK) pathway is one of the most important pathways in response to ROS. The mammalian MAPK family consists of the extracellular signal regulated kinases (ERKs), the c-Jun N-terminal kinases (JNKs) and the p38MAPKs (194). P38MAPK is usually classified as stress-responsive protein kinase and is usually activated by UV radiation, ionizing radiation, ligands for G protein-coupled receptors, etc. (195). Generally speaking, the MAPK signaling cascade begins with the activation of MAPKKK, which can phosphorylate and activate MAPKK, which in turn phosphorylate and activate MAPKs. In the context of p38MAPK, MAPKKK includes ASK1 (apoptosis signal-regulatory kinase 1), TAO (thousand-and-one amino acids 1 and 2), mixed-lineage kinase 3 (MLK3), etc.; MAPKK include MKK3 and MKK6. The activated p38MAPK can further activate transcription factors, including ATF2, STAT1, GSK3β, etc. to affect the overall cellular response (196). Therefore, p38 MAPK activation status is an important indicator of ROS-mediated signaling and possible cellular outcomes.

DNA damage and ROS accumulation may lead to apoptosis, cell cycle arrest, cellular senescence and mitotic catastrophe. Apoptosis is a programmed cell death that can be mediated through cell

surface death receptor and mitochondria (197). The non-repaired DNA double strand breaks can trigger apoptosis either through the p53-mediated pathway (198) by transactivating genes that can promote apoptosis (199) or through the p53-independent pathway by activating p53 homologs p63 and p73 (200, 201). The accumulated ROS can induce apoptosis not only through mitochondria (202) but also through stress-activated protein kinase by activating death receptors (203). Cell cycle arrest is usually triggered by DNA damage response through the activation of CDKs (204) or by ROS through the activation of p53 (205). Cellular senescence may also be a possible outcome of DNA damage and ROS accumulation. It is an irreversible cell cycle arrest mediated through p53 and cdc25 in DDR-signaling (206). It can also be triggered by the activation of p38MAPK upon ROS accumulation (207). Moreover, radiation-induced mitotic catastrophe is also one of the possibilities (208). It is resulted from premature or inappropriate entry of cells into mitosis caused by ionizing radiation and oxidative stress, and is usually morphologically characterized by gross nuclear alterations such as micro-/multi-nucleation, and accompanied by checkpoint failure, genetic inhibition of TP53, mitotic apparatus perturbations and some degree of mitotic arrest (209, 210). All these cellular outcomes are the possible pathways contribute to radiosensitization. RJ Muschel *et al*. discussed that p53, Bcl2 and Ras which play important roles in mediating apoptosis can affect the radiosensitivity (211). HM Wang *et al.* showed that nasopharyngeal carcinoma cells can be radiosensitized by inhibiting ATM expression with cell cycle arrested at G_2/M phase (212). M Wang *et al.* discovered that EGFR (epidermal growth factor receptor) inhibitor can radiosensitize non-small cell lung cancer (NSCLC) cells by inducing senescence (213). Hayman TJ *et al.* demonstrated that elF4E knockdown in MDA-MB-231 cells induced radiosensitization is resulted from mitotic

catastrophe (214). Therefore, it is possible that these cellular events also participated in CX_3CR1-dependent radiosensitization.

4.2 Materials and Methods

4.2.1 Materials

p38[pThr180, pThr182] (Novus, NB500-138, 1:1000); total p38 (Cell Signaling Technology, #9212, 1:1000); anti-rabbit IgG, HRP-linked antibody (Cell Signaling Technology, 1:1000-1:5000); anti-mouse IgG, HRP-linked antibody (Santa Cruz Biotechnology, sc-2005, 1:500-1:3000); α-tubulin (University of Iowa, AA4.3, 1:200); DCFDA-Cellular Reactive Oxygen Species Detection Assay Kit (Abcam, ab113851); Propidium iodide flow cytometry kit (Abcam, ab139418)

4.2.2 Western Blotting

Cells were harvested and lysed in RIPA buffer (1.25ml 1M Tris buffer, pH7.4, 7.5ml 1M NaCl, 0.5ml NP-40, 0.5g Sodium Deoxycholate, 0.5ml SDS, 5 tablets of complete mini EDTA-free phosphatase inhibitor, protease inhibitor). Same amount of protein separated by SDS-PAGE were electro-transferred onto PVDF membranes, blocked with 5% BSA (w/v) at room temperature for 60 minutes, and incubated with primary antibodies at 4 ℃ overnight. After incubation with secondary antibody at room temperature for 2 hours, the membranes were developed with enhanced chemiluminescence (ECL) reagents.

4.2.3 ROS Detection by DCFDA Assay

Cells were grown to 80% confluency, and transfected accordingly. Three days after transfection, cells were subjected to radiation. 30 minutes before radiation, cells were stained with 20uM DCFDA following manufacturer's instructions and incubated at 37 ℃. Cells were then collected 20 minutes and 1 hour after radiation and analyzed by flow cytometer (BD accuri C6 Flow cytometer).

4.2.4 Cell Cycle and Apoptosis Analysis

SKOV3 and OVCAR4 cells ($1*10^5$ cells/ml) were transfected accordingly for 72 hours and treated with x-ray radiation. Cells were harvested, washed with cold PBS, fixed in 66% ethanol at 4 ℃ overnight, and then washed with PBS. The single cell suspension was stained with propidium iodide and RNase staining solution according to manufacturer's instructions in dark for 30 minutes at 37 ℃. Samples were then analyzed for their cell cycle distribution and apoptosis by BD Accuri C6 Flow Cytometer (BD Biosciences, San Jose, CA, USA). The data were analyzed with FlowJo (FlowJo, LLC).

4.2.5 Statistical Analysis

The Student *t* test was performed using Excel. The results represent the mean of at least triplicate measurements with error bars corresponding to standard deviation. For each test, p values of <0.05 was considered significant.

4.3 Results

4.3.1 Loss of CX_3CR1 Leads to the Persistent Oxidative Stress

Since ionizing radiation can induce extensive oxidative DNA damage, we investigated how CX_3CR1 affect the overall oxidative status. SKOV3 cells were either non-transfected or transfected with the control siRNA or CX_3CR1 siRNA. Then cells were stained with DCFDA to assess the total ROS level followed by ionizing radiation. As shown in Figure 4.1, 20min after radiation, ROS levels are similar among the radiated group, with the average intensity at around 2500000 (Figure 4.1 A); however, 1 hour after radiation, the 3 gray CX_3CR1-downregulated group displayed the highest amount of ROS compared to the radiated control groups and non-radiated groups, with the average intensity of the radiated and CX_3CR1-downregulated group remained at around 2500000 while the radiated control groups dropped down to around 1300000 (Figure 4.1 B). Overall, this result suggests that the persistent oxidative stress also contributes to the CX_3CR1-dependent radiosensitization.

A B

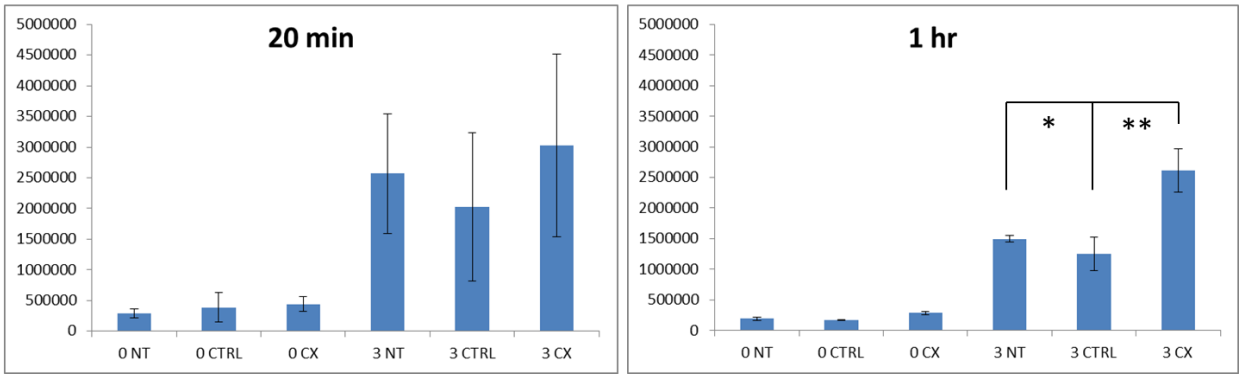

Figure 4.1 Loss of CX_3CR1 Leads to ROS Persistence. Intracellular levels of ROS were detected by flow cytometry using the DCFDA (dichlorofluorescin diacetate) fluorescence probe. Cells were collected A) 20 minutes, B) 1 hour. After DCFDA being deacetylated into a non-fluorescent compound, the presence of ROS can oxidize this compound into a highly fluorescent compound- DCF (2', 7'-dichlorofluorescein), which can be excited at 488nm and emission was measured through a 530nm band-pass filter (215). Intensity was measured by BD Accuri C6 software (BD Bioscience) and student t test was conducted by Excel. Values shown represent the mean ± SD from 3 independent experiments. *$p<0.05$, **$p<0.001$ according to student's *t* test.

4.3.2 CX_3CR1-Dependent Radiosensitization is not Mediated through Cell Cycle Arrest and Apoptosis.

To investigate the mechanism responsible for loss of CX_3CR1-induced radiosensitization, we first started with the analysis of cell cycle distribution based on my data showed in chapter 3 that transient downregulation of CX_3CR1 can inhibit the activation of checkpoint kinases chk1 and chk2 and the theory that cell cycle phase redistribution is a crucial factor deciding radiosensitivity. Therefore, SKOV3 and OVCAR4 cells were stained with propidium iodide, a DNA stain, and subjected to flow cytometer to analyze the cell cycle distribution. As shown in Figure 4.2 and 4.3, the cell cycle distribution of each phase was not significantly affected not only 0 hour, 24 hours, 48 hours after radiation, but also 10-14 days after radiation when comparing the combinational treatment group with the control groups, indicating that

synchronizing cell cycle into a more radiosensitive phase is not the result of CX_3CR1 transient knockdown-mediated enhancement in ionizing radiation-induced cell killing. Moreover, apoptosis was also not observed due to the absence of sub-G_1 phase. Therefore, both cell cycle redistribution and apoptosis are not the mechanism for the CX_3CR1-mediated alterations in radiosensitivity.

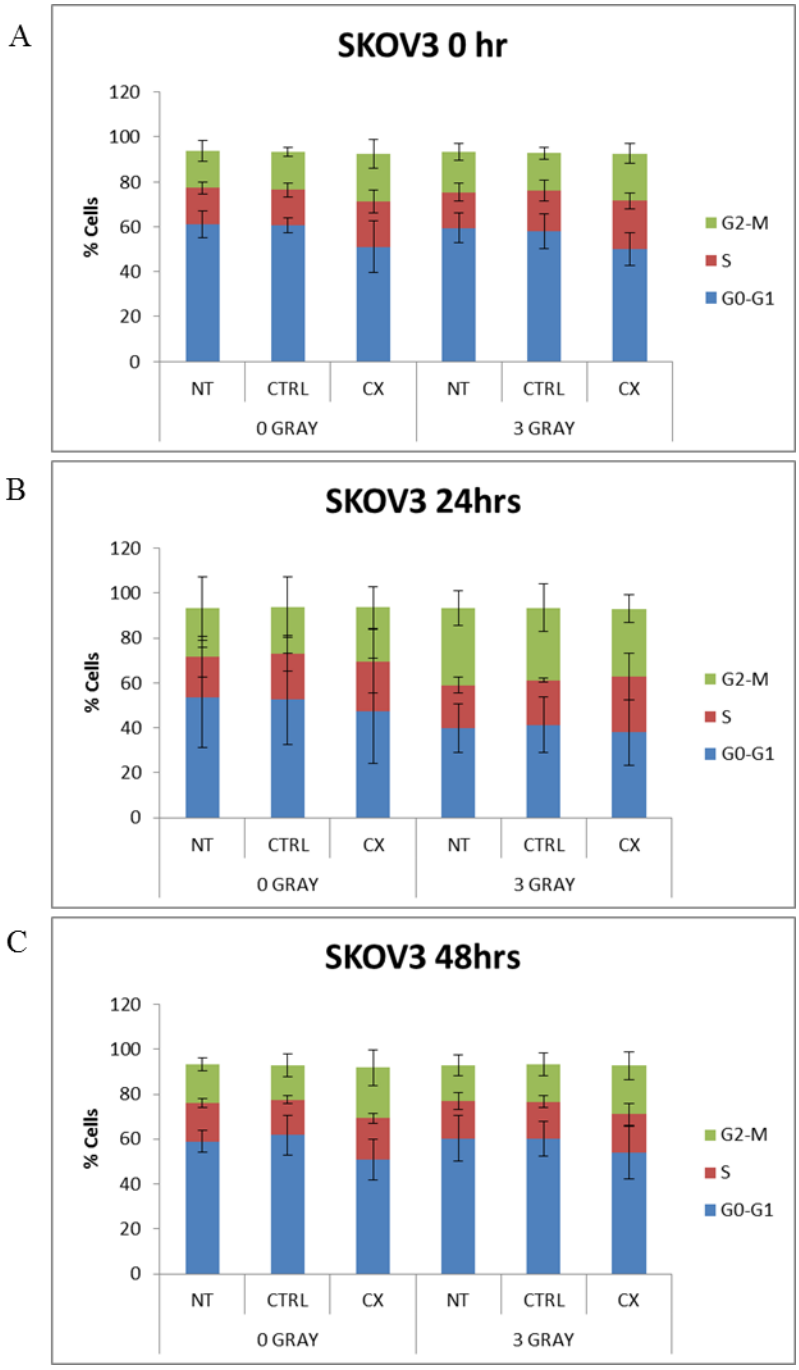

Figure 4.2 Loss of CX_3CR1 cannot Induce Cell Cycle Arrest and Apoptosis after IR. Cell cycle and apoptosis were analyzed by flow cytometry using PI. SKOV3 were collected A) 0 hour, B) 24 hours, C) 48 hours, PI is a DNA binding dye that can quantify DNA content to analysis cell cycle. The results demonstrated that CX_3CR1 downregulation cannot change the cell cycle distribution and the absence of sub-G_1 phase indicated the absence of apoptosis. Quantification analysis was conducted by FlowJo and statistical analysis was done by Excel. Values shown represent the mean $\pm$SD from 3 independent experiments.

A B

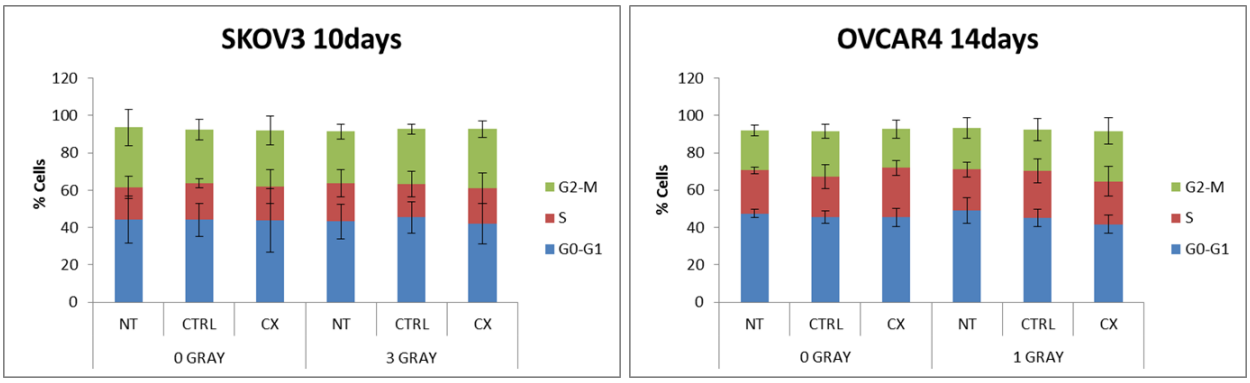

Figure 4.3 Loss of CX_3CR1 cannot Induce Cell Cycle Arrest and Apoptosis after IR. Cell cycle and apoptosis were analyzed by flow cytometry using PI. A) SKOV3 cells were collected 10 days after radiation and B) OVCAR4 cells were collected 14 days after radiation. The results demonstrated that CX_3CR1 downregulation cannot change the cell cycle distribution and the absence of sub-G_1 phase indicated the absence of apoptosis. Quantification analysis was conducted by FlowJo and statistical analysis was done by Excel. Values shown represent the mean $\pm$ SD from 3 independent experiments.

4.4 Discussion

Ionizing radiation can produce excessive amount of ROS by the radiolysis of water molecules inside the cells. The overproduced ROS can cause damage in almost all biomolecules, including DNA, membrane lipids and proteins, and ultimately lead to loss of cellular functions and viability (216). However, in cancer cells, one of the mechanisms contributing to radioresistance is the adaptation to ROS by elevating the amount of ROS-scavenging enzymes and/or by activating redox-sensitive transcriptional factors, such as NF-κB. These adaptations can help the cells to tolerate exogenous damage by enhancing DNA repair capacity and escaping from cell death. For example, ovarian cancer cells have a high capacity of ROS due to the high expression of NADPH oxidase Nox4 (217), and ovarian cancer cells can regulate the endogenous ROS level to promote their proliferation, metastasis and angiogenesis by activating NF-κB to degrade

MKP-3 and thereby activate ERK1/2 (218). Therefore, in order to sensitize ovarian cancer cells to ionizing radiation, abrogating these adaptation mechanisms by promoting ROS production and/or interfering with ROS metabolism to increase the overall level of ROS that exceed the cellular tolerability threshold could be a very important strategy to break the cellular redox homeostasis and therefore overcome the therapeutic barriers (219).

As shown in Figure 4.1, transient downregulation of CX_3CR1 leads to ROS persistence. Although 20 minutes after radiation, similar amount of free radicals was produced in all radiated group, the CX_3CR1-downregulated group displayed a weaker antioxidant ability compared to the radiated controls, indicating that the downregulation of CX_3CR1 affected the ROS metabolism. Taken together, while ionizing radiation induces ROS production, loss of CX_3CR1 can lead to persistent ROS production and therefore contribute to radiosensitization in ovarian cancer cells.

Fractalkine axis can activate the antioxidative system by activating hemeoxygenase-1 (HO-1). After CX_3CR1 get activated, the intracellular MAPK signaling is activated, among which JNK MAPK signaling plays the major role in inducing the expression of HO-1 via Nrf-2 recruitment. Nrf-2 is a transcription factor that regulates redox homeostasis by promoting the expression of multiple antioxidant enzymes such as HO-1, NADP(H) quinone oxidoreductase (NQO1), and enzymes of glutathione metabolism, etc. Therefore, in our case, it is highly possible that loss of CX_3CR1 cannot induce HO-1 expression, and the impaired anti-oxidant systems failed to scavenge ROS as effective as the radiated controls. (220, 221, 222)

Although cell cycle arrest and apoptosis are not the mechanisms contributed to CX_3CR1-dependent radiosensitization, other mechanisms, such as mitotic catastrophe, could be the possible one. As shown in chapter 3, loss of CX_3CR1 leads to the inhibition of DNA damage repair machinery, SKOV3 is p53-null, CAOV3 and OVCAR4 harbor mutated p53, and the defective DNA damage repair ultimately leads to accumulated DNA damage. These results are all consistent with the major characteristics of mitotic catastrophe. Moreover, Hayman TJ *et al.* also showed a similar result in a breast cancer cell line that elF4E transient downregulation cannot lead to cell cycle phase redistribution and apoptosis, but can induce accumulated DNA damage as characterized by the γH2A.X foci formation and mitotic catastrophe 72 hours after radiation (214). Therefore, it is highly likely that mitotic catastrophe is the mechanism for CX_3CR1-dependent radiosensitization.

4.5 Conclusion

To summarize, our present study indicated that besides DNA damage response regulation, oxidative damage responses also participate in CX_3CR1-dependent radiosensitization in ovarian cancer cells. Therefore, CX_3CR1 inhibitor can also serve as an intracellular redox state modulator to increase ovarian cancer cells' response to ionizing radiation.

CHAPTER 5.

CX_3CR1 STABLE KNOCKDOWN REDUCES OVERALL TUMOR BURDEN AND INHIBITS METASTASIS *IN VIVO*

5.1 Introduction

High-grade serous ovarian carcinoma (HGSOC) is the most aggressive form of ovarian cancer, and is a key contributor to the low overall 5-year survival rate. Most of the HGSOC are diagnosed at advanced stages when the disease has already extensively metastasized. Metastatic progression of ovarian carcinoma is very unique in that the cancer cells metastasis locoregionally in the peritoneal cavity (223), which is very different from the hematogenous dissemination, where the cancer cells intravasate into the blood vessel, transport with the blood stream, extravasate from the vessel and implant into tissues and organs (224). In ovarian carcinomas, cancer cells disseminate from the primary tumor and are carried by the peritoneal ascites following implantation at the tissues and organs in the abdominal cavity, anchorage in the submesothelial extracellular matrix and establishment of metastasis (Figure 5.1) (225, 226).

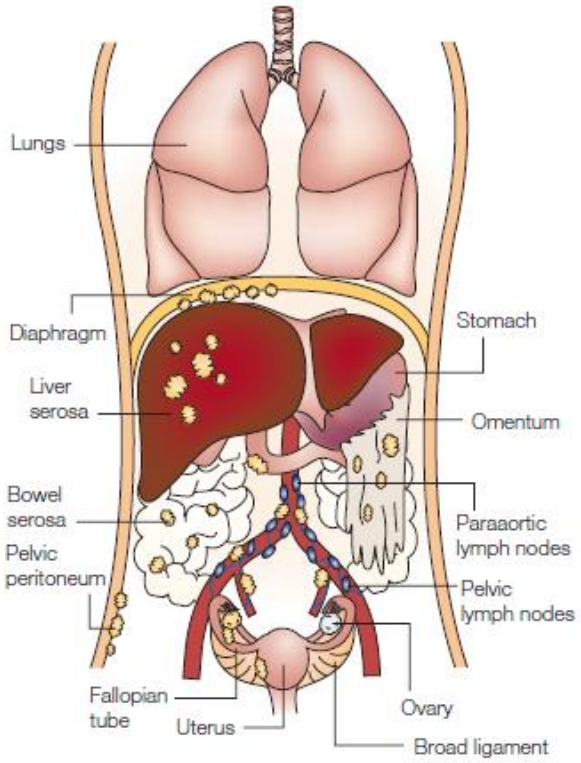

Figure 5.1 Patterns of spread of ovarian carcinoma. At its earliest stage (stage IA/IB), the tumour (shown in the figure as yellow masses) is limited to one or both ovaries, the ovarian capsule is intact, and no tumour is present on the ovarian surface or in ascites or peritoneal washings. Once the capsule is disrupted, the tumour spreads beyond the confines of the ovaries. This can occur by direct extension to, and invasion of, adjacent tissues such as the uterus, fallopian tubes, the mesothelial lining of the pelvic cavity (peritoneum), and the broad ligament (a fold of peritoneum that supports the uterus). Exfoliated tumour cells are transported by peritoneal fluid and implant on the peritoneum and mesothelial linings of pelvic and abdominal organs (serosa). Nests of tumour cells are commonly observed on the omentum (a peritoneal fold connected to the stomach and suspended over the intestines), the mesentery (a peritoneal fold anchoring the intestines to the posterior abdominal wall; not shown) and the diaphragm. Ascites is commonly associated with intraperitoneal dissemination. Tumour cells are also thought to spread through the lymphatics that drain the ovaries to the pelvic and paraaortic lymph nodes. Haematogenous dissemination is a clinically rare phenomenon, and can involve any organ including the brain, although certain organs such as the liver are more frequently involved. Reprinted with permission from *Nature Reviews Cancer*, 2005, 5: 355-366. Copyright (2005), Nature Publishing Group.

The primary metastasis site of serous ovarian carcinoma is omentum, which is a membranous double layer of fatty tissue that connects to the stomach and supports the intestines. The other metastatic sites including diaphragm, the mesentery, which is a membranous tissue anchoring the intestines to the posterior peritoneal cavity wall. Ascites are commonly observed with intraperitoneal dissemination. Ovarian cancer cells are also thought to spread through the lymphatic system that drain the ovaries to the pelvic and the paraaortic lymph nodes (227).

Despite the high clinical complete response rates of tumor-debulking surgery and chemotherapy, most of the patients with advanced ovarian carcinoma die after the cancer relapses. Therefore, it is crucial to identify new molecular targets and agents that can be used in the treatment against high-grade serous ovarian carcinoma. Fractalkine receptor, CX_3CR1, belongs to the chemokine family of G-protein coupled receptor. Our published studies have demonstrated that transient downregulation of CX_3CR1 in ovarian cancer cells can impair their migration and adhesion to peritoneal mesothelial cells *in vitro* (228). These data provided crucial evidences that the metastasis *in vivo* might also be inhibited upon CX_3CR1 downregulation.

In this chapter, we used a syngeneic model to study the ovarian cancer metastasis *in vivo*. The advantage of syngeneic models is that the immune system of the host is functional and normal, which can better represent the real situation of the tumor microenvironment.

5.2 Materials and Methods

5.2.1 Cell Line and Cell Culture

Id8 is a spontaneously tumorigenic mouse ovarian surface epithelial cell line and was purchased from Dr. Katherine F. Roby (University of Kansas Medical Center). It was cultured according to the manufacturer's instructions using minimal essential media (MEM) (Corning) supplemented with 10% fetal bovine serum (FBS) (SIGMA-ALDRICH), 0.5% penicillin/streptomycin (Corning), 0.4% amphotericin B (Corning) and 0.22% g/ml sodium bicarbonate (Santa Cruz Biotechnology) for less than 20 consecutive passages. Cells were kept at 37 ℃ and 5% CO_2 in a humidified incubator, and were routinely tested for Mycoplasma.

5.2.2 Reagents and Antibodies

Antibodies used in this research are: β-tubulin (University of Iowa, E7, 1:200), CX_3CR1 (Abcam, ab51668, 1:2000), anti-rabbit IgG, HRP-linked antibody (Cell Signaling Technology, 1:1000-1:5000), anti-mouse IgG, HRP-linked antibody (Santa Cruz Biotechnology, sc-2005, 1:500-1:3000), ECL reagents were purchased from GE Healthcare and Thermo Scientific. CX_3CR1 scrambled shRNA negative control and CX_3CR1 shRNA plasmids were purchased from Origene.

5.2.3 Stable Cell Lines Generation

Id8 cells were plated in six well plates one day before transfection. On the day of transfection, plasmids (Scrambled shRNA and CX_3CR1 shRNA plasmids) were resuspended in DNA/RNAse free water according to the manufacturer's instructions prior to use, and Id8 cells were transfected by DharmaFECT. One day post-transfection, the cells were split into 48 well plates (SIGMA-ALDRICH) and were treated with 4 μg/ml puromycin (Enzo Life Sciences) for the selection of the scrambled control clones or CX_3CR1-shRNA clones. The colonies formed from single surviving cells were isolated and re-plated into p35 plates with appropriate propagation.

CX_3CR1-shRNA/scrambled clones were maintained in regular complete MEM with 1-2 μg/ml puromycin for 2-6 weeks. Clones were screened for CX_3CR1 expression by western blot. The mouse CX_3CR1 shRNA constructs contain 4 unique sequences:

5'-AGTGCAGCACGGTGTCACCATTAGTCTGG-3',

5'-GCCTTTGGAACCATCTTCCTGTCCGTCTT-3',

5'-AGTGGCGTTCAGCCACTGTTGCCTCAACC-3',

5'-CGTGCTCCGCAACTCGGAAGTCAACATCC-3'.

5.2.4 GFP Plasmid Transfection

The appropriate amount of cells was plated onto 6 well plates one day before transfection. On the day of transfection, 1.5 μg/well GFP plasmids were transfected using DharmaFECT. Cells were maintained in antibiotic free complete media and then subjected to fluorescence microscope to check the transfection efficiency 1 day, 2 days and 3 days after transfection. The time needed to achieve the highest transfection efficiency was recorded for each cell line before being used in the experiment.

5.2.5 Animals

All animal experiments were done according to an Office of Animal Care and Institutional Biosafety (OACIB) approved protocol. Female C57BL/6 mice were used between the ages of 6-8 weeks and purchased from The Jackson Laboratory. Mice were maintained in the laminar flow room, maintaining consistent temperature and humidity and were given free access to water and a normal diet.

5.2.6 Western Blot

For the detection of CX_3CR1, the cells were lysed in lysis buffer (50mM Tris pH8, 150mM NaCl, 1% NP40, and phosphatase inhibitor cocktail tablets [Roche]) and centrifuged for 15 min at 13,200 rpm and at 4 ℃. The supernatants were quantified using the Bradford method (Bio-Rad Laboratories). The desired amount of protein was then mixed with sample loading buffer (65.8 mM Tris-HCl pH6.8, 2.1% SDS, 26.3% glycerol, 0.01% bromophenol blue and 0.5% β-mercaptoethanol right before use) and boiled for 5min. 20 μg of protein from each treatment condition was loaded on 10% SDS-PAGE, and proteins were electro-transferred onto PVDF (Millipore). The membrane was then blocked with 3% BSA for 1hr at room temperature (RT), and incubated with primary antibody for 3 hr at RT, and washed with Tris-buffered saline with 0.1% Tween 3 times, followed by incubation with secondary antibody for 1 hr at RT, and developed by enhanced chemiluminescence. The densitometric values were determined by Quantity One 1-D Analysis Software (Bio-Rad Laboratories).

5.2.7 Short-Term Adhesion Assay

One clone that harbors the stable knockdown of CX_3CR1 was used in this study, and it was named as CX2. Cells that were stably transfected with scrambled plasmids were named as SCR. In this research, 1 million cells (transfected with GFP plasmids) of each cell line: Id8, SCR and CX2 were intraperitoneally injected into the abdominal cavity of C57BL/6 mice (5 mice/group) using a 25G needle. 4 hours after injection, mice were euthanatized with carbon dioxide, followed by cervical dislocation (justified in the animal care and approved by the Animal Care Committee (ACC)). Mice were then dissected to isolate omentum, which was maintained in Leibovitz's media. Omentum was then placed under the fluorescence microscope to check the

amount of GFP-transfected cells. The number of cells that attached to omentum was calculated using the following equation:

The real number of the cells = The counted number of the cells/Transfection Efficiency

The aim of this study is to compare the difference in the adhesion ability between ovarian cancer cells and CX_3CR1-knockdown ovarian cancer cells to omentum.

5.2.8 Long-Term Overall Survival Assay

1 million cells of each cell line: Id8, SCR, CX2, CX3 and CX6 were intraperitoneally injected into the abdominal cavity of C57BL/6 mice (10 mice/group) using a 25G needle. Mice were under surveillance every other day and kept for up to 2 years until they became visibly ill. After sacrificing the animal, ascites were preserved and tumors that attached to the abdominal organs were weighed, measured and fixed in 4% para-formaldehyde.

5.2.9 Statistical Analysis

The comparison of tumor adhesion and tumor burden between different groups was done by GraphPad Prism 6, and *p* values were calculated using the student's *t* test for significance.

5.3 Results

5.3.1 Stable Downregulation of CX_3CR1 in Id8 Clones

Id8, which was cloned from the late passage mouse ovarian surface epithelial cells (MOSEC), is a spontaneously tumorigenic cell line and researchers found that after injecting Id8 into the

peritoneal cavity of C57BL/6 mice, the Id8 cells formed tumors in various organs in the abdominal cavity along with the secondary peritoneal carcinomatosis. Extensive ascites were also produced, and the histological features of the tumors resembled serous carcinoma (229). The CX_3CR1 downregulation level brought by CX_3CR1 shRNA was determined by western blot analysis (Figure 5.2). Compared to the scrambled control clones, the reduction of CX_3CR1 expression in CX2 is approximately 70%, in CX3 is approximately 78% and in CX6 is approximately 77%.

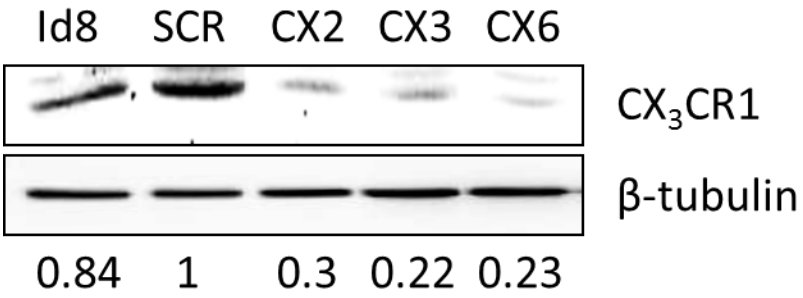

Figure 5.2 CX_3CR1 Levels in Parental Id8, Scrambled-shRNA Transfected Id8, and Three CX_3CR1-shRNA Transfected Id8 Clones. Protein levels of CX_3CR1 in various Id8 clones. CX_3CR1 was detected using anti-CX_3CR1 antibodies by Western blot analysis. Numbers below the bands are densitometry results.

5.3.2 CX_3CR1 Promotes Ovarian Cancer Cell Adhesion to Omentum

Omentum is the primary site of ovarian cancer metastasis due to its anatomical location and tissue composition. It is covered by mesothelium, which serves as a “soil” for ovarian carcinoma, and is composed of adipocytes, blood and lymph vessels, immune cells, stromal cells, and

connective matrix components (230, 231). The first step in ovarian cancer metastasis is the detachment of cancer cells from the primary tumor site, carried by the physiological movement of peritoneal fluid to omentum. Therefore, in this study, we want to examine if loss of CX_3CR1 can reduce the early adhesion of ovarian cancer cells to omentum. Our published data have demonstrated that siRNA-mediated downregulation of CX_3CR1 resulted in an approximately 50% loss of EOC cell adhesion to the human-derived peritoneal mesothelial LP-9 cells *in vitro*. In order to evaluate the *in vivo* efficacy of loss of CX_3CR1 on cancer cell adhesion, same amount of Id8, Scr and CX2 that were transfected with GFP plasmids were intraperitoneally injected into the abdomen of C57BL/6 mice. The GFP plasmid transfection efficiency for each cell line is as follows: 40% in Id8, 28% in Scr and 45% in CX2. After 4 hours of injection, the animals were dissected and omentum were isolated and observed under the fluorescent microscope for the evaluation of cancer cell adhesion. As shown in Figure 5.3, CX2 adhered significantly less to omentum compared to parental Id8 and Scr, indicating that loss of CX_3CR1 can impair the tumor cell adhesion to omentum *in vivo*.

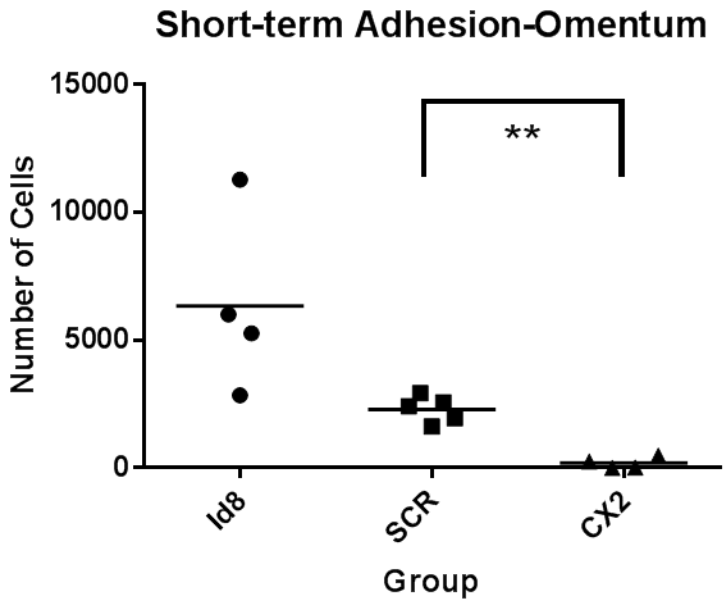

Figure 5.3 shRNA-Mediated Stable Downregulation of CX_3CR1 Resulted in Impaired Early Metastasis Event. 1 million cells of each cell line were intraperitoneally injected into each animal from each group. After 4 hours, the number of cells that were attached to omentum from each group was quantified and analyzed. The number of cells that were attached to omentum was calculated after normalizing to the transfection efficiency. Values shown represent the mean ± SEM from 5 animals. **$p<0.001$ according to student's *t* test.

5.3.3 Loss of CX_3CR1 Reduces Overall Tumor Burden

Based on the result of the short-term adhesion assay and our previously published data that fractalkine receptor may facilitate the metastatic progression of EOC by participating in migration, proliferation and peritoneal adhesion, it is logical to hypothesize that loss of CX_3CR1 can offer benefits in the reduction of overall tumor burden. In order to test this, 1 million cells from each cell line, Id8, SCR, CX2, CX3 and CX6 were intraperitoneally injected into C57BL/6 mice. Animals were under surveillance every other day and were sacrificed until they were visibly ill (unable to move and/or generated a lot of ascites). As shown in Figure 5.4, animals

that were injected with CX2, CX3 and CX6 have the least amount of overall tumor burden as assessed by tumor weight.

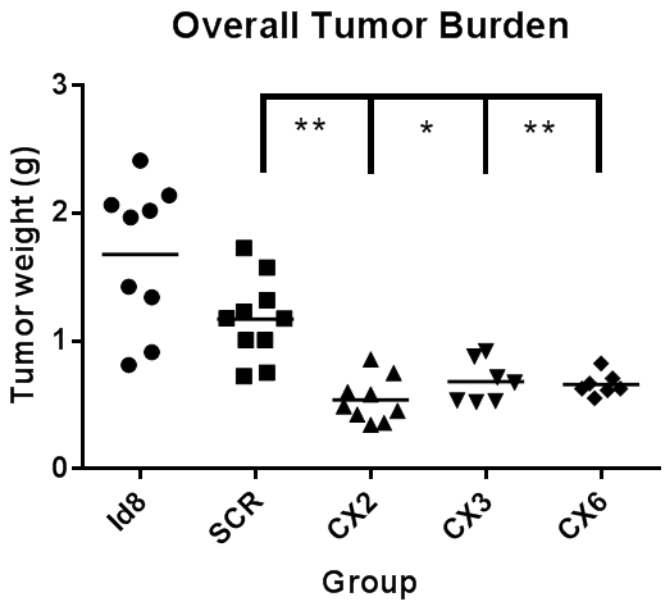

Figure 5.4 Stable Downregulation of CX_3CR1 Reduces Overall Tumor Burden. 1 million cells of each cell line were intraperitoneally injected into each animal from each group. Mice were dissected and tumors attached to each organ in the peritoneal cavity were isolated to evaluate the tumor burden when the animals were visibly ill. Values shown represent the mean ± SEM from 10 animals. *$p<0.05$, **$p<0.001$ according to student's *t* test.

5.4 Discussion

Ovarian Cancer is the most lethal gynecological malignancy due to the advanced stage of the disease at the time of diagnosis. Most disease has already spread to tissues and organs in the peritoneal cavity which makes it hard for cytoreductive surgery to be able to render patients free of disease. Ovarian cancer has a unique pattern of metastasis in which the cancer usually spreads

locoregionally in the peritoneal cavity. The transportation of cancer cells inside the abdominal cavity is frequently correlated to ascites production, which is commonly observed in patients with serous carcinoma. Moreover, since ovarian cancer cells can block part of the lymphatic system, the ascites cannot drain out of the abdomen as usual (232).

Omentum is the primary metastatic site of ovarian cancer, and it is covered by a single layer of mesothelial cells. In order to establish metastasis, cancer cells must invade through mesothelial cells. Possible mechanisms include mesothelial cell clearance through myosin-generated force and tumor-induced apoptosis (233, 234). On the other hand, Rieppi *et al.* showed that human mesothelial cells are capable of inducing ovarian cancer cell migration and promoting tumor cell adhesion (235). Therefore, mesothelial cells are also recruited by ovarian cancer cells and reprogrammed to facilitate tumor growth (236).

Why do ovarian cancer cells preferentially metastasize to omentum? Lengyel *et al.* demonstrated that human omental adipocytes, which are the main component in omentum, promote homing, migration and invasion of ovarian cancer cells through adipokines such as IL-8. Meanwhile, adipocytes can not only transfer lipids to ovarian cancer cells to promote tumor growth, but also serve as an energy source for tumor cells. Furthermore, fatty acid-binding protein 4 (FABP4) are expressed in ovarian cancer cells at the adipocyte-tumor cell interface and loss of FABP4 resulted in reduced metastatic tumor growth (237). The same group also reported that the early ovarian cancer metastasis is mediated through the interaction between fibronectin in the extracellular matrix (ECM) in omentum and α5β1 integrin in ovarian cancer cells (236). Besides adipocytes, milky spots are also part of omentum. Milky spots are comprised of immune cells,

stromal cells and structural elements surrounding glomerulus-like capillary beds. Clark *et al.* showed that milky spots and adipocytes play distinct and complementary roles in omental metastasis (230).

Our lab has also been interested in the mechanism of ovarian cancer metastasis. As our published data indicated, the interaction between CX_3CL1 that expressed in mesothelial cells and CX_3CR1 that expressed in EOC cells facilitates tumor cell migration and adhesion to peritoneal mesothelial cells *in vitro* (228). These findings were also further validated in this study. As shown in Figure 5.3, shRNA-mediated stable downregulation of CX_3CR1 resulted in impaired EOC cell adhesion to omentum *in vivo*; and as shown in Figure 5.4, the stable loss of CX_3CR1 also resulted in reduced overall tumor burden *in vivo*. Therefore, our studies demonstrated that the abrogation of the CX_3CR1-CX_3CL1 axis could be a promising approach against metastatic ovarian carcinoma.

As discussed in chapter 2, shRNA-mediated stable gene downregulation has a lot of disadvantages, such as off-target effects, unstable gene downregulation, etc. In order to overcome the technical difficulties, we are currently using the CRISPR technology to create CX_3CR1-specific knockout Id8 clones. Moreover, as discussed in chapter 1, the commercially and orally available CX_3CR1 inhibitor will also be used in our future pre-clinical models to assess its therapeutic efficacy against metastatic ovarian cancer. Furthermore, more clinical-mimic models should be applied in our animal study. Clinically, ovarian cancer patients with ascites are usually treated with ascites drainage to help relieve symptoms (238). Therefore, in the

future preclinical models, appropriate surgery procedures should be used to better evaluate the therapeutic efficacy of our approach.

5.5 Conclusion

In conclusion, our *in vivo* study indicated that loss of CX_3CR1 can abrogate ovarian cancer cells adhesion to omentum to establish metastasis and reduce overall tumor burden.

CHAPTER 6.

CONCLUSIONS AND FUTURE DIRECTIONS

6.1 Conclusions

High grade serous ovarian carcinoma is the most common of the epithelial ovarian cancers, and accounts for most of the mortality. Initially, most patients respond well to the current treatment modalities, which are the combination of cytoreductive surgery and six cycles of platinum/taxane based chemotherapy. However, the majority of the patients experience the disease recurrence, which is usually resistant to the conventional chemotherapy. Therefore, identifying novel targets and modifying current treatments could offer great benefits to these patients. Radiation therapy is usually used as a second-line therapy or palliative therapy to alleviate symptoms caused by chemotherapy. Although radiation therapy can achieve better therapeutic efficacy, especially in patients experiencing the disease recurrence, it is seldom used as a main treatment against ovarian cancer due to the dose-related severe toxicities. Therefore, discovering novel radiosensitizers could enable the widespread use of radiation therapy while control the toxicities to a tolerable level.

Fractalkine receptor, CX_3CR1, is an attractive target in ovarian cancer therapy because our publications have demonstrated that while CX_3CR1 is not expressed in the normal ovarian surface epithelium, it is expressed in the majority of pathologic ovarian surface (239). Moreover, the fractalkine axis (CX_3CR1-CX_3CL1) play a pivotal role in facilitating epithelial ovarian cancer metastasis. Therefore, targeting fractalkine axis could be a promising treatment against ovarian malignancies.

My study demonstrated that transient downregulation of fractalkine receptor in epithelial ovarian cancer cell lines leads to radiosensitization through multiple mechanisms, including impaired DNA damage repair machinery and persistence of the oxidative stress. My research indicated that CX_3CR1 inhibitor could be a radiosensitizer in ovarian cancer therapeutics.

6.1.1 Loss of CX_3CR1 Selectively Sensitizes Epithelial Ovarian Cancer Cell Lines that Resemble HGSOC Tumors to Ionizing Radiation.

Our study shows that transient downregulation of CX_3CR1 using siRNA effectively sensitized most of the epithelial ovarian cancer cells that resemble HGSOC tumors to ionizing radiation. Using the clonogenic assay, we found that transient loss of CX_3CR1 followed by increasing doses of ionizing radiation effectively decreased surviving fraction and colony formation compared to either treatment alone. (Figure 2.5-2.8 and Table 2.1). The cell lines that we used to mimic the HGSOC tumors are SKOV3, CAOV3, OVCAR4 and OVSAHO. While CAOV3, OVCAR4 and OVSAHO expressed mutated p53, SKOV3 is p53 null. These features agree with one of the most important genomic characteristics of HGSOC that TP53 mutations are universal events. IGROV-1 and A2780 were recently defined as non-HGSOC subtype, partially due to the reason that both of them have wild-type TP53. However, transient loss of CX_3CR1 cannot radiosensitize these two p53 functional cell lines, indicating that in ovarian tumors with normal p53, our treatment combination is not an ideal model; however, it also indicates that this treatment combination has little damage on normal tissue. Therefore, the enlarged therapeutic window with high selectivity in high grade serous ovarian cancer models makes the combinational treatment of CX_3CR1 inhibitor and ionizing radiation a clinically effective therapeutic strategy against this deadly disease. Moreover, even though OVSAHO is one of the

representative cellular models of high grade serous ovarian carcinoma, it cannot be sensitized to ionizing radiation upon CX_3CR1 downregulation, indicating the type of p53 mutation might also affect cellular response to ionizing radiation.

6.1.2 CX_3CR1-Dependent Radiosensitization in High Grade Serous Ovarian Cancer Cells is Mediated through Multiple Mechanisms.

There are several altered characteristics that may contribute to resistance to ionizing radiation, including enhanced DNA damage repair, acquired resistance to apoptosis, and adaptive response to the exogenous radiation-induced ROS, etc. Therefore, a combination of ionizing radiation with drugs that can modulate these resistance-related traits can theoretically enhance radiosensitivity. Since cell lines that resemble HGSOC tumors are TP53 mutated, and TP53 is the most extensively studied tumor suppressor gene, these cells are believed to be intrinsically resistant to cell cycle arrest, apoptosis, senescence and DNA damage repair (240, 241, 242). Thus, drugs that can impair DNA damage repair pathway and/or can modulate intracellular redox status are the ideal radiosensitizers. Figure 3.5-3.9 and Figure 3.12-3.15 clearly illustrate that transient downregulation of CX_3CR1 can abrogate the phosphorylation and activation of DNA damage response related genes, including ATM, chk1, chk2, DNA-PKcs and γH2A.X short after radiation, and the unrepaired DNA damage in radiated and CX_3CR1-downregulated cells lead to radiosensitization. Moreover, Figure 4.1 also show that transient downregulation of CX_3CR1 leads to persistent oxidative damage in radiated group. Furthermore, compared to combining ionizing radiation with ATM inhibitors or Chk1/2 inhibitors, the combination with the orally available CX_3CR1 inhibitor is more disease-specific, due to the specific expression of CX_3CR1

in the pathologic ovarian surface. The whole schematic summary of the mechanisms of radiosensitization is shown in Figure 6.1.

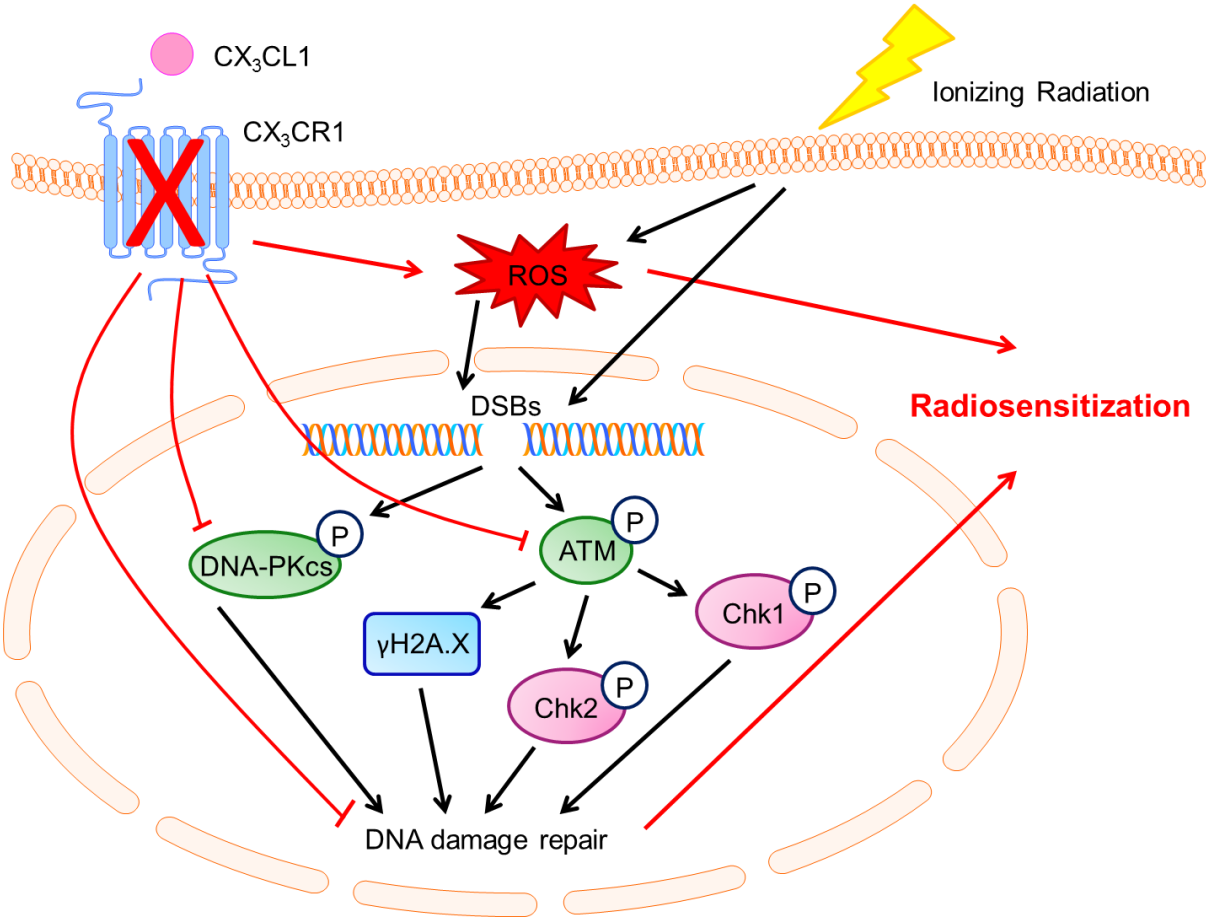

Figure 6.1 Scheme of CX_3CR1-Dependent Radiosensitization.

6.1.3 CX_3CR1 is a Promising Cellular Target against Metastatic Ovarian Cancer

Most ovarian cancer patients are diagnosed at the time when the disease has already progressed to its late stage. The current therapeutic approaches fail to keep patients in remission mainly due

to the massive uncontrollable metastasis in the abdominal organs, especially omentum. Therefore, it is very important to identify and validate a molecule that can target the malignant cells that lead to metastasis. Meanwhile, the residual tumor determines the possibility of secondary metastasis and survival for the patients. Hence, strategies to minimize and diminish peritoneal spread of EOC metastasis, retard their growth and prevent re-implantation are likely to increase the progression-free and the overall survival for the ovarian cancer patients. Our published data have already demonstrated that the abrogation of CX_3CR1-CX_3CL1 axis is potential in reducing ovarian cancer cell adhesion to human mesothelial cells *in vitro*, and my study further suggests that loss of CX_3CR1 can reduce the metastasis *in vivo*. Therefore, CX_3CR1 is a promising target against metastatic ovarian carcinoma.

Taken together, this dissertation study demonstrates that loss of CX_3CR1 can sensitize high grade serous ovarian cancer cells to ionizing radiation through the regulation of DNA damage response and intracellular redox status. Although CX_3CR1 antagonists have been commercially available, they are not evaluated in ovarian cancer animal models and clinical studies yet. Therefore, the safety, the tolerability, the pharmacokinetics and the pharmacodynamics of CX_3CR1 antagonists are remained largely unknown. Due to the promising results from our *in vitro* study, more attention should be put on the development of CX_3CR1 antagonists and used them as radiosensitizers against the disease. Moreover, the radiation technology has been significantly advanced in the past two decades. Traditionally, whole abdomen radiation therapy (WAR) was used as a major technique in radiation therapy against ovarian cancer. However, there are a lot of technology-related toxicities that prevent the widespread use of WAR. For instance, the insufficient coverage of the big target volume and the poor sparing of organs at risk

(OAR) can cause severe toxicities (243, 244). The whole abdominal-pelvic cavity is a large area with a lot of organs in different shapes, and because liver and kidney are very sensitive to radiation, even low doses of radiation can cause permanent damage. Partial kidney and liver blocks are usually used with anterior/posterior beam arrangement, which produce a highly inhomogeneous dose distribution (245, 246). Although other methods, such as moving strip technique, was used to improve dose homogeneity, the result came with very limited success (247). Nowadays, radiation techniques have been improved a lot together with the imaging technology. Linear accelerator (LA)-based intensity-modulated radiotherapy (IMRT), volumetric intensity-modulated arc therapy (IMAT), and helical tomotherapy (HT) have shown strong potential in achieving homogeneous dose distribution and better sparing of OARs (248, 249, 250). Therefore, applying the latest radiation technique with the potential CX_3CR1 inhibitor could be a promising therapy against HGSOC.

6.2 Future Directions

Our study reveals that CX_3CR1 inhibition has the potential of sensitizing ovarian cancer cells that resemble HGSOC to ionizing radiation. However, there are still several unresolved questions needed to be answered. It is still unknown how CX_3CR1 regulates ATM, how CX_3CR1 changes the antioxidant system capacity, what is the biological consequence of persistent DNA damage and oxidative damage, and what kind of clinically relevant animal model we could use to evaluate our combinational approach *in vivo*. Therefore, future studies still need to be done to clarify these problems.

NF-κB might play a crucial role in mediating CX_3CR1-dependent radiosensitization. It is important in the development of tumor radioresistance by regulating cell cycle, preventing apoptosis, increasing DNA damage repair capacity and detoxifying ROS (251). NF-κB belongs to the Rel family proteins, which include RelA, RelB, C-Rel, NF-κB1 and NF-κB2 (252). It can be activated by IR either through nuclear or cytoplasmic pathway (253). Nuclear pathway is regulated by the phosphorylation of ATM while cytoplasmic pathway involves the activation of PI3K/Akt or ROS-mediated NIK(NF-κB-inducing kinase). In inactivated cells, NF-κB is sequestered in the cytoplasm by its inhibitor IκB. After radiation, IκB is phosphorylated, ubiquitinated, proteolytically degraded, and thereby releasing NF-κB and allowing it to translocate into the nucleus and activate the downstream gene expression. Therefore, NF-κB is a crucial element in mediating cellular responses to ionizing radiation. Fractalkine axis can regulate the activation and translocation of NF-κB through multiple pathways, including PI3K pathway and MAPK pathway (254). NF-κB can also be activated upon CAMKII (calmodulin-dependent protein kinase II) expression induced by the release of intracellular Ca++ (255), and our publication showed that CX_3CR1 activation can trigger robust release of intracellular Ca++. Taken together, NF-κB is a promising bridge to connect CX_3CR1 and radiosensitivity. It is highly possible that loss of CX_3CR1 inhibits NF-κB, and then inhibits the DNA damage repair machinery as well as the antioxidant system and thereby sensitizing ovarian cancer cells to ionizing radiation. Therefore, one of the future studies should focus on the change of the NF-κB DNA-binding activity upon CX_3CR1 downregulation.

Furthermore, it is also important to test our combinational treatment *in vivo*. The growth delay assay is usually used to assess the tumor radiosensitization effect *in vivo* (256, 257). Generally

speaking, a certain amount of ovarian cancer cells that have *in vivo* tumorigenic ability are prepared in single cell suspension and injected subcutaneously into the lateral aspect of the right leg of the athymic nude mice. When the mean volume of tumors reaches a certain size (such as 200mm^3), mice are then randomized into four groups: non-treatment group, radiation only group, CX_3CR1 antagonist only group and the combinational group (radiation and CX_3CR1 antagonist). Tumors can be irradiated locally using the Linac accelerator with animals restrained in a custom designed lead jig, and CX_3CR1 antagonist can be given by oral gavage due to its good oral bioavailability. To obtain growth curves, perpendicular diameter measurement of each tumor is measured 3 times per week with caliper and volumes are calculated using the formula: length [L] * width [W] *width [W])/2 (258). The end point for each animal is when the tumor volume reaches a bigger value (such as 2000mm^3). The time to grow from the initial tumor volume to the final tumor volume of the treated mice minus that of the control mice is calculated to determine the absolute growth delays and the dose enhancement factor (DEF) is calculated based on the following formula: DEF=absolute tumor growth delay (combined treatment)/absolute growth delay (radiation alone). If DEF is more than 1.1, then the combinational treatment can be advanced into more clinically relevant models to assess therapeutic efficacy (259). My work in this dissertation together with the proposed future works will play a critical role in adjusting current ovarian cancer therapy and offering significant benefits to patients.

CITED LITERATURE

1. Prat, J. New insights into ovarian cancer pathology. *Ann Oncol*. 2012, 23, 111-117.

2. Zhang B, Barekati Z, Kohler C, Radpour R, Asadollahi R., Holzgreve W., Zhong XY. Proteomics and biomarkers for ovarian cancer diagnosis. *Ann Clin Lab Sci*. 2010. 40(3): 218-225

3. Desai, A, Xu J, Aysola K., Qin Y., Okoli C., Hariprasad, R., Chinemerem U., Gates C., Reddy A., Danner O., Franklin G., Ngozi A., Cantuaria G., Singh K., Grizzle W., Landen C., Partridge EE., Rice VM, Reddy ESP, Rao VN. Epithelial ovarian cancer: an overview. *World J Transl Med*. 3(1):1-8. 2014

4. Delair D, Soslow RA. Key features of extrauterine pelvic serous tumours (fallopian tube, ovary, and peritoneum). *Histopathology*. 2012, 61(3): 329-339

5. Berns EM, Bowtell DD. The changing view of high-grade serous ovarian cancer. *Cancer Res*. 2012. 72(11). 2701-2704.

6. Erickson BK, Conner MG, Landen CN Jr. The role of the fallopian tube in the origin of ovarian cancer. *Am J Obstet Gynecol*. 2013. 209(5):409-414.

7. Nik NN, Vang R, Shih IeM, Kurman RJ. Origin and pathogenesis of pelvic (ovarian, tubal, and primary peritoneal) serous carcinoma. *Annu Rev Pathol*. 2014. 9:27-45.

8. Adami HO, Hsieh CC, Lambe M., Trichopoulos D., Leon D, Persson I., Ekbom A., Janson PO. Parity, age at first childbirth, and risk of ovarian cancer. *Lancet*. 1994. 344(8932):1250-1254

9. Robbins CL, Whiteman MK, Hillis SD, Curtis KM, McDonald JA, Wingo PA, Kulkarni A., Marchbanks PA. Influence of reproductive factors on mortality after epithelial ovarian cancer diagnosis. *Cancer Epidemiol Biomarkers Prev*. 2009.18(7):2035-2041

10. Coticchia CM, Yang J, Moses MA. Ovarian cancer biomarkers: current options and future promise. *J Natl Compr Canc Netw*. 2008. 6(8):795-802

11. Zhang B, Cai FF, Zhong XY. An overview of biomarkers for the ovarian cancer diagnosis. *Eur J Obstet Gynecol Reprod Biol*. 2011. 158(2): 119-23

12. Cortez MA, Valdecanas D, Zhang X, Zhan Y, Bhardwaj V, Calin GA, Komaki R, Giri DK, Quini CC, Wolfe T., Peltier HJ, Badar AG, Heymach JV, Meyn RE, Welsh JW. Therapeutic delivery of miR-200c enhances radiosensitivity in lung cancer. *Mol Ther*. 2014 22(8):1494-1503

13. Resnick KE, Alder H, Hagan JP, Richardson DL, Croce CM, Cohn DE. The detection of differentially expressed microRNAs from the serum of ovarian cancer patients using a novel real-time PCR platform. *Gynecol Oncol*. 2009. 112(1):55-59

14. Taylor DD, Gercel-Taylor C. MicroRNA signatures of tumor-derived exosomes as diagnostic biomarkers of ovarian cancer. *Gynecol Oncol*. 2008. 110(1):13-21

15. Lintz KC, Penson RT, Chabner BA, Lynch TJ. Schwartz Center Rounds. A staff dialogue on caring for an intensely spiritual patient: psychosocial issues faced by patients, their families, and caregivers. *Oncologist*. 1998, 3(6) 439-445

16. Pectasides D, Pectasides E. Maintenance or consolidation therapy in advanced ovarian cancer. *Oncology*. 2006. 70(5):315-324

17. Gelblum D, Mychalczak B, Almadrones L, Spriggs D, Barakat R. Palliative benefit of external-beam radiation in the management of platinum refractory epithelial ovarian carcinoma. *Gynecol Oncol*. 1998. 69(1):36-41.

18. Tinger A, Waldron T, Peluso N, Katin MJ, Dosoretz DE, Blitzer PH, Rubenstein JH, Garton GR, Nakfoor BA, Patrice SJ, Chuang L, Orr JW Jr. Effective palliative radiation therapy in advanced and recurrent ovarian carcinoma. *Int J Radiat Oncol Biol Phys*, 2001. 51(5):1256-1263

19. Gadducci A, Cosio S, Conte PF, Genazzani AR. Consolidation and maintenance treatments for patients with advanced epithealial ovarian cancer in complete response after first-line chemotherapy: a review of the literature. *Crit Rev Oncol Hematol*. 2005 55(2):153-166

20. Lee M, Kim SW, Lee SH, Paek J, Yim GW, Kim GE, Kim S, Kim JH, Kim YT, Nam EJ. Comparison of the efficacy and toxicity between radiotherapy and chemotherapy in nodal and isolated nonnodal recurrence of ovarian cancer. *Int J Gynecol Cancer*. 2011 21(6):1032-1039

21. Lee SW, Park SM, Kim YM, Kim YS, Choi EK, Kim DY, Kim JH, Nam JH, Kim YT. Radiation therapy is a treatment to be considered for recurrent epithelial ovarian cancer after chemotherapy. *Tumori*. 2011. 97(5):590-595

22. Pickel H, Petru E, Lahousen M, Stettner H, Heydarfadai M, Arian Schad K, Hackl A. Consolidation radiotherapy following carboplatin-based chemotherapy in radically operated advanced ovarian cancer. A pilot study. *Am J Clin Oncol*. 1991. 14(3):184-187

23. Rochet N, Lindel K, Katayama S, Schubert K, Herfarth K, Schneeweiss A, Sohn C, Harms W, Debus J. Intensity-modulated whole abdomen irradiation following adjuvant carboplatin/taxane chemotherapy for FIGO stage III ovarian cancer: Four-year outcomes. *Strahlenther Onkol*. 2015. 191(7):582-589

24. Coleman R, Coleman F. Radiation therapy in the management of epithelial ovarian cancer. *Glob Libr Women's Med*. 2008. ISSN: 1756-2228. DOI 10.3843/GLOWM.10254

25. Scripture CD, Figg WD, Sparreboom A. Peripheral neutropathy induced by paclitaxel: recent insights and future perspective. *Curr Neuropharmacol*. 2006. 4(2):165-172

26. Peters CM, Jimenez-Andrade JM, Kuskowski MA, Ghilardi JR, Mantyh PW. An evolving cellular pathology occurs in dorsal root ganglia, peripheral nerve and spinal cord following intravenous administration of paclitaxel in the rat. *Brain Res*. 2007;1168:46–59

27. Corn BW, Lanciano RM, Boente M, Hunter WM, Ladazack J, Ozols RF. Recurrent ovarian cancer. Effective radiotherapeutic palliation after chemotherapy failure. *Cancer*. 1994. 74(11):2979-2983

28. Rontgen WK. A new form of radiation. *Science*. 1896. 3(72):726-729

29. Hall EJ, Giaccia AJ. *Radiobiology for the radiologist*. 7th edition

30. Elkind MM, Sutton-Gilbert H, Moses WB, Alescio T, Swain RW. Radiation response of mammalian cells grown in culture. V. temperature dependence of the repair of x-ray damage in surviving cells. (aerobic and hypoxic). *Radiat Res*. 1965. 359-376

31. H.R. Withers. The four R's of radiotherapy. J.T. Lett, H. Adler (Eds), Advances in radiation biology, *Academic Press*, New York. 1975. 241-247

32. Harrington K. A modern interpretation of the 5 Rs of radiobiology and their impact on clinical practice. *National Cancer Research Institute*

33. Williams GH, Stoeber K. The cell cycle and cancer. *J Pathol*. 2012. 226(2):352-364

34. Pawlik TM, Keyomarsi K. Role of cell cycle in mediating sensitivity to radiotherapy. *Int J. Radiat Oncol. Biol Phys*. 2004. 59(4):928-942

35. Pajonk F., Vlashi E, McBride WH. Radiation resistance of cancer stem cells: the 4 R's of radiobiology revisited. *Stem cells*. 2010. 28(4):639-648

36. Chatterjee A. Reduced glutathione: a radioprotector or a modulator of DNA-repair activity? *Nutrients*. 2013 5(2):525-542

37. Baird MC, Hendry JH, Testa NG. Radiosensitivity increases with differentiation status of murine hemopoietic progenitor cells selected using enriched marrow subpopulations and recombinant growth factors. *Radiat Res.* 1990. 123(3):292-298

38. Povinelli B, Kokolus KM, Curtin L, Repasky EA, Nemeth M. The influence of metabolic stress on radiosensitivity of hematopoietic stem and progenitor cells. *Blood*. 122(21), 2447

39. Schwachofer JH, Crooijmans RP, Hoogenhout J, Jerusalem CR, Kal HB, Theeuwes AG. Radiosensitivity of human melanoma spheroids influenced by growth rate. *Int J Radiat Oncol Biol Phys*. 1990. 19(5)"1191-1197

40. DeVita VT Jr, Chu E. A history of cancer chemotherapy. *Cancer Res*. 2008. 68(21):8643-8653

41. Mihlon F, Ray CE, Messersmith W. Chemotherapy agents: a primer for the interventional radiologist. *Semin Intervent Radiol*. 2010. 27(4):384-390

42. Agarwal R, Kaye SB. Ovarian cancer: strategies for overcoming resistance to chemotherapy. *Nat Rev Cancer*. 2003. 3(7):502-516

43. Kelland L. The resurgence of platinum-based cancer chemotherapy. *Nat Rev Cancer*. 2007. 7(8):573-584

44. Burger RA, Brady MF, Bookman MA, Fleming GF, Monk BJ, Huang H, Mannel RS, Homesley HD, Flowler J, Greer BE, Boente M, Birrer MJ, Liang SX, Gynecologic Oncology Group. Incorporation of bevacizumab in the primary treatment of ovarian cancer. *N Engl J Med*. 2011. 365(26):2473-2483

45. Perren TJ, Swart AM, Pfisterer J, Ledermann JA, Pujade-Lauraine E, Kristensen G, Carey MS, Beale P, Cervantes A, Kurzeder C, du Bios A, Sehouli J, Kimmiq R, Stahle A, Collinson F, Essapen S, Gourley C, Lortholary A, Selle F, Mirza MR, Leminen A, Plante M, Stark D, Qian W, Parmar MK, Oza AM, ICON7 Investigators. A phase 3 trial of bevacizumab in ovarian cancer. *N Eng J Med*. 2011. 365(26):2484-2496

46. Keighobadi M, Fakhar M, Emami S. Hypothesis: The potential application of doxorubicin against cutaneous leishmaniasis. *Trop Parasitol*. 2015. 5(1):69-70

47. Chatterjee K, Zhang J, Honbo N, Karliner JS. Doxorubicin Cardiomyopathy. *Cardiology*. 2010. 115(2):155-162

48. Sorbe B, Swedish-Norgewian Ovarian Cancer Study Group. Consolidation treatment of advanced (FIGO stage III) ovarian carcinoma in complete surgical remission after induction chemotherapy: a randomized, controlled, clinical trial comparing whole abdominal radiotherapy, chemotherapy, and no further treatment. *Int J Gynecol Cancer*. 2003. 13(3):278-286

49. Menczer J, Ben-Baruch G, Rizel S, Brenner H. Intraperitoneal cisplatin chemotherapy in ovarian carcinoma patients who are clinically in complete remission. *Gynecol Oncol*. 1992. 46(2):222-225

50. Bookman MA, Brady MF, McGuire WP, Harper PG, Alberts DS, Friedlander M, Colombo N, Fowler JM, Argenta PA, De Geest K, Mutch DG, Burger RA, Swart AM, Trimble EL, Accario-Winslow C, Roth LM. Evaluation of new platinum-based treatment

regimens in advanced-stage ovarian cancer: a phase III trial of the gynecologic cancer intergroup. *J Clin Oncol*. 2009. 27(9):1419-1425

51. Bicher HI, Hetzel FW, Sandhu TS, Frinak S, Vaupel P, O'Hara MD, O'Brien T. Effects of hyperthermia on normal and tumor microenvironment. *Radiology*. 1980. 137(2):523-530

52. Griffin RJ, Dings RPM, Jamshidi-Parsian A, Song CW. Mild temperature hyperthermia and radiation therapy: role of tumor vascular thermotolerance and relevant physiological factors. *Int J Hyperthermia*. 2010. 26(3):256-263

53. Kalamida D, Karagounis IV, Mitrakas A, Kalamide S, Giatromanolaki A, Koulourakis MI. Fever-range heperthermia vs. hypothermia effects on cancer cell viability, proliferation and HSP90 expression. *PloS One*. 2015. 10(1): e0116021

54. Peer AJ, Grimm MJ, Zynda ER, Repasky EA. Diverse immune mechanisms may contribute to the survival benefit seen in cancer patients receiving hyperthermia. *Immunol Res*. 2010. 46(1-3):137-154

55. Muenyi CS, States VA, Masters JH, Fan TW, Helm CW, States JC. Sodium arsenite and hyperthermia modulate cisplatin-DNA damage responses and enhance platinum accumulation in murine metastatic ovarian cancer xenograft after hyperthermic intraperitoneal chemotherapy (HIPEC). *J Ovarian Res*. 2011. 4:9

56. Deraco M, Kusamura S, Virzi S, Puccio F, Macri A, Famulari C, Solazzo M, Bonomi S, Lusco DR, Baratti D. Cytoreductive surgery and hyperthermic intraperitoneal chemotherapy as upfront therapy for advanced epithelial ovarian cancer: multi-institutional phase-II trial. *Gynecol Oncol*. 2011. 122(2):215-220

57. Thomas GM, Dembo AJ. Integrating radiation therapy into the management of ovarian cancer. *Cancer*. 1993. 71(4 Suppl):1710-1718

58. Arian-Schad KS, Kapp DS, Hackl A, Juettner FM, Leitner H, Porsch G, Lahousen M, Pickel H. Radiation therapy in stage III ovarian cancer following surgery and chemotherapy: prognostic factors, patterns of relapse, and toxicity: a preliminary report. *Gynecol Oncol*. 1990. 39(1):47-55

59. Kim M, Rooper L, Xie J, Kajdacsy-Balla AA, Barbolina MV. Fractalkine receptor CX_3CR1 is expressed in epithelial ovarian carcinoma cells and required for motility and adhesion to peritoneal mesothelial cells. *Mol Cancer Res*. 2012 10(1):11-24

60. Wojdasiewicz P, Poniatowski LA, Kotela A, Deszczynski J, Kotela I, Szukiewicz D. The chemokine CX_3CL1 (fractalkine) and its receptor CX_3CR1: occurrence and potential role in osteoarthritis. *Arch Immunol Ther Exp (Warsz).* 2014 62(5):395-403

61. Tang XL, Wang Y, Li DL, Luo J, Liu MY. Orphan G protein-coupled receptors (GPCRs): biological functions and potential drug targets. *Acta Pharmacol Sin*. 2012. 33(3): 363-371

62. Muralidhar GG, Barbolina MV. Chemokine receptors in epithelial ovarian cancer. *Int J Mol Sci*. 2014. 15(1):361-376

63. Ferretti E, Pistoia V, Corcione A. Role of fractalkine/CX_3CL1 and its receptor in the pathogenesis of inflammatory and malignant diseases with emphasis on B cell malignancies. *Mediators Inflamm*. 2014. 2014:480941

64. Bacon K, Baggiolini M, Broxmeyer H, Horuk R, Lindley I, Mantovani A, Maysushima K, Murphy P, Nomiyama H, Oppenheim J, Rot A, Schall T, Tsang M, Thorpe R, Van Damme J, Wadhwa M, Yoshie O, Zlotnik A, Zoon K,IUIS/WHO subcommittee on chemokine nomenclature. Chemokine/chemokine receptor nomenclature. *J Interferon Cytokine Res*. 2002. 22(10): 1067-1068

65. Apostolakis S, Spandidos D. Chemokines and atherosclerosis: focus on the CX_3CL1/CX_3CR1 pathway. *Acta Pharmacol Sin*. 2013. 34(10):1251-1256

66. White GE, Tan TC, John AE, Whatling C, McPheat WL, Greaves DR. Fractalkine has anti-apoptotic and proliferative effects on human vascular smooth muscle cells via epidermal growth factor receptor signaling. *Cardiovasc Res*. 2010. 85(4):825-835

67. Fernandez EJ, Lolis E. Structure, function, and inhibition of chemokines. *Annu Rev Pharmacol Toxicol*. 2002. 42:469-499

68. Schwarz N, Pruessmeyer J, Hess FM, Dreymueller D, Pantaler E, Koelsch A, Windoffer R, Voss M, Sarabi A, Weber C, Sechi AS, Uhliq S, Ludwig A. Requirements for leukocyte transmigration via the transmembrane chemokine CX_3CL1. *Cell Mol Life Sci*. 2010. 67(24):4233-4248

69. Allen SJ, Crown SE, Handel TM. Chemokine: receptor structure, interactions, and antagonism. *Annu Rev Immunol*, 2007. 25:787-820

70. Denis C, Sauliere A, Galandrin S, Senard JM, Gales C. Probing heterotrimeric G protein activation: applications to biased ligands. *Curr Pharm Des*. 2012, 18(2):128-144

71. Zoughlami Y, Voermans C, Brussen K, van Dort KA, Kootstra NA, Maussang D, Smit MJ, Hordijk PL, van Hennik PB. Regulation of CXCR4 conformation by the small GTPase Rac1: implications for HIV infection. *Blood*. 2012. 119(9):2024-2032

72. McCudden CR, Hains MD, Kimple RJ, Siderovski DP, Willard FS. G-protein signaling: back to the future. *Cell Mol Life Sci*. 2005. 62(5):551-557

73. Smrcka AV. Molecular targeting of Gα and Gβγ subunits: a potential approach for cancer therapeutics. *Trends Pharmacol Sci*. 2013. 34(5):290-298

74. Green MM, Petreaca M, Wang L. Chemokines and their receptors are key players in the orchestra that regulates wound healing. *Adv Wound Care (New Rochelle)*. 2013. 2(7):327-347

75. McComb JG, Ranganathan M, Liu XH, Pilewski JM, Ray P, Watkins SC, Choi AMK, Lee JS. CX_3CL1 up-regulation is associated with recruitment of CX_3CR1^+ mononuclear phagocytes and T lymphocytes in the lungs during cigarette smoke-induced emphysema. *Am J Pathol*. 2008. 173(4):949-961

76. Fong AM, Robinson LA, Steeber DA, Tedder TF, Yoshie O, Imai T, Patel DD. Fractalkine and CX_3CR1 mediate a novel mechanism of leukocyte capture, firm adhesion, and activation under physiologic flow. *J Exp Med*. 1998. 188(8):1413-1419

77. Harrison JK, Jiang Y, Chen S, Xia Y, Maciejewski D, McNamara RK, Streit WJ, Salafranca MN, Adhikari S, Thompson DA, Botti P, Bacon KB, Feng L. Role for neuronally derived fractalkine in mediating interactions between neurons and CX_3CR1-expressing microglia. *Proc Natl Acad Sci U S A*. 1998. 95(18):10896-10901

78. Shulby SA, Dolloff NG, Stearns ME, Meucci O, Fatatis A. CX_3CR1-fractalkine expression regulates cellular mechanisms involved in adhesion, migration, and survival of human prostate cancer cells. *Cancer Res*. 2004. 64(14):4693-4698

79. Erreni M, Solinas G, Brescia P, Osti D, Zunino F, Colombo P, Destro A, Roncalli M, Mantovani A, Draghi R, Levi D, Rodriguez Y Baena R, Gaetani P, Pelicci G, Allavena P. Human glioblastoma tumours and neural cancer stem cells express the chemokine CX_3CL1 and its receptor CX_3CR1. *Eur J Cancer*. 2010. 46(18):3383-3392

80. Marchesi F, Piemonti L, Fedele G, Destro A, Roncalli M, Albarello L, Doglioni C, Anselmo A, Doni A, Bianchi P, Laghi L, Malesci A, Cervo L, Malosio M, Reni M, Zerbi A, Di Carlo V, Mantovani A, Allavena P. The chemokine receptor CX_3CR1 is involved in the neural tropism and malignant behavior of pancreatic ductal adenocarcinoma. *Cancer Res*. 2008. 68(21) 9060-9069

81. Jamieson-Gladney WL, Zhang Y, Fong AM, Meucci O, Fatatis A. The chemokine receptor CX_3CR1 is directly involved in the arrest of breast cancer cells to the skeleton. *Breast Cancer Res*. 2011. 13(5):R91

82. Lavergne E, Combadiere B, Bonduelle O, Iga M, Gao JL, Maho M, Boissonnas A, Murphy PM, Debre P, Combadiere C. Fractalkine mediates natural killer-dependent antitumor responses *in vivo*. *Cancer Res*. 2003. 63(21):7468-7474

83. Hart KM, Bak SP, Alonso A, Berwin B. Phenotypic and functional delineation of murine CX_3CR1 monocyte-derived cells in ovarian cancer. *Neoplasia*. 2009. 11(6):564-573

84. Gaudin F, Nasreddine S, Donnadieu AC, Emilie D, Combadiere C, Prevot S, Machelon V, Balabanian K. Identification of the chemokine CX_3CL1 as a new regulator of malignant cell proliferation in epithelial ovarian cancer. *PLoS One*. 2011. 6(7):e21546

85. Rooper L, Gurler H, Kajdacsy-Balla AA, Barbolina MV. Fractalkine receptor is expressed in mature ovarian teratomas and required for epidermal lineage differentiation. *J Ovarian Res*. 2013. 6(1):57

86. Dorgham K, Ghadiri A, Hermand P, Rodero M, Poupel L, Iga M, Hartley O, Gorochov G, Combadiere C, Deterre P. An engineered CX_3CR1 antagonist endowed with anti-inflammatory activity. *J Leukoc Biol*. 2009. 86(4): 903-911

87. Karlstrom S, Nordvall G, Sohn D, Hettman A, Turek D, Ahlin K, Kers A, Claesson M, Slivo C, Lo-Alfredsson Y, Petersson C, Bessidskaia G, Svensson PH, Rein T, Jerning E, Malmberg A, Ahlgen C, Ray C, Vares L, Ivanov V, Johansson R. Substituted 7-amino-5-thio-thiazolo [4,5-d] pyrimidines as potent and selective antagonists of the fractalkine receptor (CX_3CR1). *J Med Chem*. 2013. 56(8):3177-3190

88. Ridderstad Wollberg A, Ericsson-Dahlstrand A, Jureus A, Ekerot P, Simon S, Nilsson M, Wiklund SJ, Berg AL, Ferm M, Sunnemark D, Johansson R. Pharmacological inhibition of the chemokine receptor CX_3CR1 attenuates disease in a chronic-relapsing rat model for multiple sclerosis. *Proc Natl Acad Sci U S A*. 2014. 111(14):5409-5414

89. Old EA, Nadkarni S, Grist J, Gentry C, Bevan S, Kim KW, Mogg AJ, Perretti M, Malcangio M. Monocytes expressing CX_3CR1 orchestrate the development of vincristine-induced pain. *J Clin Invest*. 2014. 124(5):2023-2036

90. Obata K, Morland SJ, Watson RH. Frequent PTEN/MMAC mutations in endometrioid but not serous or mucinous epithelial ovarian tumors. *Cancer Res* 1998; 58: 2095–2097

91. Sato N, Tsunoda H, Nishida M. Loss of heterozygosity on 10q23.3 and mutation of the tumor suppressor gene PTEN in benign endometrial cyst of the ovary: possible sequence progression from benign endometrial cyst to endometrioid carcinoma and clear cell carcinoma of the ovary. *Cancer Res* 2000; 60: 7052–7056.

92. Prat J. *Pathology of the Ovary*. Philadelphia: Saunders 2004

93. Lee KR, Tavassoli FA, Prat J. Surface epithelial-stromal tumours (Ch 2: tumours of the ovary and peritoneum). In Tavassoli FA, Devilee P (eds), World Health Organization classification of tumours: pathology and genetics of tumours of the breast and female genital organs. *Lyon: IARC Press* 2003; 117–145

94. Vang R, Levine DA, Soslow RA, Zaloudek C, Shih IM, Kurman RJ. Molecular Alterations of TP53 are a Defining Feature of Ovarian High-Grade Serous Carcinoma: A Rereview of Cases Lacking TP53 Mutations in The Cancer Genome Atlas Ovarian Study. *Int J Gynecol Pathol*, 2015

95. Hyman, DM and Spriggs DR. Unwrapping the Implications of BRCA1 and BRCA2 mutations in ovarian cancer. *JAMA*. 2012. 307(4): 408-410

96. Cunningham JM, Cicek MS, Larson NB, David J, Wang C, Larsen MC, Song H, Dicks EM, Harrington P, Wick M, Winterhoff BJ, Hamidi H, Konecny GE, Chien J, Bikikova M, Fan JB, Kalli KR, Lindor NM, Fridley BL, Pharoah PP, Goode EL. Clinical characterization of ovarian cancer classified by BRCA1, BRCA2, and Rad51C status. *Sci Rep*. 2014. 4: 4026

97. Vang R, Shih IM, Kurman RJ. Ovarian low-grade and high-grade serous carcinoma: pathogenesis, clinicopathologic and molecular biologic features, and diagnostic problems. *Adv Anat Pathol*. 2009. 16(5): 267-282.

98. Casagrande JT, Louie EW, Pike MC, Roy S, Ross RK, Henderson BE. "Incessant ovulation" and ovarian cancer. *Lancet*. 1979; 2:170-173

99. Fathalla MF. Incessant ovulation-a factor in ovarian neoplasia? *Lancet*. 1979; 2; 163.

100. Pruthi S, Gostout BS, Lindor NM. Identification and Management of Women with BRCA Mutations or Hereditary Predisposition for Breast and Ovarian Cancer. *Mayo Clin Proc*. 2010. 85(12): 1111-1120

101. Huber SM, Butz L, Stegen B, Klumpp D, Braun N, Ruth P, Eckert F. Ionizing radiation, ion transports, and radioresistance of cancer cells. *Front Physiol*. 2013. 4:212

102. Fung C, Fossa SD, Milano MT, Sahasrabudhe DM, Peterson DR, Travis LB. Cardiovascular disease mortality after chemotherapy or surgery for testicular nonseminoma: a population-based study. *J Clin Oncol*. 2015. Aug.3

103. Stanton RA, Gernert KM, Nettles JH, Aneja R. Drugs that target dynamic microtubules: a new molecular perspective. *Med. Res. Rev*. 2011. 31(3): 443-481

104. Behar A, Pujade-lauraine E, Maurel A, Brun MD, Chauvin FF, Feuinade de Chauvin F, Oulid-Aissa D, Hille D. The pathophysiological mechanism of fluid retention in advanced cancer patients treated with docetaxel, but not receiving corticosteroid comedication. *Br J Clin Pharmacol*. 1997. 43(6): 653-658

105. Budd GT, Ganapathi R, Wood L, Snyder J, McLain D, and Bukowski RM. Approaches to managing carboplatin-induced thrombocytopenia: focus on the role of amifostine. *Semin Oncol*. 1999. 26(2): 41-50

106. Scripture CD, Figg WD, Sparreboom A. Peripheral neuropathy induced by paclitaxel: recent insights and future perspectives. *Curr Neuropharmacol*. 2006. 4(2): 165-172

107. Agarwai R, Kaye SB. Ovarian cancer: strategies for overcoming resistance to chemotherapy. *Nat Rev Cancer*. 2003. 3(7): 502-516

108. Inai T, Mancuso M, Hashizume H, Baffert F, Haskell A, Baluk P, Hu-lowe DD, Shalinsky DR, Thurston G, Yancopoulos GD, McDonald DM. Inhibition of vascular endothelial growth factor (VEGF) signaling in cancer causes loss of endothelial fenestrations, regression of tumor vessels, and appearance of basement membrane ghosts. *Am J Pathol*. 2004. 165(1): 35-52

109. www.gene.com/patients/medicines/avastin

110. Starlinger P, Brugger P, Schauer D, Sommerfeldt S, Tamandl D, Kuehrer I, Schoppmann SF, Gnant M, Brostjan C. Myelosuppression of thrombocytes and monocytes is associated with a lack of synergy between chemotherapy and anti-VEGF treatment. *Neoplasia*. 13(5): 419-427

111. Domcke S, Sinha R, Levine DA, Sander C, Schultz N. Evaluating cell lines as tumour models by comparison of genomic profiles. *Nat Commun*. 2013. 4:2126

112. Pease JC, Brewer M, Tirnauer JS. Spontaneous spheroid budding from monolayers: a potential contribution to ovarian cancer dissemination. *Biol Open*. 2012. 1(7):622-628

113. Benard J, Da Silva J, De Blois MC, Boyer P, Duvillard P, Chiric E, Riou G. Characterization of a human ovarian adenocarcinoma line, IGROV1, in tissue culture and in nude mice. *Cancer Res*. 1985. 45(10):4970-4979

114. Behrens BC, Hamilton TC, Masuda H, Grotzinger KR, Whang-Peng J, Louie KG, Knutsen T, McKoy WM, Young RC, Ozols RF. Characterization of a cis-diamminedichloroplatinum(II)-resistant human ovarian cancer cell line and its use in evaluation of platinum analogues. *Cancer Res*. 1987. 47(2):414-418

115. Okaichi K, Ide-Kanematsu M, Izumi N, Morita N, Okumura Y, Ihara M. Variations in sensitivity to ionizing radiation in relation to p53 mutation point. *Anticancer Res*. 2008. 28(5A):2687-2690

116. Batinac T, Gruber F, Lipozencic J, Zamolo-Koncar G, Stasic A, Brajac I. Protein p53—structure, function, and possible therapeutic implications. *Acta Dermatovenerol Croat*. 2003. 11(4):225-230

117. Franken NA, Rodermond HM, Stap J, Haveman J, van Bree C. Clonogenic assay of cells *in vitro*. *Nat Protoc*. 2006. 1(5):2315-2319

118. Chapman JP. Target theory revisited: why physicists are essential for radiobiology research. *Clin Oncol*. 2007. 19(3):S12

119. Nomiya T. Discussions on target theory: past and present. *J Radiat Res*. 2013. 54(6):1161-1163

120. Yu T. Xiong Z, Chen S, Tu G. The use of models in "target" theory to evaluate the survival curves of human ovarian carcinoma cell line exposure to Adriamycin combined with ultrasound. *Ultrason Sonochem*. 2005. 12(5): 345-348

121. Hall EJ, Giaccia AJ. *Radiobiology for the radiologist*. 7th edition

122. Sutherland JC. Repair dependent radiation survival: a stochastic model with Euler gamma function solutions. *Phys Med Biol*. 2006. 51(19): 4883-4901

123. Bloomer WD, Adelstein SJ. The mammalian radiation survival curve. *J Nucl Med*. 1982. 23(3):259-265

124. Chu PM, Chiou SH, Su TL, Lee YJ, Chen LH, Chen YW, Yen SH, Chen MT, Chen MH, Shih YH, Tu PH, Ma HI. Enhancement of radiosensitivity in human glioblastoma cells by the DNA N-mustard alkylating agent BO-1051 through augmented and sustained DNA damage response. *Radiat Oncol*. 2011. 19;6:7

125. Tishler RB, Geard CR. Correlation of sensitizer enhancement ratio with bromodeoxyuridine concentration and exposure time in human cervical carcinoma cells treated with low dose rate irradiation. *Int J Radiat Oncol Biol Phys*. 1992. 22(3):495-498

126. Gunderson LL, Tepper JE. *Clinical Radiation Oncology*. 3rd edition

127. Fertil B, Malaise EP. Inherent cellular radiosensitivity as a basic concept for human tumor radiotherapy. *Int J Radiat Biol*. 1981. 7:621-629

128. Petersen C, Petersen S, Milas L, Lang FF, Tofilon PJ. Enhancement of intrinsic tumor cell radiosensitivity induced by a selective cyclooxygenase-2 inhibitor. *Clin Cancer Res*. 2000. 6(6):2513-2520

129. Brunner TB, Cengel KA, Hahn SM, Wu J, Fraker DL, McKenna WG, Bernhard EJ. Pancreatic cancer cell radiation survival and prenyltransferase inhibition: the role of K-Ras. *Cancer Res*. 2005. 65(18):8433-8441

130. Halling-Brown MD, Bulusu KC, Patel M, Tym JE, Al-Lazikani B. canSAR: an integrated cancer public translational research and drug discovery resource. *Nucleic Acids Res*. 2012; 40:D947-56

131. Geske FJ, Nelson AC, Lieberman R, Strange R, Sun T, Gerschenson LE. DNA repair is activated in early stages of p53-induced apoptosis. *Cell Death Differ*. 2000. 7(4):393-401

132. Cmelak AJ, KappDS. Long-term survival with whole abdominopelvic irradiation in platinum-refractory persistent or recurrent ovarian cancer. *Gynecol Oncol*. 1997. 65(3):453-460

133. Gelblum D, Mychalczak B, Almadrones L, Spriggs D, Barakat R. Palliative benefit of external-beam radiation in the management of platinum refractory epithelial ovarian carcinoma. *Gynecol Oncol*. 1998. 69(1):36-41

134. Faul C, Gerszten K, Edwards R, Land S, D'Angelo G, Kelley J 3rd, Price F. A phase I/II study of hypofractionated whole abdominal radiation therapy in patients with chemoresistant ovarian carcinoma: Karnofsky score determines treatment outcome. *Int J Radiat Oncol Biol Phys*. 2000. 47(3):749-754

135. Firat S, Murray K, Erickson B. High-dose whole abdominal and pelvic irradiation for treatment of ovarian carcinoma: long-term toxicity and outcomes. *Int J Radiat Oncol Biol Phys*. 2003. 57(1):201-207

136. Kvols LK. Radiation sensitizers: a selective review of molecules targeting DNA and non-DNA targets. *J Nucl Med*. 2005. 46 Suppl 1: 187S-190S

137. Gao Y, Liu Z, Chen X, Luo W, Zhang L, Wang J. Intraoperative radiotherapy electron boost in advanced and recurrent epithelial ovarian carcinoma: a retrospective study. *BMC Cancer*. 2011. 11:439

138. Rochet N, Kieser M, Sterzing F, Krause S, Lindel K, Harms W, Eichbaum MH, Schneeweiss A, Sohn C, Debus J. Phase II study evaluating consolidation whole abdominal intensity-modulated radiotherapy (IMRT) in patients with advanced ovarian cancer stage FIGO III—the OVAR-IMRT-02 study. *BMC Cancer*. 2011. 11:41

139. Mahantshetty U, Jamema S, Engineer R, Deshpande D, Sarin R, Fogliata A, Nicolini G, Clivio A, Vanetti E, Shrivastava S, Cozzi L. Whole abdomen radiation therapy in ovarian cancers: a comparison between fixed beam and volumetric arc based intensity modulation. *Radiat Oncol*. 2010. 5:106

140. Kim M, Rooper L, Xie J, Kajdacsy-Balla AA, Barbolina MV. Fractalkine receptor CX_3CR1 is expressed in epithelial ovarian carcinoma cells and required for motility and adhesion to peritoneal mesothelial cells. *Mol Cancer Res*. 2012. 10(1):11-24

141. Kim M, Rooper L, Xie J, Rayahin J, Burdette JE, Kajdacsy-Balla AA, Barbolina MV. The lymphotactin receptor is expressed in epithelial ovarian canrcinoma and contributes to cell migration and proliferation. *Mol Cancer Res*. 2012. 10(11):1419-1429

142. Acosta JC, O'Loghlen A, Banito A, Guijarro MV, Augert A, Raguz S, Fumagalli M, Da Costa M, Brown C, Popov N, Takatsu Y, Melamed J, d'Adda di Fagagna F, Bernard D, Hernando E, Gil J. Chemokine signaling via the CXCR2 receptor reinforces senescence. *Cell*. 133(6):1006-1018

143. Attardi LD, de Vries A, Jacks T. Activation of the p53-dependent G_1 checkpoint response in mouse embryo fibroblasts depends on the specific DNA damage inducer. *Oncogene*. 2004. 23(4):973-980

144. Vance S, Liu E, Zhao L, Parsels JD, Parsels LA, Brown JL, Maybaum J, Lawrence TS, Morgan MA. Selective radiosensitization of p53 mutant pancreatic cancer cells by combined inhibition of Chk1 and PARP1. *Cell Cycle*. 2011. 10(24):4321-4329

145. Powell SN, DeFrank JS, Connell P, Eogan M, Preffer F, Dombkowski D, Tang W, Friend S. Differential sensitivity of p53(-) and p53 (+) cells to caffeine-induced radiosensitization and override of G_2 delay. *Cancer Res*. 1995. 55(8):1643-1648

146. Lee YJ, Chung DY, Lee SJ, Ja Jhon G, Lee YS. Enhanced radiosensitization of p53 mutant cells by oleamide. *Int J Radiat Oncol Biol Phys*. 2006. 64(5):1466-1474

147. Jung M, Notario V, Dritschilo A. Mutations in the p53 gene in radiation-sensitive and –resistant human squamous carcinoma cells. *Cancer Res*. 1992. 52(22):6390-6393

148. Selivanova G, Wiman KG. Reactivation of mutant p53: molecular mechanisms and therapeutic potential. *Oncogene*. 2007. 26(15): 2243-2254

149. Okaichi K, Izumi N, Takamura Y, Fukui S, Kudo T. Radiation-sensitivity and transcription profiles in various mutant p53 cells. *Current topics in ionizing radiation research*. 2012

150. Singh S, Narang AS, Mahato RI. Subcellular fate and off-target effects of siRNA, shRNA, and miRNA. *Pharm Res*. 2011. 28(12):2996-3015

151. Sander JD, Joung JK. CRISPR-Cas systems for genome editing, regulation and targeting. *Nat Biotechnol*. 2014. 32(4):347-355

152. Mali P, Yang L, Esvelt KM, Aach J, Guell M, DiCarlo JE, Norville JE, Church GM. RNA-Guided Human Genome Engineering via Cas9. *Science*. 2013. 339(6121):823-826

153. Petitjean A, Achatz MI, Borresen-Dale AL, Hainaut P, Olivier M. TP53 mutations in human cancers: functional selection and impact on cancer prognosis and outcomes. *Oncogene*. 2007. 26(15): 2157-2165

154. Nomiya T. Discussions on target theory: past and present. *J Radiat Res*. 2013. 54(6): 1161-1163.

155. Fowler JF. Differences in survival curve shapes for formal multi-target and multi-hit models. *Phys Med Biol*. 1964. 9:177–188.

156. Haynes RH. The interpretation of microbial inactivation and recovery phenomena. *Radiat Res.* 1966. 6:97–116.

157. Douglas BG, Fowler JF. The effect of multiple small doses of X-rays on skin reactions in the mouse and a basic interpretation. *Radiat Res*. 1976. 66:401–426.

158. (http://www.origene.com/cdna/search/seq_fl.aspx?est_name=SC328568&type=Human)

159. Chene P. The role of tetramerization in p53 function. *Oncogene.* 2001. 20(21): 2611-2617

160. Brachova P, Mueting SR, Carlson MJ, Goodheart MJ, Button AM, Mott SL, Dai D, Thiel KW, Devor EJ and Leslie KK. TP53 oncomorphic mutations predict resistance to platinum- and taxane-based standard chemotherapy in patients diagnosed with advanced serous ovarian carcinoma. *Int J Oncol*. 2015. 46(2): 607-618.

161. Hall EJ, Giaccia AJ. *Radiobiology for the radiologist*. 7th edition

162. Robertson AB, Klungland A, Rognes T, Leiros I. DNA repair in mammalian cells: base excision repair: the long and short of it. *Cell Mol Life Sci*. 2009. 66(6):981-993

163. Matsumura Y, Ananthaswamy HN. Short-term and long-term cellular and molecular events following UV irradiation of skin: implications for molecular medicine. *Expert Rev Mol Med*. 2002. 4(26):1-22

164. Davis AJ, Chen DJ. DNA double strand break repair via non-homologous end-joining. *Transl Cancer Res*. 2013. 2(3):130-143

165. Betermier M, Bertrand P, Lopez BS. Is non-homologous end-joining really an inherently error-prone process. *PLoS Genet*. 2014. 10(1):e1004086

166. Jasin M, Rothstein R. Repair of strand breaks by homologous recombination. *Cold Spring Harb Perspect Biol*. 2013. 5(11):a012740

167. Geuting V, Reul C, Lobrich M. ATM release at resected double-strand breaks provides heterochromatin reconstitution to facilitate homologous recombination. *PLoS Genet*. 2013. 9(8): e1003667

168. Krejci L, Altmannova V, Spirek M, Zhao X. Homologous recombination and its regulation. *Nucleic Acids Res*. 2012. 40(13):5795-5818

169. Polo SE, Jackson SP. Dynamics of DNA damage response proteins at DNA breaks: a focus on protein modifications. *Genes Dev*. 2011. 25(5):409-433

170. Cleaver JE, Feeney L, Revet I. Phosphorylated H2Ax is not an unambiguous marker for DNA double-strand breaks. *Cell Cycle*. 2011. 10(19):3223-3224

171. Bryant HE, Schultz N, Thomas HD, Parker KM, Flower D, Lopez E, Kyle S, Meuth M, Curtin NJ, Helleday T. Specific killing of BRCA2-deficient tumours with inhibitors of poly(ADP-ribose) polymerase. *Nature*. 2005. 434(7035):913-917

172. Rouleau M, Patel A, Hendzel MJ, Kaufmann SH, Poirier GG. PARP inhibition: PARP1 and beyond. *Nat Rev Cancer*. 2010. 10(4):293-301

173. Walsh CS. Two decades beyond BRCA1/2: homologous recombination, hereditary cancer risk and a target for ovarian cancer therapy. *Gynecol Oncol*. 2015. 137(2):343-350

174. Moding EJ, Kastan MB, Kirsch DG. Strategies for optimizing the response of cancer and normal tissues to radiation. *Nat Rev Drug Discov*. 2013. 12(7):526-542

175. Tichy A, Vavrova J, Pejchal J, Rezacova M. Ataxia-telangiectasia mutated kinase (ATM) as a central regulator of radiation-induced DNA damage response. *Acta Medica (Hradec Kralove)*. 2010. 53(1):13-17

176. Hickson I, Zhao Y, Richardson CJ, Green SJ, Martin NM, Orr AI, Reaper PM, Jackson SP, Curtin NJ, Smith GC. Identification and characterization of a novel and specific inhibitor of the ataxia-telangiectasia mutated kinase ATM. *Cancer Res*. 2004. 64(24):9152-9159

177. Biddlestone-Thorpe L, Sajjad M, Rosenberg E, Beckta JM, Valerie NC, Tokarz M, Adams BR, Wagner AF, Khalil A, Gilfor D, Golding SE, Deb S, Temesi DG, Lau A, O'Connor MJ, Choe KS, Parada LF, Lim SK, Mukhopadhyay ND, Valerie K. ATM kinase inhibition preferentially sensitizes p53-mutant glioma to ionizing radiation. *Clin Cancer Res*. 2013. 19(12):3189-3200

178. Rainey MD, Charlton ME, Stanton RV, Kastan MB. Transient inhibition of ATM kinase is sufficient to enhance cellular sensitivity to ionizing radiation. *Cancer Res*. 2008. 68(18):7466-7474

179. Zhao Y, Thomas HD, Batey MA, Cowell IG, Richardson CJ, Griffin RJ, Calvert AH, Newell DR, Smith GC, Curtin NJ. Preclinical evaluation of a potent novel DNA-dependent protein kinase inhibitor NU7441. *Cancer Res*. 2006. 66(10):5354-5362

180. White GE, Tan TC, John AE, Whatling C, McPheat WL, Greaves DR. Fractalkine has anti-apoptotic and proliferative effects on human vascular smooth muscle cells via epidermal growth factor receptor signaling. *Cardiovasc Res*. 2010. 85(4):825-835

181. Golding SE, Rosenberg E, Neill S, Dent P, Povirk LF, Valerie K. Extracellular signal-related kinase positively regulates ataxia telangiectasia mutated, homologous recombination repair, and the DNA damage response. *Cancer Res*. 2007. 67(3):1046-1053

182. Wei F, Xie Y, Tao L, Tang D. Both ERK1 and ERK2 kinases promote G_2/M arrest in etoposide-treated MCF7 cells by facilitating ATM activation. *Cell Signal*. 2010. 22(11):1783-1789

183. Lodish H, Berk A, Zipursky SL, Matsudecira P, Baltimore D, Darnell JE. *Molecular Cell Biology. 4th Edition*. New York: W.H. Freeman: 2000.

184. Williiamson CT, Kubota E, Hamill JD, Klimowicz A, Ye R, Muzik H, Dean M, Tu L, Gilley D, Magliocco AM, McKay BC, Bebb DG, Lees-Miller SP. Enhanced cytotoxicity of PARP inhibition in mantle cell lymphoma harbouring mutations in both ATM and p53. *EMBO Mol Med*. 2012. 4(6): 515-527.

185. Racila D, Bickenbach JR. Are epidermal stem cells unique with respect to aging. *Aging(Albany NY)*. 2009. 1(8):746-750

186. Subba Rao K. Mechanisms of disease: DNA repair defects and neurological disease. *Nat Clin Pract Neurol*. 2007. 3(3):162-172

187. Massaad CA, Klann E. Reactive oxygen species in the regulation of synaptic plasticity and memory. *Antioxid Redox Signal*. 2011. 14(10):2013-2054

188. Fridovich I. Superoxide dismutases. *Adv Enzymol Relat Areas Mol Biol*. 1986. 58:61-97

189. Vaziri ND, Lin CY, Farmand F, Sindhu RK. Superoxide dismutase, catalase, glutathione peroxidase and NADPH oxidase in lead-induced hypertension. *Kidney Int*. 2003. 63(1):186-194

190. Ahmad ST, Arjumand W, Seth A, Kurman Saini A, Sultana S. Impact of glutathione transferase M1, T1, and P1 gene polymorphisms in the genetic susceptibility of North Indian population to renal cell carcinoma. *DNA Cell Biol*. 2012. 31(4):636-643

191. Mustacich D, Powis G. Thioredoxin reductase. *Biochem J*. 2000. 346(Pt1):1-8

192. Trachootham D, Lu W, Ogasawara MA, Valle NRD, Huang P. Redox regulation of cell survival. *Antioxid Redox Signal*. 2008. 10(8):1343-1374

193. Liou GY, Storz P. Reactive oxygen species in cancer. *Free Radic Res*. 2010. 44(5):10.3109

194. Wada T, Penninger JM. Mitogen-activated protein kinases in apoptosis regulation. *Oncogene*. 2004. 23(16):2838-2849

195. Roux PP, Blenis J. ERK and p38 MAPK-activated protein kinases: a family of protein kinases with diverse biological functions. *Microbiol Mol Biol Rev*. 2004. 68(2):320-344

196. Koul HK, Pal M, Koul S. Role of p38 MAP kinase signal transduction in solid tumors. *Genes Cancer*. 2013. 4(9-10):342-359

197. Hengartner MO. The biochemistry of apoptosis. *Nature*. 2000. 407(6805):770-776

198. Fridman JS, Lowe SW. Control of apoptosis by p53. *Oncogene*. 2003. 22(56):9030-9040

199. el-Deiry WS. Regulation of p53 downstream genes. *Semin Cancer Biol*. 1998. 8(5):345-357

200. Melino G, De Laurenzi V, Vousden KH. P73: Friend or foe in tumorigenesis. *Nat Rev Cancer*. 2002. 2(8):605-615

201. Roos WP, Kaina B. DNA damage-induced cell death by apoptosis. *Trends Mol Med*. 2006. 12(9):440-450

202. Manna SK, Zhang HJ, Yan T, Oberley LW, Aggarwal BB. Overexpression of managanese superoxide dismutase suppresses tumor necrosis factor-induced apoptosis and activation of nuclear transcription factor-kappa B and activated protein-1. *J Biol Chem*. 1998. 273(21):13245-13254

203. Huang HL, Fang LW, Lu SP, Chou CK, Luh TY, Lai MZ. DNA-damaging reagents induce apoptosis through reactive oxygen species-dependent Fas aggregation. *Oncogene*. 2003. 22(50):8168-8177

204. Lapenna S, Giordano A. Cell cycle kinases as therapeutic targets for cancer. *Nat Rev Drug Discov*. 2009. 8(7):547-566

205. Haigis KM, Sweet-Cordero A. New insights into oncogenic stress. *Nat Genet*. 2011. 43(3):177-178

206. d'Adda di Fagagna F. Living on a break: cellular senescence as a DNA-damage response. *Nat Rev Cancer*. 2008. 8(7): 512-522

207. Freund A, Patil CK, Campisi J. p38MAPK is a novel DNA damage response-independent regulator of the senescence-associated secretory phenotype. *EMBO J*. 2011. 30(8):1536-1548

208. Vakifahmetoglu H, Olsson M, Zhivotovsky B. Death through a tragedy: mitotic catastrophe. *Cell Death Differ*. 2008. 15(7):1153-1162

209. Galluzzi L, Vitale I, Abrams JM, Alnemri EH, Blagosklonny MV, Dawson TM, Dawson VL, EI-Deiry WS, Fulda S, Gottlieb E, Green DR, Hengartner MO, Kepp O, Knight RA, Kumar S, Lipton SA, Lu X, Madeo F, Malorni W, Mehlen P, Gunez G, Peter ME, Piacentini M, Rubinsztein DC, Shi Y, Simon HU, Vandenabeele P, White E, Yuan J, Zhivotosky B, Melino G, Kroemer G. Molecular definitions of cell death subroutines:

recommendations of the nomenclature committee on cell death 2012. *Cell Death Differ*. 2012. 19(1):107-120

210. Lanz HL, Zimmerman RM, Brouwer J, Noteborn MH, Backendorf C. Mitotic catastrophe triggered in human cancer cells by the viral protein apoptin. *Cell Death Dis*. 2013. 4:e487

211. Muschel RJ, Soto DE, McKenna WG, Bernhard EJ. Radiosensitization and apoptosis. *Oncogene*. 1998. 17(25):3359-3363

212. Wang HM, Chen LH, Zheng XK, Wu XY, Xia YF. The role of cell cycle arrest in radiosensitization of nasopharyngeal carcinoma cell line CNE1 by inhibiting ATM expression. *Ai Zheng*. 2008. 27(5):466-470

213. Wang M. Morsbach F, Sander D, Gheorghiu L, Nanda A, Benes C, Kriegs M, Krause M, Dikomey E, Baumann M, Dahm-Daphi J, Settleman J, Willers H. EGF receptor inhibition radiosensitizes NSCLC cells by inducing senescence in cells sustaining DNA double-strand breaks. *Cancer Res*. 2011. 71(19):6261-6269

214. Hayman TJ, Williams ES, Jamal M, Shankavaram UT, Camphausen K, Tofilon PJ. Translation initiation factor eIF4E is a target for tumor cell radiosensitization. *Cancer Res*. 2012. 72(9):2362-2372

215. Kim JB, Jung JY, Ahn JC, Rhee CK, Hwang HJ. Antioxidant and anti-apoptotic effect of melatonin on the vestibular hair cells of rat utricles. *Clin Exp Otorhinolaryngol*. 2009. 2(1):6-12

216. Bhardwaj R, Sharma PK, Jadon SS, Varshney R. A combination of 2-deoxy-D-glucose and 6-aminonicotinamide induces oxidative stress mediated selective radiosensitization of malignant cells via mitochondrial dysfunction. *Tumor Biol*. 2011. 32(5):951-964

217. Xia C, Meng Q, Liu LZ, Rojanasakul R, Wang XR, Jiang BH. Reactive oxygen species regulate angiogenesis and tumor growth through vascular endothelial growth factor. *Cancer Res*. 2007. 67(22):10823-10830

218. Chan DW, Liu VW, Tsao GS, Yao KM, Furukawa T, Chan KK, Ngan HY. Loss of MKP3 mediated by oxidative stress enhances tumorigenicity and chemoresistance of ovarian cancer cells. *Carcinogenesis*. 2008. 29(9):1742-1750

219. Trachootham D, Alexandre J, Huang P. Targeting cancer cells by ROS-mediated mechanisms: a radical therapeutic approach? *Nat Rev Drug Discov*. 2009. 8(7):579-591

220. Noda M, Doi Y, Liang J, Kawanokuchi J, Sonobe Y, Takeuchi H, Mizuno T, Suzumura A. Fractalkine attenuates excite-neurotoxicity via microglial clearance of damaged neurons and antioxidant enzyme heme oxygenase-1 expression. *J Biol Chem*. 2011. 286(3):2308-2319

221. Lastres-Becker I, Innamorato NG, Jaworski T, Rabano A, Kugler S, Van Leuven F, Cuadrado A. Fractalkine activates NRF2/NFE2L2 and heme oxygenase 1 to restrain tauopathy-induced microgliosis. *Brain*. 2014. 137(Pt1):78-91

222. Inui M, Ishida Y, Kimura A, Kuninaka Y, Mukaida N, Kondo T. Protective roles of CX_3CR1-mediated signals in toxin A-induced enteritis through the induction of heme oxygenase-1 expression. *J Immunol*. 2011. 186(1):423-431

223. Cannistra SA. Cancer of the ovary. *N Engl J Med*. 2004. 351(24):2519-2529

224. Wong SY, Hynes RO. Lymphatic or hematogenous dissemination: how does a metastatic tumor cell decide? *Cell cycle*. 2006. 5(8):812-817

225. Burleson KM, Casey RC, Skubitz KM, Pambuccian SE, Oegema TR Jr, Skubitz AP. Ovarian carcinoma ascites spheroids adhere to extracellular matrix components and mesothelial cell monolayers. *Gynecol Oncol*. 2004. 93(1):170-181

226. Casey RC, Skulbitz AP. CD44 and beta1 integrins mediate ovarian carcinoma cell migration toward extracellular matrix proteins. *Clin Exp Metastasis*. 2000. 18(1):67-75

227. Naora H, Montell DJ. Ovarian cancer metastasis: integrating insights from disparate model organisms. *Nat Rev Cancer*. 2005. 5(5):355-366

228. Kim M, Rooper L, Xie J, Kajdacsy-Balla AA, Barbolina MV. Fractalkine receptor CX_3CR1 is expressed in epithelial ovarian carcinoma cells and required for motility and adhesion to peritoneal mesothelial cells. *Mol Cancer Res*. 2012. 10(1):11-24

229. Roby KF, Taylor CC, Sweetwood JP, Cheng Y, Pace JL, Tawfik O, Persons DL, Smith PG, Terranova PF. Development of a syngeneic mouse model for events related to ovarian cancer. *Carcinogenesis*. 2000. 21(4):585-591

230. Clark R, Krishnan V, Schoof M, Rodriguez I, Theriault B, Chekmareva M, Rinker-Schaeffer C. Milky spots promote ovarian cancer metastatic colonization of peritoneal adipose in experimental models. *Am J Pathol*. 2013. 183(2):576-591

231. Kenny HA, Krausz T, Yamada SD, Lengyel E. Use of a novel 3D culture model to elucidate the role of mesothelial cells, fibroblasts and extra-cellular matrices on adhesion and invasion of ovarian cancer cells to the omentum. *Int J Cancer*. 2007. 121(7):1463-1472

232. Ahmed N, Stenvers KL. Getting to know ovarian cancer ascites: opportunities for targeted therapy-based translational research. *Front Oncol*. 2013. 3:256

233. Iwanicki MP, Davidowitz RA, Ng MR, Besser A, Muranen T, Merritt M, Danuser G, Ince T, Brugge JS. Ovarian cancer spheroids use myosin-generated force to clear the mesothelium. *Cancer Discov*. 2011. 1(2):144-157

234. Heath RM, Jayne DG, O'Leary R, Morrison EE, Guillou PJ. Tumor-induced apoptosis in human mesothelial cells: a mechanism of peritoneal invasion by Fas Ligand/Fas interaction. *Br J Cancer*. 2004. 90(7):1437-1442

235. Rieppi M, Vergani V, Gatto C, Zanetta G, Allavena P, Taraboletti G, Giavazzi R. Mesothelial cells induce the motility of human ovarian carcinoma cell. *Int J Cancer*. 1999. 80(2):303-307

236. Kenny HA, Chiang CY, White EA, Schryver EM, Habis M, Romero IL, Ladanyi A, Penicka CV, George J, Matlin K, Montag A, Wroblewski K, Yamada SD, Mazar AP, Bowtell D, Lengyel E. Mesothelial cells promote early ovarian cancer metastasis through fibronectin secretion. *J Clin Invest*. 2014. 124(10):4614-4628

237. Nieman KM, Kenny HA, Penicka CV, Ladanyi A, Buell-Gutbrod R, Zillhardt MR, Romero IL, Carey MS, Mills GB, Hotamisligil GS, Yamada SD, Peter ME, Gwin K, Lengyel E. Adipocytes promote ovarian cancer metastasis and provide energy for rapid tumor growth. *Nat Med*. 2011. 17(11): 1498-1503

238. Fischer DS. Abdominal paracentesis for malignant ascites. *Arch Intern Med*. 1979. 139:235

239. Kim M, Rooper L, Xie J, Kajdacsy-Balla AA, Barbolina MV. Fractalkine receptor CX_3CR1 is expressed in epithelial ovarian carcinoma cells and required for motility and adhesion to peritoneal mesothelial cells. *Mol Cancer Res*. 2012. 10(1):11-24

240. Bieging KT, Mello SS, Attardi LD. Unravelling mechanisms of p53-mediated tumour suppression. *Nat Rev Cancer*. 2014. 14(5):359-370

241. Meek DW. Tumour suppression by p53: a role for the DNA damage response? *Nat Rev Cancer*. 2009. 9(10):714-723

242. Khoo KH, Verma CS, Lane DP. Drugging the p53 pathway: understanding the route to clinical efficacy. *Nat Rev Drug Discov*. 2014. 13(3):217-236

243. Einhorn N, Lundell M, Nilsson B, Ragnarsson-Olding B, Sjovall K. Is there place for radiotherapy in the treatment of advanced ovarian cancer? *Radiother Oncol*. 1999. 53(3):213-218

244. Einhorn N, Trope C, Ridderheim M, Boman K, Sorbe B, Cavallin-Stahl E. A systematic overview of radiation therapy effects in ovarian cancer. *Acta Oncol*. 2003. 42(5-6):562-566

245. Fyles AW, Dembo AJ, Bush RS, Levin W, Manchul LA, Pringle JF, Rawlings GA, Sturgeon JF, Thomas GM, Simm J. Analysis of complications in patients treated with

abdomino-pelvic radiation therapy for ovarian carcinoma. *Int J Radiat Oncol Biol Phys*. 1992. 22(5):847-851

246. Lindner H, Willich H, Atzinger A. Primary adjuvant whole abdominal irradiation in ovarian carcinoma. *Int J Radiat Oncol Biol Phys*. 1990. 19(5):1203-1206

247. Smith JP, Rutledge FN, Delclos L. Postoperative treatment of early cancer of the ovary: a random trial between postoperative irradiation and chemotherapy. *Natl Cancer Inst Monogr*. 1975. 42:149-153

248. Hong L, Alektiar K, Chui C, LoSasso T, Hunt M, Spirou S, Yang J, Amols H, Ling C, Fuks Z, Leibel S. IMRT of large fields: whole-abdomen irradiation. *Int J Radiat Oncol Biol Phys*. 2002. 54(1):278-289

249. Duthoy W, De Gersem W, Vergote K, Coghe M, Boterberg T, De Deene Y, De Wagter C, Van Belle S, De Neve W. Whole abdominopelvic radiotherapy (WAPRT) using intensity-modulated arc therapy (IMAT): first clinical experience. *Int J Radiat Oncol Biol Phys*. 2003. 57(4):1019-1032

250. De Meerleer G, Vandecasteele K, Ost P, Delrue L, Denys H, Makar A, Speleers B, Van Belle S, Van den Broecke R, Fonteyne V, De Neve W. Whole abdominopelvic radiotherapy using intensity-modulated arc therapy in the palliative treatment of chemotherapy-resistant ovarian cancer with bulky peritoneal disease: a single-institution experience. *Int J Radiat Oncol Biol Phys*. 2011. 79(3):775-781

251. Kim BY, Kim YA, Kwon O, Kim SO, Kim MS, Kim BS, Oh WK, Kim GD, Jung M, Ahn JS. NF-kappaB inhibition radiosensitizes Ki-Ras-transformed cells to ionizing radiation. *Carcinogenesis*. 2005. 26(8):1395-1403

252. Kabe Y, Ando K, Hirao S, Yoshida M, Handa H. Redox regulation of NF-kappaB activation: distinct redox regulation between the cytoplasm and the nucleus. *Antioxid Redox Signal*. 2005. 7(3-4):395-403

253. Ahmed KM, Li JJ. NF-kappa B-mediated adaptive resistance to ionizing radiation. *Free Radic Biol Med*, 2008; 44(1):1-13.

254. Sheridan GK, Murphy KJ. Neuron-glia crosstalk in health and disease: fractalkine and CX_3CR1 take centre stage. *Open Biol*. 2013. 3(12):130181

255. Ishiguro K, Green T, Rapley J, Wachtel H, Giallourakis C, Landry A, Cao Z, Lu N, Takafumi A, Goto H, Daly MJ, Xavier RJ. Ca2+/calmodulin-dependent protein kinase II is a modulator of CARMA1-mediated NF-kappaB activation. *Mol Cell Biol*. 2006. 26(14):5497-5508

256. Camphausen K, Cerna D, Scott T, Sproull M, Burgan WE, Cerra MA, Fine H, Tofilon PJ. Enhancement of in vitro and in vivo tumor cell radiosensitivity by valproic acid. *Int J Cancer*. 2005. 114(3):380-386

257. Zwicker F, Kirsner A, Peschke P, Roeder F, Debus J, Huber PE, Weber KJ. Dichloroacetate induces tumor-specific radiosensitivity in vitro but attenuates radiation-induced tumor growth delay in vivo. *Strahlenther Onkol*. 2013. 189(8):684-692

258. Camphausen K, Moses MA, Beecken WD, Khan MK, Folkman J, O'Reilly MS. Radiation therapy to a primary tumor accelerates metastatic growth in mice. *Cancer Res*. 2001. 61(5):2207-2211

259. Loriot Y, Mordant P, Duque D, Geneste O, Gombos A, Opolon P, Guegan J, Perfettini JL, Pierre A, Berthier LK, Kroemer G, Soria JC, Depil S. Deutsch E. Radiosensitization by a novel Bcl-2 and Bcl-XL inhibitor S44563 in small-cell lung cancer. *Cell Death Dis*. 2014. 5:e1423

APPENDICES

APPENDIX.A Approved ACC Animal Protocol

UIC UNIVERSITY OF ILLINOIS AT CHICAGO

Office of Animal Care and Institutional
Biosafety Committee (OACIB) (M/C 672)
Office of the Vice Chancellor for Research
206 Administrative Office Building
1737 West Polk Street
Chicago, Illinois 60612

4/16/2014

Maria Barbolina
Biopharmaceutical Sciences
M/C 865

Dear Dr. Barbolina:

The protocol indicated below was reviewed in accordance with the Animal Care Policies and Procedures of the University of Illinois at Chicago and **renewed on 4/16/2014.**

Title of Application: **Role of the Fractalkine Signaling In EOC**
ACC NO: **13-051**
Original Protocol Approval: **4/22/2013(3 year approval with annual continuation required).**
Current Approval Period: **4/16/2014 to 4/16/2015**

Funding: ***Portions of this protocol are supported by the funding sources indicated in the table below.***
Number of funding sources: 3

Funding Agency	**Funding Title**			**Portion of Funding Matched**
NIH	*Role of the Fractalkine Signaling in EOC*			*All matched*
Funding Number	**Current Status**	**UIC PAF NO.**	**Performance Site**	**Funding PI**
R21 CA160917 (yrs 1-2 original)	*Funded*	*2011-01793*	*UIC*	*Maria Barbolina*
Funding Agency	**Funding Title**			**Portion of Funding Matched**
NIH	*Role Of The Fractalkine Axis In Metastiatic Ovarian Carcinoma*			*All matched*
Funding Number	**Current Status**	**UIC PAF NO.**	**Performance Site**	**Funding PI**
RO1 CA181114 (yrs 1-5 original)	*Pending*	*2013-03810*	*UIC*	*Maria Barbolina*
Funding Agency	**Funding Title**			**Portion of Funding Matched**
NIH	*CX3CR1- Dependent miRNA Transfer in Epithelial Ovarian Carcinoma*			*All matched*
Funding Number	**Current Status**	**UIC PAF NO.**	**Performance Site**	**Funding PI**
R21 CA181854 (yrs 1-2 original)	*Pending*	*2013-04400*	*UIC*	*Maria Barbolina*

This institution has Animal Welfare Assurance Number A3460.01 on file with the Office of Laboratory Animal Welfare, NIH. **This letter may only be provided as proof of IACUC approval for those specific funding sources listed above in which all portions of the grant are matched to this ACC protocol.**

Thank you for complying with the Animal Care Policies and Procedures of the UIC.

Sincerely,

Bradley Merrill, PhD
Chair, Animal Care Committee

BM/*kg*
cc: BRL, ACC File, Randi Zillmer

Phone (312) 996-1972 • Fax (312) 996-9088

APPENDIX.A Approved ACC Animal Protocol (continued)

UIC UNIVERSITY OF ILLINOIS AT CHICAGO

Office of Animal Care and Institutional
Biosafety Committee (OACIB) (M/C 672)
Office of the Vice Chancellor for Research
206 Administrative Office Building
1737 West Polk Street
Chicago, Illinois 60612

12/18/2014

Maria Barbolina
Biopharmaceutical Sciences
M/C 865

Dear Dr. Barbolina:

The protocol indicated below was reviewed in accordance with the Animal Care Policies and Procedures of the University of Illinois at Chicago and **renewed on 12/18/2014.**

Title of Application: **Chemokine-Dependent Control of Survival in Ovarian Carcinoma**
ACC NO: **12-222**
Original Protocol Approval: **1/2/2013 (3 year approval with annual continuation required).**
Current Approval Period: **12/18/2014 to 12/18/2015**

Funding: ***Portions of this protocol are supported by the funding sources indicated in the table below.***
Number of funding sources: 1

Funding Agency	Funding Title			Portion of Funding Matched
Ovarian Cancer Research Fdtn.	*Chemokine- Dependent Control of Survival in Ovarian Carcinoma*			*All matched*
Funding Number	**Current Status**	**UIC PAF NO.**	**Performance Site**	**Funding PI**
258934	*Funded*	*2013-00908*	*UIC*	*Maria Barbolina*

This institution has Animal Welfare Assurance Number A3460.01 on file with the Office of Laboratory Animal Welfare, NIH. **This letter may only be provided as proof of IACUC approval for those specific funding sources listed above in which all portions of the grant are matched to this ACC protocol.**

Thank you for complying with the Animal Care Policies and Procedures of the UIC.

Sincerely,

Bradley Merrill, PhD
Chair, Animal Care Committee

BM/*kg*
cc: BRL, ACC File, Randi Zillmer

Phone (312) 996-1972 • Fax (312) 996-9088

APPENDIX.B Permission of Reprint/Reproduce

Copyright Clearance Center RightsLink®

Home | Account Info | Help | Live Chat

OXFORD JOURNALS
OXFORD UNIVERSITY PRESS

Title: Complicating the complexity of p53:
Author: Karen S. Yee, Karen H. Vousden
Publication: Carcinogenesis
Publisher: Oxford University Press
Date: August 2005

Logged in as:
Jia Xie
Account #:
3000896914

LOGOUT

Order Completed

Thank you very much for your order.

This is a License Agreement between Jia Xie ("You") and Oxford University Press ("Oxford University Press"). The license consists of your order details, the terms and conditions provided by Oxford University Press, and the payment terms and conditions.

Get the printable license.

License Number	3653311072999
License date	Jun 20, 2015
Licensed content publisher	Oxford University Press
Licensed content publication	Carcinogenesis
Licensed content title	Complicating the complexity of p53:
Licensed content author	Karen S. Yee, Karen H. Vousden
Licensed content date	August 2005
Volume number	26
Issue number	8
Type of Use	Thesis/Dissertation
Requestor type	Academic/Educational institute
Format	Print and electronic
Portion	Figure/table
Number of figures/tables	1
Will you be translating?	No
Author of this OUP article	No
Order reference number	None
Title of your thesis / dissertation	Fractalkine Receptor Regulates Cellular Response to X-ray Radiation in Ovarian Cancer Cells
Expected completion date	Aug 2015
Estimated size(pages)	150
Publisher VAT ID	GB 125 5067 30
Total	0.00 USD

ORDER MORE... | CLOSE WINDOW

APPENDIX.B Permission of Reprint/Reproduce (continued)

ELSEVIER LICENSE
TERMS AND CONDITIONS

Jul 31, 2015

This is a License Agreement between Jia Xie ("You") and Elsevier ("Elsevier") provided by Copyright Clearance Center ("CCC"). The license consists of your order details, the terms and conditions provided by Elsevier, and the payment terms and conditions.

All payments must be made in full to CCC. For payment instructions, please see information listed at the bottom of this form.

Supplier	Elsevier Limited The Boulevard,Langford Lane Kidlington,Oxford,OX5 1GB,UK
Registered Company Number	1982084
Customer name	Jia Xie
Customer address	833 South Wood Street (MC865) CHICAGO, IL 60612
License number	3660860685448
License date	Jun 20, 2015
Licensed content publisher	Elsevier
Licensed content publication	Elsevier Books
Licensed content title	Clinical Radiation Oncology
Licensed content author	Leonard L. Gunderson
Licensed content date	2012
Number of pages	40
Start Page	3
End Page	42
Type of Use	reuse in a thesis/dissertation
Intended publisher of new work	other
Portion	figures/tables/illustrations
Number of figures/tables/illustrations	1
Format	both print and electronic
Are you the author of this Elsevier chapter?	No
Will you be translating?	No
Original figure numbers	Figure 1-7
Title of your thesis/dissertation	Fractalkine Receptor Regulates Cellular Response to X-ray Radiation in Ovarian Cancer Cells
Expected completion date	Aug 2015
Estimated size (number of pages)	
Elsevier VAT number	GB 494 6272 12
Permissions price	0.00 USD
VAT/Local Sales Tax	0.00 USD / 0.00 GBP
Total	0.00 USD

APPENDIX.B Permission of Reprint/Reproduce (continued)

Copyright Clearance Center RightsLink®

Home | Account Info | Help | Live Chat

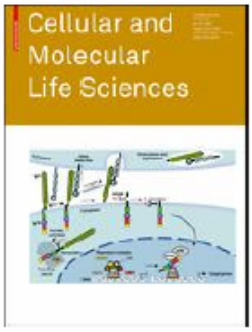

Title: DNA Repair in Mammalian Cells
Author: A. B. Robertson
Publication: Cellular and Molecular Life Sciences
Publisher: Springer
Date: Jan 1, 2009

Logged in as:
Jia Xie
Account #:
3000896914
LOGOUT

Order Completed

Thank you very much for your order.

This is a License Agreement between Jia Xie ("You") and Springer ("Springer"). The license consists of your order details, the terms and conditions provided by Springer, and the payment terms and conditions.

Get the printable license.

License Number	3658920148210
License date	Jun 30, 2015
Licensed content publisher	Springer
Licensed content publication	Cellular and Molecular Life Sciences
Licensed content title	DNA Repair in Mammalian Cells
Licensed content author	A. B. Robertson
Licensed content date	Jan 1, 2009
Volume number	66
Issue number	6
Type of Use	Thesis/Dissertation
Portion	Figures
Author of this Springer article	No
Original figure numbers	Figure 1
Title of your thesis / dissertation	Fractalkine Receptor Regulates Cellular Response to X-ray Radiation in Ovarian Cancer Cells
Expected completion date	Aug 2015
Estimated size(pages)	150
Total	0.00 USD

CLOSE WINDOW

APPENDIX.B Permission of Reprint/Reproduce (continued)

Copyright Clearance Center RightsLink®

Home | Account Info | Help | Live Chat

CAMBRIDGE JOURNALS

Title: Short-term and long-term cellular and molecular events following UV irradiation of skin: implications for molecular medicine

Author: Yasuhiro Matsumura and Honnavara N. Ananthaswamy

Publication: Expert Reviews in Molecular Medicine

Publisher: Cambridge University Press

Date: Feb 13, 2004

Logged in as:
Jia Xie
Account #:
3000896914

LOGOUT

Order Completed

Thank you very much for your order.

This is a License Agreement between Jia Xie ("You") and Cambridge University Press ("Cambridge University Press"). The license consists of your order details, the terms and conditions provided by Cambridge University Press, and the payment terms and conditions.

Get the printable license.

License Number	3660351394786
License date	Jul 01, 2015
Licensed content publisher	Cambridge University Press
Licensed content publication	Expert Reviews in Molecular Medicine
Licensed content title	Short-term and long-term cellular and molecular events following UV irradiation of skin: implications for molecular medicine
Licensed content author	Yasuhiro Matsumura and Honnavara N. Ananthaswamy
Licensed content date	Feb 13, 2004
Volume number	4
Issue number	26
Start page	1
End page	22
Type of Use	Dissertation/Thesis
Requestor type	Not-for-profit
Portion	Text extract
Number of pages requested	1
Order reference number	None
Territory for reuse	North America Only
Title of your thesis / dissertation	Fractalkine Receptor Regulates Cellular Response to X-ray Radiation in Ovarian Cancer Cells
Expected completion date	Aug 2015
Estimated size(pages)	150
Billing Type	Invoice
Billing address	Jia Xie 833 South Wood Street (MC865) 335 College of Pharmacy Building CHICAGO, IL 60612 United States Attn: Jia Xie

Tax (0.00%)	0.00 USD
Total	0.00 USD

ORDER MORE... | CLOSE WINDOW

APPENDIX.B Permission of Reprint/Reproduce (continued)

Copyright Clearance Center RightsLink®

Home | Account Info | Help | Live Chat

nature publishing group

Title: End-joining, translocations and cancer
Author: Samuel F. Bunting, Andre Nussenzweig
Publication: Nature Reviews Cancer
Publisher: Nature Publishing Group
Date: Jun 13, 2013

Logged in as:
Jia Xie
Account #: 3000896914
LOGOUT

Order Completed

Thank you very much for your order.

This is a License Agreement between Jia Xie ("You") and Nature Publishing Group ("Nature Publishing Group"). The license consists of your order details, the terms and conditions provided by Nature Publishing Group, and the payment terms and conditions.

Get the printable license.

License Number	3660920257903
License date	Jul 02, 2015
Licensed content publisher	Nature Publishing Group
Licensed content publication	Nature Reviews Cancer
Licensed content title	End-joining, translocations and cancer
Licensed content author	Samuel F. Bunting, Andre Nussenzweig
Licensed content date	Jun 13, 2013
Type of Use	reuse in a dissertation / thesis
Volume number	13
Issue number	7
Requestor type	academic/educational
Format	print and electronic
Portion	figures/tables/illustrations
Number of figures/tables/illustrations	1
High-res required	no
Figures	Figure 4
Author of this NPG article	no
Your reference number	None
Title of your thesis / dissertation	Fractalkine Receptor Regulates Cellular Response to X-ray Radiation in Ovarian Cancer Cells
Expected completion date	Aug 2015
Estimated size (number of pages)	150
Total	0.00 USD

ORDER MORE... | CLOSE WINDOW

APPENDIX.B Permission of Reprint/Reproduce (continued)

Copyright Clearance Center RightsLink®

Home | Account Info | Help | Live Chat

nature publishing group

Title: Regulation and mechanisms of mammalian double-strand break repair
Author: Kristoffer Valerie and Lawrence F Povirk
Publication: Oncogene
Publisher: Nature Publishing Group
Date: Sep 1, 2003

Logged in as:
Jia Xie
Account #: 3000896914
LOGOUT

Order Completed

Thank you very much for your order.

This is a License Agreement between Jia Xie ("You") and Nature Publishing Group ("Nature Publishing Group"). The license consists of your order details, the terms and conditions provided by Nature Publishing Group, and the payment terms and conditions.

Get the printable license.

License Number	3660930506580
License date	Jul 02, 2015
Licensed content publisher	Nature Publishing Group
Licensed content publication	Oncogene
Licensed content title	Regulation and mechanisms of mammalian double-strand break repair
Licensed content author	Kristoffer Valerie and Lawrence F Povirk
Licensed content date	Sep 1, 2003
Type of Use	reuse in a dissertation / thesis
Volume number	22
Issue number	37
Requestor type	academic/educational
Format	print and electronic
Portion	figures/tables/illustrations
Number of figures/tables/illustrations	1
High-res required	no
Figures	Figure 4
Author of this NPG article	no
Your reference number	None
Title of your thesis / dissertation	Fractalkine Receptor Regulates Cellular Response to X-ray Radiation in Ovarian Cancer Cells
Expected completion date	Aug 2015
Estimated size (number of pages)	150
Total	0.00 USD

ORDER MORE... | CLOSE WINDOW

APPENDIX.B Permission of Reprint/Reproduce (continued)

Copyright Clearance Center RightsLink®

Home | Account Info | Help | Live Chat

nature publishing group

Title: Ovarian Cancer Metastasis: Integrating insights from disparate model organisms

Author: Honami NaoraandDenise J. Montell

Publication: Nature Reviews Cancer

Publisher: Nature Publishing Group

Date: May 1, 2005

Logged in as:
Jia Xie
Account #:
3000896914

LOGOUT

Order Completed

Thank you very much for your order.

This is a License Agreement between Jia Xie ("You") and Nature Publishing Group ("Nature Publishing Group"). The license consists of your order details, the terms and conditions provided by Nature Publishing Group, and the payment terms and conditions.

Get the printable license.

License Number	3660940271634
License date	Jul 02, 2015
Licensed content publisher	Nature Publishing Group
Licensed content publication	Nature Reviews Cancer
Licensed content title	Ovarian Cancer Metastasis: Integrating insights from disparate model organisms
Licensed content author	Honami NaoraandDenise J. Montell
Licensed content date	May 1, 2005
Type of Use	reuse in a dissertation / thesis
Volume number	5
Issue number	5
Requestor type	academic/educational
Format	print and electronic
Portion	figures/tables/illustrations
Number of figures/tables/illustrations	1
High-res required	no
Figures	Figure 2
Author of this NPG article	no
Your reference number	None
Title of your thesis / dissertation	Fractalkine Receptor Regulates Cellular Response to X-ray Radiation in Ovarian Cancer Cells
Expected completion date	Aug 2015
Estimated size (number of pages)	150
Total	0.00 USD

ORDER MORE... CLOSE WINDOW

VITA

Jia Xie

EDUCATION

2010-2015	Ph.D.	University of Illinois at Chicago, Chicago, Illinois, USA. (GPA: 3.58)
2006-2010	B.S.	Wuhan University, Wuhan, Hubei, China. (GPA: 3.58)

RESEARCH EXPERIENCE

Jan. 2011-Sep. 2015	Research Assistant, Department of Biopharmaceutical Sciences, University of Illinois at Chicago, Chicago, IL, USA Fractalkine Receptor, CX_3CR1, Can Regulate the Response of Ovarian Carcinoma Cells to Radiation Therapy. CX_3CR1, a Fractalkine Receptor, can Regulate Peritoneal Dissemination of Epithelial Ovarian Cancer Cells.
May 2009-Jun. 2010	Research Assistant, Laboratory of Cell Biology, Wuhan University, Wuhan, Hubei, China CS055 (Chidamide/HBI-8000), a Novel Histone Deacetylase Inhibitor, Induces G_1 Arrest, ROS-Dependent Differentiation and Apoptosis in Human Leukemia Cells.
Dec.2008-Mar.2009	Research Assistant, Laboratory of Pharmacology, Wuhan University, Wuhan, Hubei, China The Preparation of Eugenol Nanoemulsion Gel and Its Therapeutic Effect against Chronic Neuralgia.
Oct.2008-Dec. 2008	Research Assistant, Laboratory of Biopharmaceutics, Wuhan University, Wuhan, Hubei, China The Design of Moisturizing Face Mask in which the Main Constituent is Nostoc Sphaeroides.

SELECTED CONFERENCES AND WORKSHOP

1. **Xie J.,** Gurler H., Barbolina M.V. Fractalkine Receptor, CX_3CR1, Regulates Cellular Response to X-Ray Radiation in Ovarian Cancer Cells. *Pharmaceutics Graduate Student Research Meeting (PGSRM)*, Chicago, IL. 2014. (Also participated in hosting the meeting)

VITA

2. **Xie J.,** Gurler H., Barbolina M.V. Fractalkine Receptor, CX_3CR1, Regulates Cellular Response to X-Ray Radiation in Ovarian Cancer Cells. *Indiana-Illinois End Epithelial Ovarian Cancer Coalition (IIEEOCC) Workshop,* South Bend, IN. 2014.

3. **Xie J.**, Gurler H., Barbolina M.V. Fractalkine Receptor, CX_3CR1, Can Regulate the Response of Ovarian Carcinoma Cells to Radiation Therapy. *American Association of Cancer Research Conference, Advances in Ovarian Cancer Research: From Concept to Clinic,* Miami, FL. 2013.

4. **Xie J.,** Gurler H., Barbolina M.V. CX_3CR1, a Fractalkine Receptor, can Regulate Peritoneal Dissemination of Epithelial Ovarian Cancer Cells. *American Association of Cancer Research Conference, Tumor Invasion and Metastasis.* San Diego, CA. 2013.

5. **Xie J.**, Barbolina M.V. The Role of CX_3CR1 in Resistance of Ovarian Carcinoma Cells to Radiation Therapy. *American Association of Cancer Research Conference, Annual Meeting*, Chicago, IL. 2012.

BIBLIOGRAPHY

1. Mitra A., Davis D.A., Tomar S., Roy L., Gurler H., **Xie J**., Lantvit D.D., Cardenas H., Fang F., Liu Y., Loughram E., Yang J., Stack S., Emerson R.E., Dahl K.D., Barbolina M.V., Nephew K.P., Matei D., Burdette J. *In Vivo* Tumor Growth of High-Grade Serous Ovarian Cancer Cell Lines. *Gynecologic Oncology*. 2015.

2. Desjardins M., **Xie J**., Gurler H., Muralidhar G., Sacks J., Burdette J. Barbolina M.V. Versican Regulates Metastasis of Epithelial Ovarian Carcinoma Cells and Spheroids. *Journal of Ovarian Research*. 2014, 7:70.

3. Kim M., Rooper L., **Xie J.**, Rayahin J., Burdette J., Kajdacsy-Balla A.A., Barbolina M.V. The Lymphotactin Receptor is Expressed in Epithelial Ovarian Carcinoma and Contributes to Cell Migration and Proliferation. *Mol. Cancer Res.* 2012.

4. Kim M., Rooper L., **Xie, J.**, Kajdacsy-Balla A.A., Barbolina M.V. Fractalkine Receptor CX_3CR1 is Expressed in Epithelial Ovarian Carcinoma Cells and Required for Motility and Adhesion to Peritoneal Mesothelial Cells. *Mol. Cancer Res.* 2012, 11-24.

5. Gong, K., **Xie, J.**, Yi, H., Li, W. CS055 (Chidamide/HBI-8000), a Novel Histone Deacetylase Inhibitor, Induces G_1 Arrest, ROS-Dependent Differentiation and Apoptosis in Human Leukemia Cells. *Biochem. J.* 2012, 735-746.

MANUSCRIPTS IN PREPARATION

1. **Xie J.,** Gurler H, Barbolina M.V. Fractalkine Receptor, CX_3CR1, Regulates Cellular Response to X-ray Radiation in Ovarian Cancer Cells.

2. **Xie J.,** Gurler H., Burdette J. Barbolina M.V. CX_3CR1, a Fractalkine Receptor, can Regulate Peritoneal Dissemination of Epithelial Ovarian Cancer Cells.

HONOR

2013	Graduate Student Council-Travel Award, University of Illinois at Chicago, Chicago, IL, USA
2008	Second-class scholarship and "Three Goods" student, Wuhan University, Wuhan, Hubei, China
2007	Second-class scholarship, Wuhan University, Wuhan, Hubei, China

TECHNICAL SKILLS

1. Biological Techniques: Western Blot, Immunofluorescence, Flow Cytometry (Apoptosis, Cell Cycle Arrest, ROS Accumulation, Cell Surface and Cytoplasm Protein Expression, Data Acquisition and Analysis), RT-PCR, Real-Time PCR, Tissue Section Preparation, Immunohistochemistry, Cell Culture, Transfection (siRNA/shRNA/CRISPR), DNA Ladder, Luciferase Reporter Assay, Clonogenic Assay, ELISA, Plasmid Extraction and Following Analysis with Agarose Gel Electrophoresis.

2. Pharmacologic Techniques: In vivo study of tumor formation, adhesion and metastasis, including subcutaneous injection, intraperitoneal injection and gastric perfusion. Animal handling and dissection, tissue sectioning, paraffin embedding and arterial cannula.

3. Instrumental Techniques: High Performance Liquid Chromatography Analysis (HPLC), Gas Chromatography Analysis (GC) and UV spectrophotometry.

4. Pharmaceutical Techniques: Organic Synthesis, Preparation of Tablets, Sustained Release, injection, etc.

Proficient in MS Word, Excel, Outlook, Powerpoint, FlowJo, GraphPad Prism, Image J and SigmaPlot.